The *Ustilago maydis* MAP kinase signaling pathway: Identification of MAP kinase targets by phospho-peptide enrichment

Dissertation

Zur

Erlangung des Doktorgrades

der Naturwissenschaften

(Dr. rer. nat.)

Dem Fachbereich Biologie

der Philipps-Universität Marburg

vorgelegt von

Vikram Naik

aus Sirsi, Karnataka/Indien

Marburg/Lahn, 2015

Die Untersuchungen der vorliegenden Arbeit wurden von Juli 2010 bis Juli 2014 unter Betreuung von Frau Prof. Dr. Regine Kahmann in Marburg am Max-Planck-Institut für terrestrische Mikrobiologie in der Abteilung Organismische Interaktionen durchgeführt.

Vom Fachbereich Biologie

der Philipps-Universität Marburg als Dissertation

angenommen am: 13.07.2015

Erstgutachter: Frau Prof. Dr. Regine Kahmann

Zweitgutachter: Herr Prof. Dr. Hans-Ulrich Mösch

Tag der mündlichen Prüfung: 22.07.2015

Other publications:

Lanver, D., Berndt, P., Tollot, M., Naik, V., Vranes, M., Warmann, T., Munch, K., Rossel, N., and Kahmann, R. (2014). Plant surface cues prime *Ustilago maydis* for biotrophic development. PLoS Pathog **10,** e1004272.

Perez-Nadales, E., Almeida Nogueira, M.F., Baldin, C., Castanheira, S., El Ghalid, M., Grund, E., Lengeler, K., Marchegiani, E., Mehrotra, P.V., Moretti, M., Naik, V., Oses-Ruiz, M., Oskarsson, T., Schäfer, K., Wasserstrom, L., Brakhage, A.A., Gow, N.A.R., Kahmann, R., Lebrun, M.-H., Perez-Martin, J., Di Pietro, A., Talbot, N.J., Toquin, V., Walther, A., and Wendland, J. (2014). Fungal model systems and the elucidation of pathogenicity determinants. Fungal Genet. Biol. **70,** 42-67.

Declaration

I hereby declare that the dissertation entitled "**The *Ustilago maydis* MAP kinase signaling pathway: Identification of MAP kinase targets by phospho-peptide enrichment**" submitted to the Department of Biology, Philipps-Universität Marburg, is the original and independent work carried out by me under the guidance of the PhD committee, and the dissertation is not formed previously on the basis of any award of Degree, Diploma or other similar titles.

Marburg, 10 June 2015

Vikram Naik

Dedication: “To insatiable curiosity that keeps ever searching for new challenges”

- Desmond Morris

Summary

The plant pathogen *Ustilago maydis* is the causative agent of maize smut disease and serves as a model system to study plant-fungal interactions. In this pathogen, a mitogen-activated protein kinase (MAPK) cascade controls mating, invasive growth and virulence on maize plants. The key players for infection-related processes and pathogenicity are the conserved mitogen-activated protein kinases (MAPKs) Kpp2 and Kpp6. Specifically, the MAP kinase Kpp2 is involved in appressorium development while Kpp6 is required for penetration of plant epidermal cells. Neither for Kpp2 nor for Kpp6 have the immediate downstream phosphorylation targets been identified.

The aim of this work was to identify crucial virulence factors which act downstream of the MAP kinases Kpp2 and Kpp6. To artificially induce MAP kinase signaling we used the strain FB1fuz7DD in which a constitutive active allele of the MAP kinase-kinase Fuz7 (Fuz7DD) is expressed under the control of an arabinose inducible promoter. Using a phospho-proteomic approach we detected phosphorylated proteins upon induction of the MAP kinase cascade in the presence and absence of *kpp2* and *kpp6*. Enrichment of phosphorylated proteins involved a two-step chromatographic procedure, using $Al(OH)_3$-based metal oxide affinity chromatography (MOAC), tryptic digestion of enriched phospho-proteins, and TiO_2-based MOAC for phospho-peptide enrichment. LC-MS/MS analysis of the phospho-peptide fraction yielded 111 potential MAP kinase substrates that were differentially phosphorylated in strains FB1fuz7DD and FB1Δkpp6Δkpp2fuz7DD. Fifteen of these differentially phosphorylated proteins, that could possibly be targets of Kpp2 and Kpp6, were selected for further studies based on extensive bioinformatic analysis.

To assess a possible contribution of the selected genes to mating and virulence, the respective genes were deleted in a solopathogenic strain and for some of the genes also in compatible haploid strains. Analysis of the respective deletions strains showed that, *um12335* was required for virulence. Subsequent studies suggest that Um12235 is a microtubule-associated protein that is a direct substrate of the MAP kinase Kpp2 and/or Kpp6.

Zusammenfassung

Ustilago maydis ist der Erreger des Maisbeulenbrands und dient als Modellorganismus um Interaktionen zwischen Pilz und Pflanze zu untersuchen. Pilzliche Paarung, invasives Wachstum in Maispflanzen und Virulenz werden in *U. maydis* über eine MAP-Kinase(MAPK) Kaskade reguliert. Zentrale Faktoren für Pathogenität sind die konservierten MAP-Kinasen (MAPKs) Kpp2 und Kpp6. Die MAP-Kinase Kpp2 ist in den Prozess der Appressorienbildung involviert, wohingegen Kpp6 eine Rolle während der Penetration pflanzlicher Epidermiszellen spielt. Weder für Kpp2 noch für Kpp6 wurden bisher die Substratproteine identifiziert welcher direkt phosphoryliert werden.

Ziel dieser Arbeit war es wichtige Virulenzfaktoren zu identifizieren, welche in der MAP-Kinase Kaskade direkt unterhalb von Kpp2 und Kpp6 agieren. Zur artifiziellen Induktion der MAP-Kinase Kaskade wurde der Stamm FB1fuz7DD genutzt, welcher ein konstitutiv aktives allel der MAP-Kinase-Kinase Fuz7 (Fuz7DD) unter Kontrolle eines Arabinose induzierbaren Promotors exprimiert. Mittels eines phosphoproteomischen Ansatzes konnten nach Induktion der MAP-Kinase Kaskade phosphorylierte Proteine in Anwesenheit und Abwesenheit von *kpp2* und *kpp6* detektiert werden. Anreicherung phosphorylierter Proteine erfolgte in einem zweistufigen chromatographischen Prozess, bei welchem zunächst mittels einer $Al(OH)_3$ Metalloxid Affinitätschromatographie (MOAC) Phosphoproteine angereichert wurden, um nach tryptischer Hydrolyse, mittels TiO_2 MOAC Phosphopeptide zu isolieren. LC-MS/MS Analyse der Phosphopeptid Fraktion ergab 111 potentielle MAP-Kinase Substrate, welche in den Stämmen FB1fuz7DD und FB1Δkpp6Δkpp2fuz7DD differenziell phosphoryliert vorlagen. Fünfzehn dieser differenziell phosphorylierten Proteine, welche möglicherweise direkte Substrate von Kpp2 und Kpp6 sind, wurden nach umfassender bioinformatischer Analyse ausgewählt und weiter untersucht.

Um zu prüfen ob diese Gene möglicherweise zu pilzlicher Paarung oder Virulenz beitragen wurden die entsprechenden Gene in einem solopathogenen Stamm, z.T auch in kompatiblen wiltyp Stämmen, deletiert. Analyse der entsprechenden Deletionsstämme zeigte, dass *um12335* für Virulenz benötigt wird. Weiterführende Untersuchungen ergaben, dass es

sich bei Um12235 möglicherweise um ein Mikrotubuli-assoziiertes Protein handelt, welches ein direktes Substrat der MAP-Kinasen Kpp2 und/ oder Kpp6 ist.

Abbreviations

Δ	Deletion
A	Adenine
aa	amino acid
Amp	Ampicillin
Cbx	Carboxin
cDNA	complementary DNA
CM	Complete medium
C-terminal	Carboxy-terminal
d	days
dpi	days post infection
DIC	Differential interference contrast
EDTA	Ethylene Diamine Tetraacetic Acid
DMSO	Dimethyl sulphoxide
eGFP	Enhanced green fluorescence protein
G	Guanine
GDP	Guanosine diphosphate
h	Hour
HA	Hemagglutinin
HMG	high-mobility-group
IP	Immuno-precipitation
kb	kilobase
k DA	kilodalton
LC	liquid chromatography
min	Minute
M	Molar
MAPK	Mitogen Activated Protein Kinase
MAPKK	MAPK kinase
MAPKK	MAPK kinase kinase
MOAC	Metal-oxide affinity chromatography
MS	Mass spectrometry
MTs	Microtubules
Nat	Nourseothricin
OD600	Optical density at 600 nm
ORF	Open reading frame
PCR	Polymerase chain reaction
PD	Potato dextrose
PEG	Polyethylene glycol
PKA	Protein kinase A
RT- PCR	Real time PCR or reverse transcription PCR
RNA	Ribonucleic acid
rRNA	Ribosomal RNA
Ser	Serine
SDS-PAGE	Sodium dodecyl sulfate polyacrylamide gel electrophoresis
T	Thymine
TCA	Trichloroacetic acid
Thr	Threonin
V	Voltage
WD	tryptophan-aspartic acid

Contents

1 Introduction

1.1 MAP kinase signaling in fungal pathogens

Mitogen-activated protein kinases (MAPKs) are a family of serine/threonine protein kinases that are involved in a variety of eukaryotic signal transduction pathways. In the MAP kinase pathway, an extracellular stimulus triggers a signaling cascade leading to the activation of transcription factors. These can then regulate the expression of genes involved in cellular programs such as differentiation or proliferation (Lengeler *et al*., 2000; Chang and Karin, 2001). In fungi, MAP kinase pathways control fundamental aspects of growth, development and reproduction (Xu, 2000). MAPK pathways function as signaling modules consisting of three hierarchic kinases: the activated MAP kinase kinase kinase (MAPKKK) first phosphorylates two Ser and/or Thr residues located within the activation loop of MAP kinase kinase (MAPKK), which in turn activates the terminal effector MAP kinase (MAPK) through dual phosphorylation of a highly-conserved activation loop that contains a –TXY- motif (Chang and Karin, 2001). Activated MAP kinases can then phosphorylate downstream substrates (Figure 1) (Hamel *et al*., 2012).

Studies on the regulation of MAP kinases in *Saccharomyces cerevisiae,* have served as a basis for the study of MAP kinase signaling in fungal pathogens (Chen and Thorner, 2007; Rispail *et al*., 2009). In *S. cerevisiae,* MAP kinase pathways control the basic aspects of the yeast life cycle (Chen and Thorner, 2007). There are five MAPK pathways in *S. cerevisiae* which regulate mating, invasive growth, cell wall integrity, hyperosmolarity responses and ascospore formation (Chen and Thorner, 2007). *S. cerevisiae* has become a standard model for studying the mechanisms that control MAP kinase signaling pathways (Chen and Thorner, 2007; Correia *et al*., 2010; Kramer *et al*., 2009; Klosterman *et al.*, 2007; Krantz *et al*.,2006; Rispail *et al*., 2009).

The pheromone response pathway regulates the mating process and it is initiated by the binding of a peptide mating pheromone to the G protein coupled receptors Ste2 or Ste3 (Figure 1). This binding results in the disassociation of inhibitory Gα subunit (Gpa1) from stimulatory Gβγ (Ste4, Ste18) subunits (Hamel *et al*., 2012; Rispail *et al*., 2009). Gβγ is

associated with the scaffolding protein Ste5 and the P21-activated kinase (PAK) Ste20 and it has been shown to be essential for activating Ste11 (MAPKK kinase), MAPK kinase (Ste7) and MAP kinase (Fus3/Kss1) cascades (Chen and Thorner, 2007; Rispail *et al*., 2009). The scaffold protein Ste5 plays an essential role in *S. cerevisiae* by recruiting the Ste11-Ste7-Fus3 complex to the plasma membrane (Pryciak and Hunters, 1998). The partially redundant MAP kinases Fus3 and Kss1 regulate the yeast mating process (Chen and Thorner, 2007; Hamel *et al*., 2012) (Figure 1).

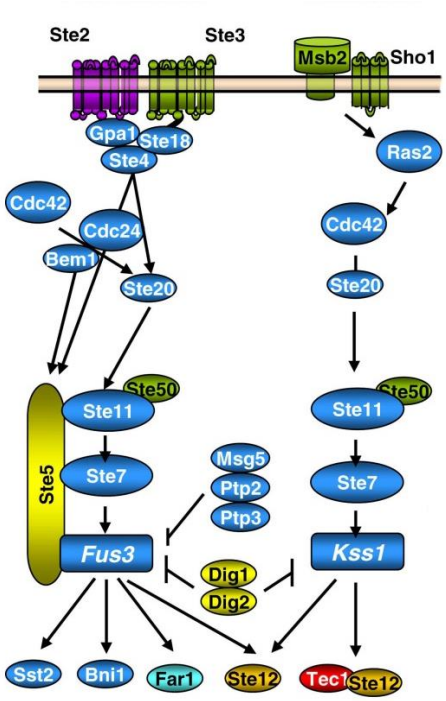

Figure 1: **Schematic view of fungal Fus3 and Kss1 MAP kinase signaling components.** MAP kinase cascades regulating mating and invasive growth are shown. Modified from Rispail *et al*., 2009.

Many components of the pheromone response pathway, including Ste20, Ste50, Ste11, Ste7, Kss1, and Ste12, are also involved in the regulation of filamentous/invasive growth pathway (Figure 1) (Hamel *et al*., 2012; Rispail *et al*., 2009). In this pathway, the mucin-like protein Msb2 and the plasma membrane protein Sho1 recognize the environmental signals (Boisnard *et al*., 2008; Krantz *et al*., 2006; Liu *et al*., 2011; Ma *et al*., 2008; Roman *et al*., 2005; Roman *et al*., 2009; Rispail *et al*., 2009). Activation of Ste11 by Sho1and Msb2 requires the small G protein Cdc42, the adaptor protein Ste50 and the PAK kinase Ste20 (Raitt *et al*., 2000). The inactive Kss1, which localizes to the nucleus, is a negative regulator of

filamentation. Ste7 phosphorylates Kss1 to relieve the negative regulation of filamentation (Hamel *et al*., 2012). However, upstream components of the pheromone pathway, such as the pheromone receptors, heterotrimeric G proteins, and the Ste5 scaffold protein, are not required for filamentation. Instead, activation of the Ste11–Ste7–Kss1 module is dependent on the osmosensors Sho1 and Msb2 (Figure 1) (Hamel *et al*., 2012; Rispail *et al*., 2009).

Fus3/Kss1-type MAP kinases have been well characterized in different fungal pathogens (Hamel *et al*., 2012; Rispail *et al*., 2009). One of the well-studied appressorium-forming fungi is *Magnaporthe oryzae,* which causes rice blast disease (Talbot, 2003). *M. oryzae* has three MAP kinase genes, *Mor-Kss1* (previously named PMK1), *Mps1* (penetration and sporulation), and *Osm1* (Osmoregulation MAP kinase), that are homologous to *S. cerevisiae* Fus3/Kss1, Slt2, and Hog1, respectively (Xu *et al*., 2000). The Mor-Kss1 MAP kinase stimulates the appressorium formation and it is required for pathogenic development in rice plants. In *M. oryzae*, the MAPKK Mor-Ste7 (Mst7) and MAPKKK Mor-Ste11 (Mst11) have been positioned upstream of Mor-Kss1 (Zhao *et al*., 2005). *M. oryzae* strains lacking *ste7* and *ste11* fail to form appressoria and are nonpathogenic (Zhao *et al*., 2005). The adaptor protein Mst50, an homologue of the yeast adaptor protein Ste50, interacts with Ste7 and Ste11 (Zhao *et al*., 2005). Both Mst50 and Ste11 interact with the GTPases Ras1 and Ras2 (Mosch *et al*., 1996; Park *et al*., 2006). At least one function of Ras2 is mediated through the Kss1 pathway (Leberer *et al*., 2001; Park *et al*., 2006).

Kss1/Fus3-type MAP kinases have also been characterized in other plant pathogenic fungi. Functional analysis shows that this class of protein kinases plays an important role in the establishment of various infection strategies (Hamel *et al*., 2012). *Pyrenophora teres*, *Colletotrichum orbiculare*, and *Cochliobolus heterostrophus*, are fungal plant pathogens that require Kss1/Fus3-type MAPKs for appressorium formation (Lev *et al*., 1999; Takano *et al*., 2000; Ruiz-Roldán *et al*., 2001; Hamel *et al*., 2012). However, for non-approssoria forming fungi such as the wheat pathogen *Mycosphaerella graminicola* (*Zymoseptoria tritici*), the MAP kinase gene Fus3 (Mgr-Kss1 pathway) is essential for the colonization of the host plant (Cousin *et al*., 2006).

In soil-born fungal pathogens that cause wilt disease symptoms in a variety of crops, virulence is attributed to the activity of Kss1/Fus3-type MAP kinases (Di Pietro *et al*., 2001;

Rauyaree *et al*., 2005) In *Fusarium oxysporum,* deletion of the MAP kinase genes Fmk1 or Kss1 results in a nonpathogenic phenotype in tomato plants (Di Pietro *et al*., 2001). In *Verticillium dahliae,* disruption of the MAP kinase *Vmk1* also results in reduced virulence phenotype, against a variety of host plants (Rauyaree *et al*., 2005). In the necrotrophic fungus *Alternaria brassicicola, disruption* of the MAP kinase *Amk1* results in strains that are nonpathogenic on healthy plants but, they are still able to colonize physically damaged host tissues (Cho *et al*., 2007). Inactivation of the MAP kinase Bmp1 in *Botrytis cinerea* also results in strains that are nonpathogenic, and in this case hyphae fails to penetrate and macerates plant tissues during infection (Zheng *et al*., 2000; Doehlemann *et al*., 2006). The *B. cinerea* MAP kinase Bmp1 has high homology to the *M. oryzae* Mor-Kss1 (Zheng *et al*., 2000). Studies have also revealed that deletion of the MAPK gene MAP1/Gpmk1 of *Fusarium graminearum*, the causal agent of wheat head-blight disease, reduces pathogenicity (Jenczmionka *et al*., 2003; Urban *et al*., 2003).

The function of Kss1/Fus3-type MAP kinases has also been analyzed in biotrophic fungi, including the hemibiotroph pathogen *Claviceps purpurea*. In *C. purpurea,* mutants lacking the MAP kinase gene *mk1* are nonpathogenic (Mey *et al*., 2002). In obligate biotrophic fungi *Blumeria graminis*, *Puccinia triticina* and *Puccinia striiformis*, Kss1/Fus3-type MAP kinases have been shown to play an important role in appressorial development, mating and virulence, although they lack the genetic transformation system (Guo *et al*., 2011: Hu *et al*., 2007; Kinane and Oliver, 2003). These genetic studies in obligate bio-trophic fungi were conducted using complementation assays in surrogate basidiomycete *U. maydis, F. graminearum* and *M. oryzae* (Guo *et al*., 2011: Hu *et al*., 2007).

Upon stimulation, MAP kinases phosphorylate a large number of substrates (Cargnello and Roux, 2011). MAP kinase substrates can be of any type of protein that co-localizes with a given MAP kinase in a cell at some point (Pitzschke, 2015). MAP kinases phosphorylate their targets at serine (S) or threonine (T) residues adjacent to a proline (P) (Park *et al*., 2011; Pitzschke, 2015). Prominent MAP kinase targets are transcription factors that elicit well defined transcriptional programs (Hamel *et al*., 2012; Turra *et al*., 2014). MAP kinase Kss1 can both negatively and positively regulate filamentation transcription factors Tec1 and Ste12 (Cook *et al*., 1997). Ste12 is a key transcription factor downstream of the pheromone-response

cascade, which binds to pheromone response elements (PREs) in the upstream activating sequences of its target genes and, in cooperation with Tec1 (Madhani and Fink, 1997). Ste12 orthologue are detected in different fungal species examined, except *S. pombe* and *U. maydis* (Rispail *et al*., 2009). Two nuclear proteins Dig1 and Dig2 are substrates of Kss1, which negatively regulate the invasive growth pathway by repressing Ste12 action (Cook *et al*., 1996). Dig1 and Dig2 orthologues has been detected only in *A. gossypii* (Rispail *et al*., 2009). Phopshorylated MAP kinase Fus3 in *S. cerevisiae* activates downstream effectors Ste12, Far1 or Sst2 (Elion *et al*., 1993). Far1 mediates the cell cycle arrest in response to pheromone (Peter *et al*., 1993). Far1 orthologues were found in all fungal species examined except in *S. pombe* and *R. oryzae* (Rispail *et al*., 2009). Sst2 is a GTPase-activating regulator of G protein signaling (RGS) for Gpa1, which regulates pheromone desensitization and prevents receptor-independent signaling of the mating pathway (Dohlman *et al*., 1996). Orthologues of Sst2 were identified in all fungal species examined, including two orthologues in *R. oryzae* (Figure1) (Rispail *et al*., 2009). Many of the MAP kinase substrates are elusive and remain to be discovered.

In summary, most components of the Fus3 and Kss1 MAP kinase cascades are well conserved in different fungal species (Rispail *et al*., 2009). In all taxonomically diverse phytopathogenic fungi studied to date, Fus3 and Kss1 type MAP kinases function as pathogenic factors required for virulence in these fungi (Hamel *et al*., 2012).

1.2 Life cycle of *U. maydis*

U. maydis is a hemibasidiomycete and has a very narrow host range (Bolker, 2001). *U. maydis* only infects maize (*Zea mays*) and its progenitor plant teosinte (Bolker, 2001). The life cycle of *U. maydis* (Figure 2) starts when two haploid compatible cells that differ in *a* locus recognize each other and then arrest their cell cycle in the G2 phase to coordinate their cell cycle prior to fusion, then they stop budding and start to form a conjugation tube (Garcia-Muse *et al*., 2003; Perez-Martin *et al*., 2006). These cells grow towards each other and fuse to form a dikaryotic filament (Figure 2). These filaments are parasitic and have the ability to infect maize plants (Banuett, 1995). Generation of the infectious dikaryotic filament is controlled by a tetrapolar mating system, regulated by the biallelic *a* locus and the multiallelic

b locus (Banuett, 2007; Brefort *et al*., 2009). The *a* locus has two alleles, *a1* and *a2*, coding for lipopeptide pheromone precursor (*mfa*) and pheromone receptor (*pra*) genes, which control cell recognition and fusion of compatible mating type cells (Brefort *et al*., 2009). The fate of the resulting dikaryon depends on *b* locus, which encodes for pair of homeodomain proteins bE and bW which are the subunits of a non-self-recognition heterodimeric transcription factor that regulates filamentation, dikaryon maintenance and pathogenicity (Banuett, 2007; Brefort *et al*., 2009). bE and bW polypeptides encoded by the same allele are unable to interact, whereas bE and bW encoded by different alleles can dimerize and form an active heterodimer (Kamper *et al*., 1995). bE/bW heterodimer functions as a transcription factor, which directly and indirectly regulates expression of genes involved in filamentous growth and establishment of the biotrophic stage (Brachmann *et al.*, 2001; Heimel *et al.*, 2010; Wahl *et al.*, 2010). Replacement of *bW1* by *bW2* and the introduction of *mfa2* into the *a1b1* background strain produced a solopathogenic strain SG200, which is haploid but can filament and induce tumor formation without prior cell fusion (Bolker *et al.*, 1995).

On the leaf surface, the dikaryotic filament develops approssoria-like structure, responsible for infection and this process is mediated by sensing the presence of hydroxy-fatty acids and hydrophobicity (Mendoza-Mendoza *et al.*, 2009). Following penetration, *U. maydis* grows intracellularly and the hyphae pass from one cell to another and are surrounded by the host plasma membrane, establishing a biotrophic interaction with the plant (Brefort *et al*., 2009). Once inside the host, *U. maydis* establishes both intracellular and intercellular growth leading to massive proliferation of fungal hyphae (Brefort *et al*., 2009). The latter stage of infection leads to the formation of tumors on plant surface (Figure 2). Inside the tumors proliferation of fungus is followed by sporogenesis where hyphal sections fragment, round up and differentiate into heavily melanized diploid teliospores (Brefort *et al*., 2009). Eventually, under favorable conditions, the diploid spores can germinate into haploid cells to reenter life cycle (Bolker, 2001). *U. maydis* is completely dependent on its maize host to complete the life cycle because it is incapable of ex planta sporulation (Figure 2) (Banuett, 1995; Bolker, 2001; Brefort *et al.*, 2009; Klosterman *et al.*, 2007).

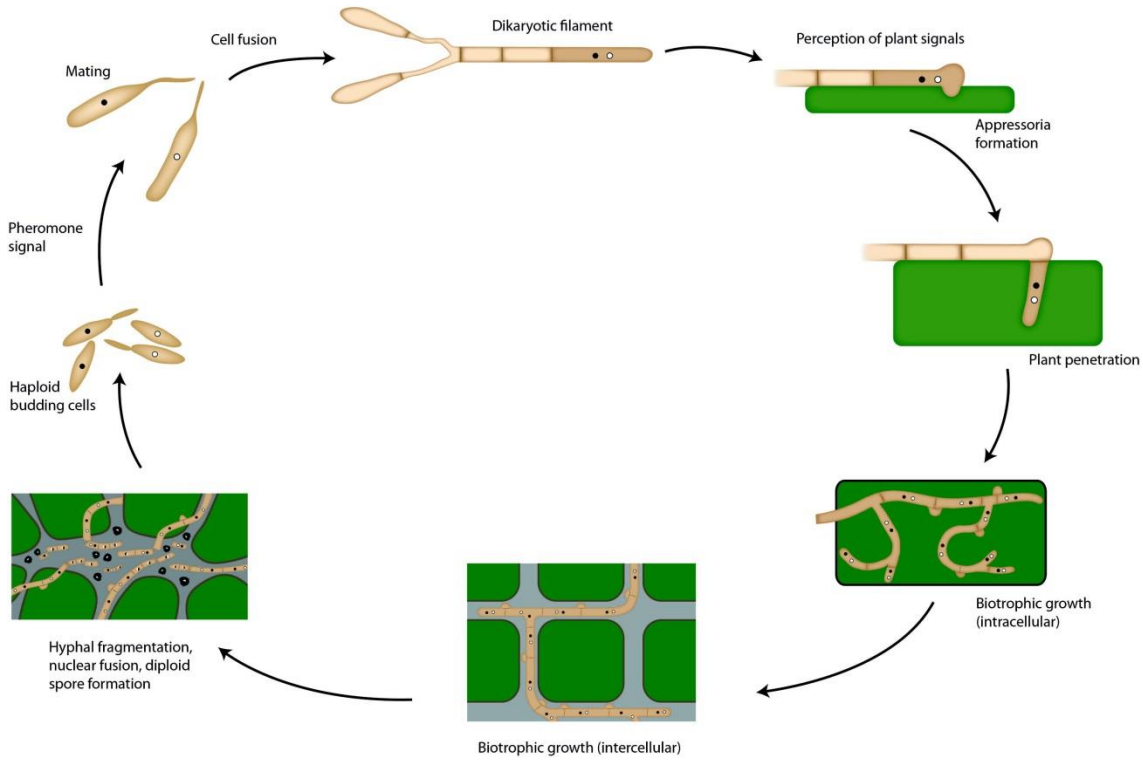

Figure 2: Life cycle of *U. maydis.* Developmental stages of *U. maydis* life cycle. (Adapted from Perez-Nadales *et al*., 2014 (see text for details).

1.3 Pheromone signaling in *U. maydis* life cycle

Transition from the non-pathogenic to pathogenic form requires the fusion of two haploid compatible cells of opposite mating type (Bölker *et al*., 1995). This process is initiated by lipopeptide pheromones which are perceived by cognate pheromone receptors (Pra1/2) in compatible mating type cells (Bolker *et al*., 1992). This pheromone receptor activates two conserved signaling pathways: the MAP kinase signaling pathway (Figure 3) and cAMP-dependent protein kinase A (PKA) pathway (Andrews *et al*., 2000; Kruger *et al*., 1998; Lee und Kronstad, 2002; Muller *et al*., 1999; Muller *et al*., 2003b).

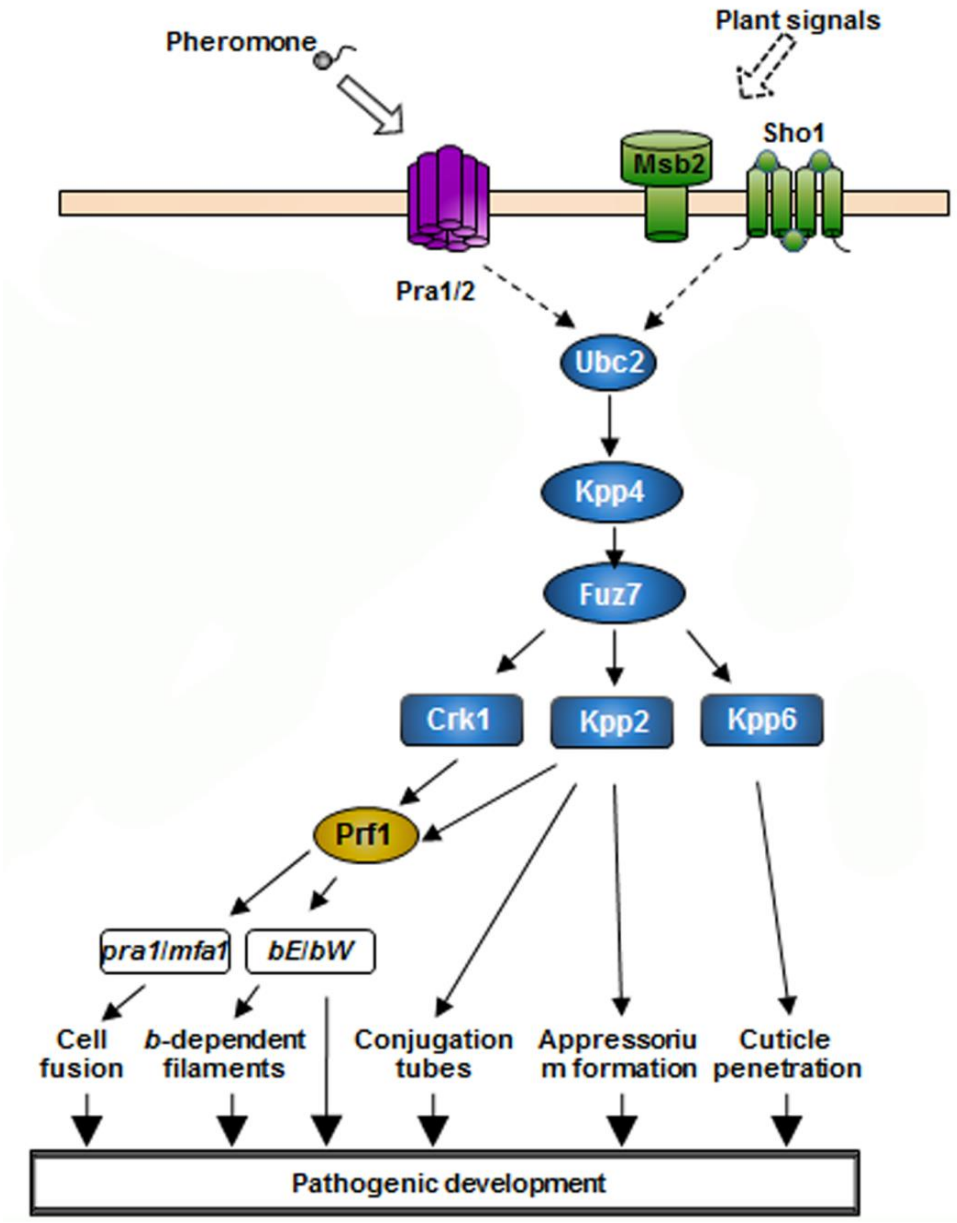

Figure 3: Pheromone signaling pathway in *U. maydis*. Main Components of MAP kinase pathways (blue) are indicated (Adapted from Lanver, 2011).

The *U. maydis* pheromone response MAP kinase module serves three different MAP kinases: Kpp2, Kpp6 and Crk1 (Figure 3) (Brachmann *et al*., 2003; Garrido *et al*., 2004; Mayorga and Gold, 1999). These kinases receive the pheromone and plant signal from the series of upstream kinases consisting of Kpp4/Ubc4, Fuz7/Ubc5 (Banuett and Herskowitz, 1994; MendozaMendoza *et al*., 2009b; Muller *et al*., 2003b). The protein kinases Kpp4/Ubc4 are regulated through its SAM domain, by interacting with Ubc2, an adaptor protein

(Klosterman *et al*., 2008; Mayorga and Gold, 2001). All the components of the MAP kinase module are needed for the conjugation tube formation and ultimately for pathogenicity (Brefort *et al*., 2009). Disruption of any component of the MAP kinase module causes a severe mating defect, inability to form appressoria and the abolishment of pathogenicity, exception is for Kpp6 (MendozaMendoza *et al.*, 2009; Muller *et al.*, 2003b). Kpp6 is rather required for the appressorial penetration step (Brachmann *et al*., 2003). The putative dual specificity phosphatase Rok1 negatively regulates the phosphorylation of Kpp2 and Kpp6 (Di Stasio *et al*., 2009). Deletion of *rok1* results in increased filamentation and hypervirulence are observed (Di Stasio *et al*., 2009) (Figure 2).

The dikaryotic filament formed upon mating grows in a polar mode producing infective appressoria-like structure. Both Sho1 and Msb2 play a key role during surface sensing and appressoria differentiation and they are shown to act upstream of the MAP kinases Kpp2 and Kpp6 (Lanver *et al.*, 2010). Penetration of the plant by appressoria is dependent on the MAP kinase Kpp6 (Brachmann *et al*., 2003). MAP kinase signaling leads to the activation of the pheromone response factor Prf1 through a complex interplay of transcriptional factors including Rop1, Hap2 and Prf1 itself (Hartmann *et al*., 1996; Garrido *et al.*, 2004; Mayorga and Gold, 1999; Mendoza-Mendoza *et al*., 2009). Prf1 receives pheromone signals from both the MAP kinase and cAMP pathways (Kaffarnik *et al*., 2003). Activated Prf1 regulates the transcription of genes located at *a* and *b* loci (Hartmann *et al*., 1996). Cyclic AMP activated PKA (protein kinase) leads to phosphorylation of Prf1, resulting in transcriptional activation of the *a* genes (Kaffarnik *et al*., 2003). The pheromone-induced *mfa1* expression is dependent on the intact PKA sites in Prf1 (Krüger *et al*., 1998). Activated-MAP kinase Kpp2 also phosphorylates Prf1 at distinct MAP kinase sites (Kaffarnik *et al*., 2003). The dual phosphorylation of Prf1 by Adr1 and Kpp2 triggers the expression of *b* genes (Kaffarnik *et al*., 2003; Zarnack *et al*., 2008). The expression of genes at the ‘a’ mating type locus occurs only if Prf1 is phosphorylated by the cyclic-AMP dependent protein kinase (PKA) while the expression of genes from the ‘b’ locus requires phosphorylation of Prf1 via PKA and the pheromone responsive MAP kinase (Kaffarnik *et al*., 2003). Deletion of *prf1* impairs expression of the *a* and *b* genes and conjugation tube formation as well as pathogenicity (Hartmann *et al*., 1996). MAP kinases cascade play a significant role in the recognition of compatible mating haploid cells, in the formation of dikaryotic filament, in sensing of plant

surfaces and the penetration of host plant tissue (Brachmann *et al*., 2003; Garrido *et al*., 2004; MendozaMendoza *et al.*, 2009; Muller *et al.*, 2003b; Mayorga and Gold, 1999). However, the direct targets of MAP kinases Kpp2 and Kpp6 that lead to conjugation tube formation, approssorium development and penetration of plant cuticle have not yet been identified (Figure 3).

1.4 The use of phospho-proteomic approaches for the detection of phosphorylated proteins in various systems

The detection of protein phosphorylation is a rapidly evolving field. These approaches can be broadly grouped into different categories: labelling, enriching, mass spectrometry and indirect methods. Labeling approaches use reagents that tag phosphorylated proteins with a detectable marker. Examples include Western blotting, *in vivo* labeling with ^{32}P or ^{33}P, (Adamczyk *et al*., 2001), and the use of phospho-protein-staining fluorescent dyes (Goodman *et al*., 2004). Affinity methods include immune-precipitation, immobilized metal affinity chromatography, and proprietary phospho-protein-binding materials (Gronborg *et al*., 2002; Gruhler *et al*., 2005; Kinoshita *et al*., 2014). Indirect measures of protein phosphorylation such as sensitivity to phosphatase treatment can help in the detection of phospho-proteins (Yamagata *et al*., 2002).

One of the most widely used phospho-peptide enrichment method is immobilized metal affinity chromatography (IMAC) (Feng *et al*., 2007). IMAC is performed in a column-based format, where positively charged metal ions, such as Fe(III) (Andersson *et al*., 1986) or gallium(III) (Posewitz *et al*., 1999) are chelated onto a solid phase nitrilotriacetic/iminodiacetic acid resin and presented for interaction with negatively charged phosphoryl groups (Grimsrud *et al*., 2010). Another frequently used affinity-based approach is metal oxide affinity chromatography (MOAC). MOAC uses microstage tip columns that take advantage of titania or zirconia as metal oxide chromatography modifiers (Sugiyama *et al*., 2007). In this method, phospho-peptides are loaded onto metal oxide at acidic pH and eluted at basic pH. MOAC uses various acids, including DHB (2,5-dihydroxybenzoic acid) (Jensen *et al*., 2007), glycolic acid and lactic acid, to increase phospho-peptide specificity

(Sugiyama *et al*., 2007). There are many variations of metal oxide presentation and staging (Sturm *et al*., 2008; Wang *et al*., 2009; Zhou *et al*., 2007).

Both immobilized metal affinity chromatography (IMAC) and metal oxide affinity chromatography (MOAC) methods are suitable for selectively enriching phospho-peptides. Often, a combination of enrichment techniques is used to achieve the highest phospho-peptide coverage in analysis of protein phosphorylation, for example in *Drosophila melanogaster* Kc167 cells (Bodenmiller *et al*., 2007). In *Arabidopsis thaliana*, dual metal oxide affinity chromatography (MOAC) of proteins and peptides was combined with LC-MS/MS to allow the identification of *in vivo* MAP kinase substrate candidates (Hoehenwarter *et al*., 2013).

Phosphorylated substrates of kinases can also be identified through a chemical genetics approach in which residues of the ATP- binding pocket of the target kinase is mutated in such a way that it can uniquely accept a bulky ATP analogue (Alaimo *et al*., 2001). In the presence of such bulky, labeled ATP analogues only mutated kinases can phosporylate their targets, which can then be identified (Alaimo *et al*., 2001). Sometimes, phosphorylated proteins migrate on gels at an apparent higher molecular weight than the un-phosphorylated form. And such mobility shifts can also be used as an indication of phosphorylation (Peck, 2006). This approach was used to identify a number of candidate proteins phosphorylated by casein kinase I (Gao *et al*., 2000) or the PAN GU kinase involved in cell cycle regulation (Lee *et al*., 2005). However, a shift in mobility upon phosphorylation depends on protein specific structural characteristics, and the number phospho-proteins that can be analyzed by the SDS-PAGE for detection of the phosphorylation is limited (Kinoshita *et al*., 2009). There are a number of additional approaches for the detection of phosphorylation by combination of conventional SDS-PAGE and other techniques including autoradiography studies, using radioactive compounds of [γ-^{32}P]- labeled ATP and [^{32}P]- labeled orthophosphate (Thingholm *et al*., 2009), immunoblotting with phospho-specific antibodies, use of phospho-specific Pro-Q Diamond gel/blot stain (Steinberg *et al*., 2003; Goodman *et al*., 2004) or the use of phospho-specific Phos-Tag gel/blot for separation of phosphorylated proteins (Kinoshita *et al*., 2009; Barbieri *et al*., 2008).

Combining the phospho-proteomic approaches with recent advances in mass spectrometry (MS) have revolutionized the analysis of signaling, allowing the identification of

phosphorylation sites with precision and sensitivity (Dephoure *et al*., 2013). Using this phosphoproteomic approach in the study of transgenic *A. thaliana* plant, where MAP kinase (MPK3/6) is artificially activated using constitutively-active variant of *MKK5* from *Petroselinum crispum*, expressed under the control of a DEX- inducible promoter, identified early and late putative substrates of MPK3 and MPK6 (Lassowskat *et al*., 2014).

1.5 Main goals of this study

The goal of this study was to identify downstream substrates of the two MAP kinases Kpp2 and/or Kpp6 and link the genes with mating and/or virulence by deleting them in *U. maydis* solopathogenic strains SG200 and in haploid strains and to elucidate the function of potential substrates.

2 Results

2.1 Generation and phenotypic characterization of FB1fuz7DD, FB1Δkpp2Δkpp6fuz7DD and FB1Δkpp6fuz7DD strains with respect to conjugation tube formation

In *U. maydis*, activation of the MAP kinase signaling pathway leads to the formation of conjugation tubes in haploid compatible strains (Brefort *et al*., 2009). To search for downstream substrates of the MAP kinase Kpp2 and Kpp6, strains were constructed in which MAP kinases could be artificially induced in presence or absence of *kpp2* and *kpp6*. The strain FB1fuz7DD was previously generated by Müller, P (Müller *et al*., 2003b). In this strain, MAP kinases could be artificially induced (Müller *et al*., 2003b; Di Stasio *et al*., 2009). Generation of the FB1Δkpp2Δkpp6fuz7DD and FB1Δkpp6fuz7DD strains, was accomplished by using the plasmid p123crg1fuz7DD (Müller *et al*., 2003b), which contains constitutively active allele of *fuz7* (*fuz7DD*) under the control of the *crg1* promoter which is repressed by glucose and induced by arabinose (Bolker *et al*., 1992). Then, these alleles were introduced in a single copy into the *ip* locus of FB1Δkpp2Δkpp6 and FB1Δkpp6 (Brachmann *et al*., 2003; Di Stasio *et al*., 2009; Loubradou *et al*., 2001; Refer to Material & Methods section for more details).

The MAP kinase inducible strains FB1Δkpp6fuz7DD, FB1Δkpp6Δkpp2fuz7DD and FB1fuz7DD were checked for the formation of the conjugation tube upon induction of MAP kinase signaling pathway.

2.1.1 Pheromone stimulation assay

Pheromone signaling pathway can be induced by the use of an artificial a2 pheromone (Müller *et al*., 1999). Pheromone stimulation leads to the formation of conjugation tube-like structures (Müller *et al*., 1999). Pheromone stimulation assay was done to assess whether the pheromone stimulation leads to the activation of MAP kinase signaling pathway in the strains FB1Δkpp6fuz7DD, FB1Δkpp6Δkpp2fuz7DD and FB1fuz7DD.

The effect of pheromones on conjugation tube formation was assessed in the strains FB1fuz7DD, FB1Δkpp6fuz7DD and FB1Δkpp6Δkpp2fuz7DD. These strains were grown in CM-glucose until reaching an OD_{600} of 0.6. Synthetic a2 pheromone (Szabó *et al*., 2002) was dissolved in dimethyl sulfoxide (DMSO) and added to a final concentration of 2.5 µg/ml. Cells were harvested for microscopic observation after 5 h of incubation at 28°C. The strains FB1fuz7DD and FB1Δkpp6fuz7DD showed formation of conjugation tubes upon pheromone stimulation (Figure 4). FB1Δkpp6Δkpp2fuz7DD did not form conjugation tubes after addition of pheromone (Figure 4). These results confirmed earlier findings where Kpp2 is shown to be required for the conjugation tube formation (Müller *et al*., 1999). These results indicate that the above tested strains are suitable for induction of the pheromone signaling pathway.

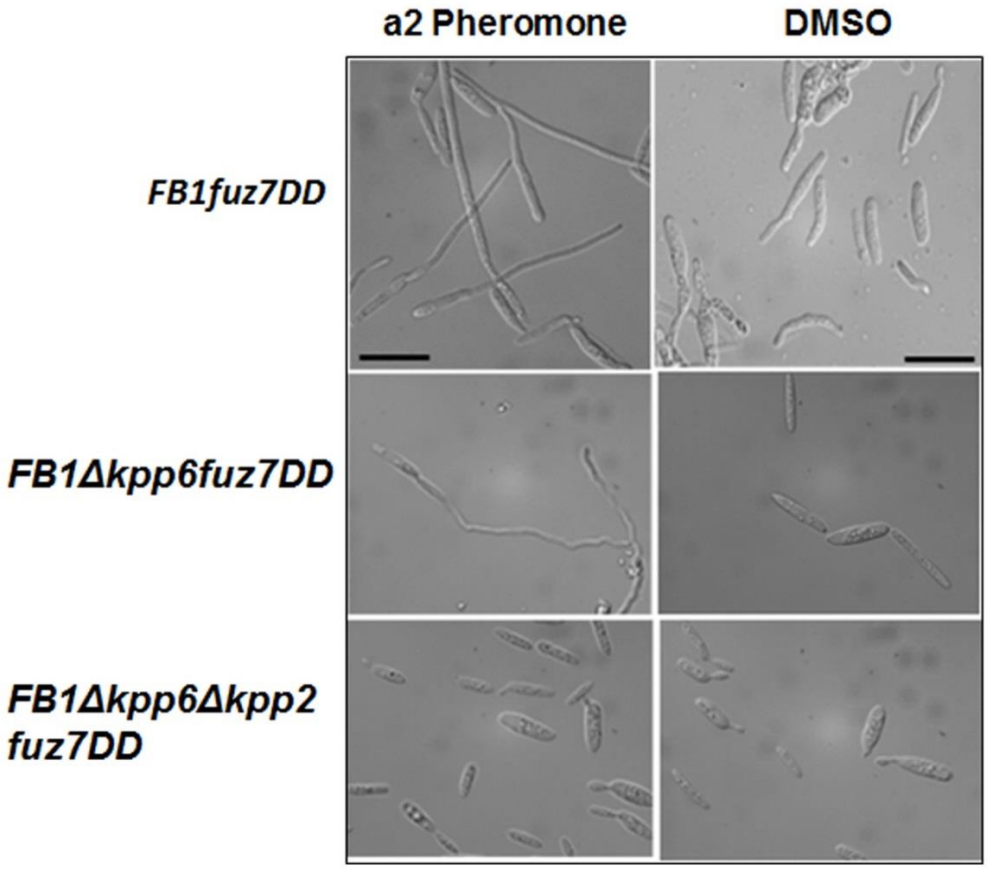

Figure 4: Conjugation tube formation in Fuz7DD strains after pheromone stimulation. The three strains listed on the left were either treated with synthetic a2 pheromone for 5 h or treated with DMSO as a control. FB1Δkpp6fuz7DD and FB1fuz7DD show the formation of conjugation tubes whereas the FB1Δkpp6Δkpp2fuz7DD does not. Scale bars indicate 10 µm.

2.1.2 Induction of conjugation tube formation in Fuz7DD strains by inducing *fuz7DD*

The MAP kinase can be directly induced by *fuz7DD* under the control of *crg1* promoter (Müller *et al*., 2003b). Induction of *fuz7DD* leads to the activation of MAP kinases, which can be measured by the formation of conjugation tube like structures (Müller *et al*., 2003b). This assay was done to measure the induction of *fuz7DD,* which leads to the activation of MAP kinases in FB1Δkpp6fuz7DD, FB1Δkpp6Δkpp2fuz7DD and FB1fuz7DD.

Induction of *fuz7DD* is under the control of *crg1* promoter which is repressed by glucose and induced by arabinose. Three strains FB1fuz7DD, FB1Δkpp6fuz7DD and FB1Δkpp6Δkpp2fuz7DD were also tested for the functionality of *fuz7DD* by growing the cells in CM-arabinose and CM-glucose medium. Overnight cultures grown in CM medium with 2% glucose were diluted in CM medium with 2% glucose until an OD_{600} of 0.8. Cells were then washed with water to remove all of the glucose and were transferred to CM medium containing 2% arabinose as a carbon source. Arabinose acts as an inducer of the *crg1* promoter, thus transcriptionally inducing the MAPK kinase Fuz7DD. This should lead to the formation of conjugation tubes in FB1Δkpp6fuz7DD and FB1fuz7DD strains. However, under the same conditions, the FB1Δkpp6Δkpp2fuz7DD strain should not show the conjugation tube formation due to the absence of the MAP kinase Kpp2 gene. The results (Figure 5) indicate that functional Fuz7DD was expressed from the *crg1* promoter.

2.1.3 Phenotypic characterization of FB1fuz7DD, FB1Δkpp2Δkpp6fuz7DD and FB1Δkpp6fuz7DD strains with respect to *mfa1* and *fuz7* gene expression

It has been demonstrated that *fuz7DD* can trigger expression of the *a* and *b* locus genes, presumably by increasing Kpp2 kinase activity (Müller *et al*., 2003b). Activation of the MAP kinase pathway increases transcription of genes in the *a* locus (*mfa1*) as well as in the *b* locus (Müller *et al*., 2003b). First, expression of fuz7 was assayed in FB1Δkpp6fuz7DD, FB1Δkpp6Δkpp2fuz7DD and FB1fuz7DD grown in CM medium containing 2% arabinose and as control in CM medium containing 2% glucose. Results showed the expression of fuz7

only after *fuz7DD* induction which is under the control of *crg1* promoter, repressed by glucose and induced by arabinose (Figure 6).

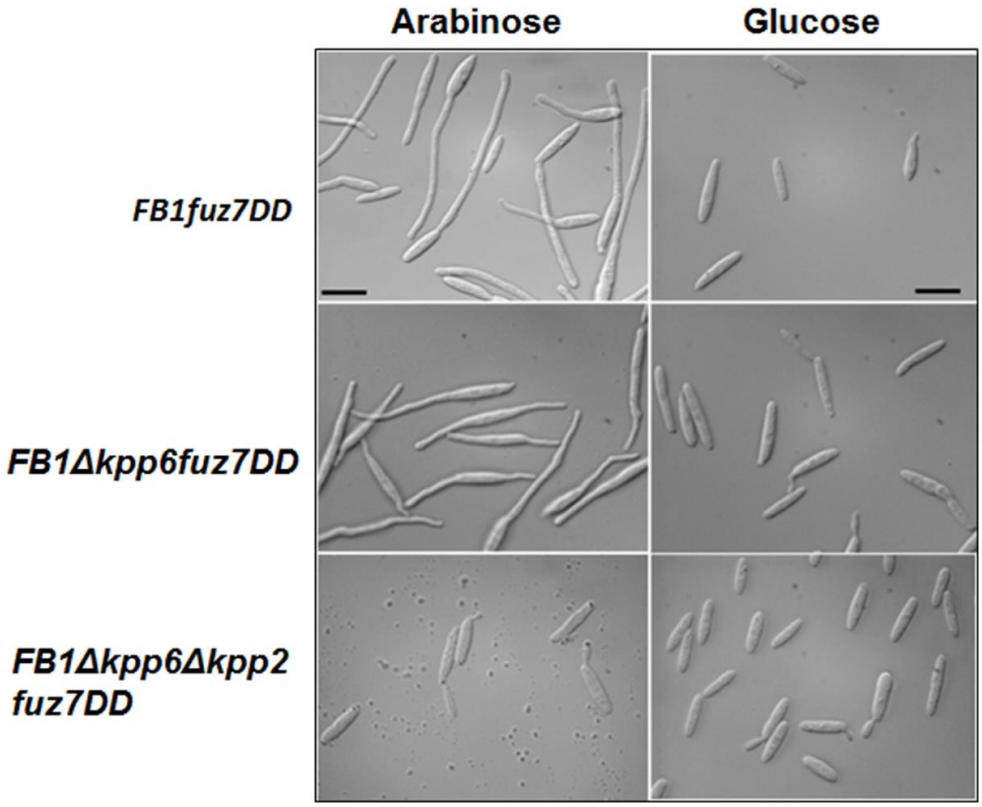

Figure 5: Conjugation tube formation in Fuz7DD strains after induction of *fuz7DD*. The three strains listed on the left were either treated with CM medium containing 2 % arabinose or treated with 2% glucose as control. FB1Δkpp6fuz7DD and FB1fuz7DD show the formation of conjugation tubes whereas the FB1Δkpp6Δkpp2fuz7DD does not. Scale bars indicate 10 µm.

Pheromone induced *mfa1* gene expression was assessed in the strains FB1Δkpp6fuz7DD, FB1Δkpp6Δkpp2fuz7DD and FB1fuz7DD to show that the transcriptional responses downstream of Kpp2 are inducible in these strains and depend on *kpp2*.

All the above three strains expressed *mfa1* upon induction for *fuz7DD*. A basal expression of mfa1 was also observed in glucose-grown cells, which has been previously observed for FB1fuz7DD (Müller *et al*., 2003). Expression of *mfa1* gene depends on both the MAP kinase and cAMP signaling pathways (Hartmannet *et al.*, 1996; Kaffarnik *et al*., 2003; Regenfelder *et al*., 1997). Consequently, *mfa1* expression is not affected by the deletion of MAP kinase *kpp2* and *kpp6*, which confirms previous findings (Müller *et al*., 2003b). These

results confirmed that fuz7DD activates the downstream regulators of MAP kinases *mfa1* in the constructed strains (Figure 6).

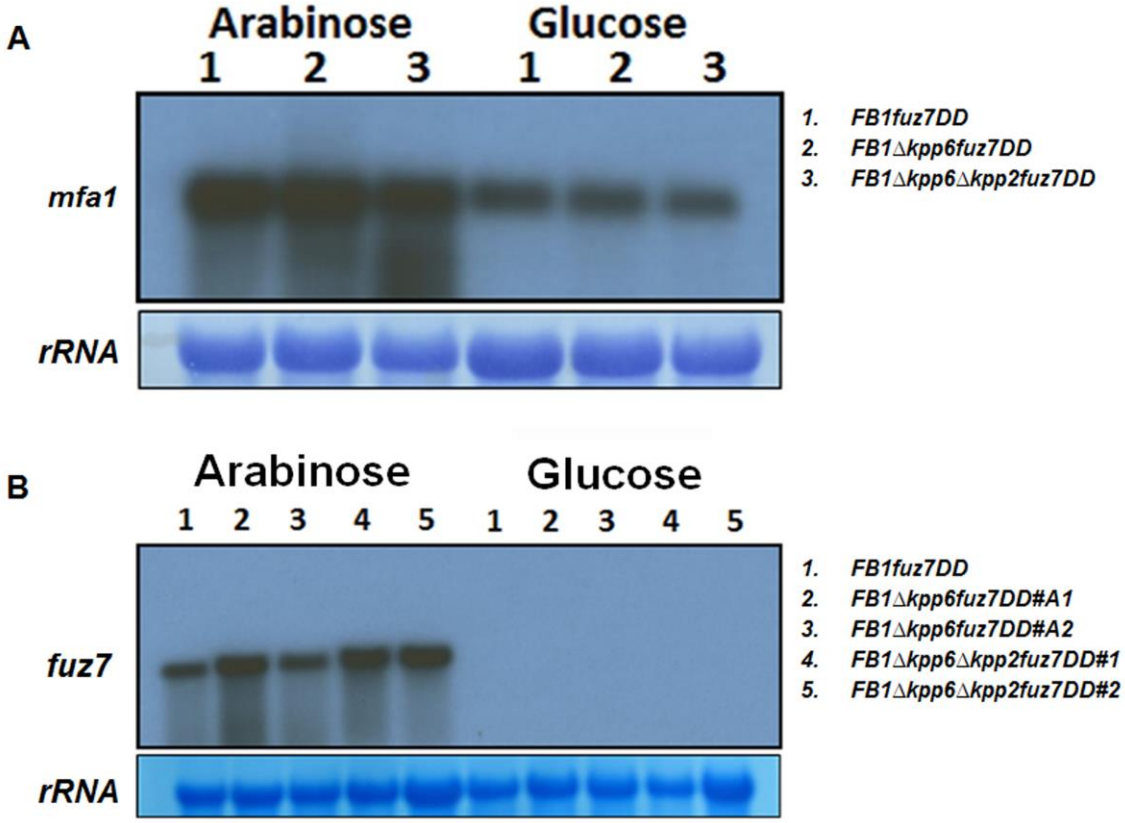

Figure 6: *fuz7DD* induces *mfa1* expression. FB1fuz7DD, FB1Δkpp6fuz7DD and FB1Δkpp6Δkpp2fuz7DD strains were grown for 5 h in CM medium containing 2% of arabinose or maintained in CM-glucose medium for the same period of time. 10 µg of total RNA was separated in each lane. (A) Northern blot was probed with a *mfa1* specific probe. (B) Northern blot was probed with a *fuz7*-specific probe. rRNA stained with methylene blue is shown as a loading control.

2.2 Phosphorylation status of Kpp2 after *fuz7DD* induction in the strains FB1fuz7DD, FB1Δkpp2Δkpp6fuz7DD and FB1Δkpp6fuz7DD

In *U. maydis*, the pheromone signaling MAPK kinase Fuz7 phosphorylates Kpp2 resulting in its activation (Müller *et al*., 2003b). Phosphorylation of Kpp2 can be detected by the phospho-specific antibody p44/p42 (Müller *et al*., 2003b). Kpp2 was shown to be

phosphorylated after Fuz7DD induction for 120 and 180 min (Di Stasio *et al*., 2009). Based on these earlier findings, three strains FB1Δkpp6fuz7DD, FB1Δkpp6Δkpp2fuz7DD and FB1fuz7DD were tested for their ability to phosphorylate Kpp2 after *fuz7DD* induction at the time points of 0, 120 and 180 min. This was accomplished by shifting the cells growing in CM-glucose to CM-arabinose medium (see Material and Methods). In FB1fuz7DD and FB1Δkpp6fuz7DD strains, phosphorylation of Kpp2 could be detected at 120 and 180 min after *fuz7DD* induction, whereas in FB1Δkpp6Δkpp2fuz7DD, phosphorylation could not be detected at any of the time points studied after activation of *fuz7DD* (Figure 7). This is in line with previous experiments for *fuz7dd* induction (Di Stasio *et al*., 2009). In Figure 7 an additional strong signal is detected at 55 kDa, which is likely reflecting phosphorylation of the cell wall integrity MAP kinase Mpk1 (Supplementary figure 2). Phosphorylation of Mpk1 in *U. maydis* is induced by cell wall stress and it can be detected with TEY motif antibody (Carbó *et al*., 2010). These stress condition could be induced during preparation of cells for protein isolation. Phosphorylation of Kpp2 was also checked at different time points after *fuz7DD* induction in FB1fuz7DD. It was observed that phosphorylation of Kpp2 starts at around 90 min after the induction of *fuz7DD* and keeps activated until 240 min (Figure 7) .These results confirm previous experiments, where Kpp2 phosphorylation was shown to occur until 180 min after *fuz7DD* induction (Di Stasio *et al*., 2009).

It was previously demonstrated that phosphorylation of Kpp6 starts after 30 min of *fuz7DD* induction and continues until 180 min (Di Stasio *et al*., 2009). Based on current findings on phosphorylation of Kpp2 after *fuz7DD* induction, clearly showed that in order to isolate MAP kinase substrates, 90 min *fuz7DD* induced FB1fuz7DD and FB1Δkpp6Δkpp2fuz7DD could be used for isolating potential MAP kinase substrates, using phosphopeptide enrichment approach.

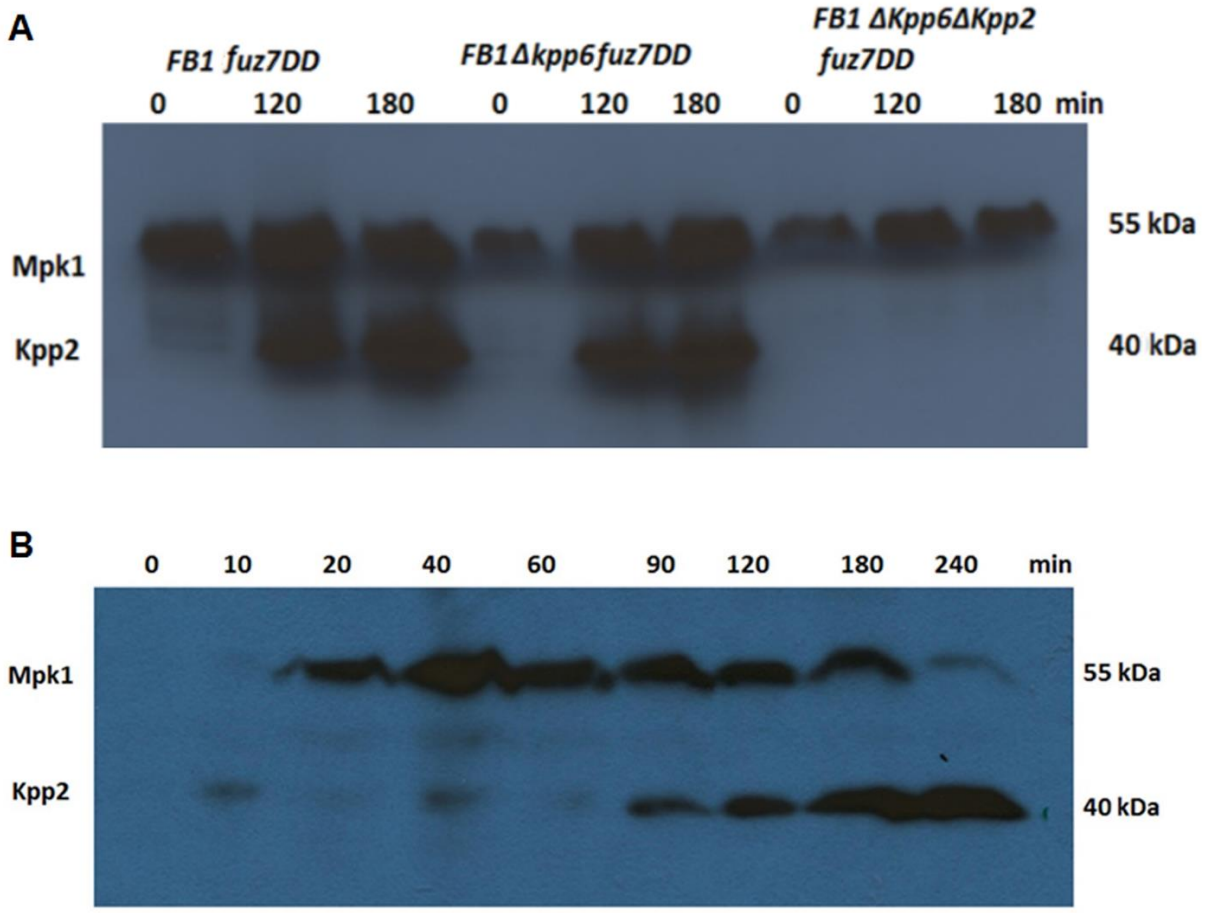

Figure 7: Phosphorylation of the MAP kinase Kpp2 after fuz7DD induction. (A) Analysis of the phosphorylation status of MAP kinase Kpp2 in the strains FB1Δkpp6fuz7DD, FB1Δkpp6Δkpp2fuz7DD and FB1fuz7DD. The expression of Kpp2 was induced for 0, 120 and 180 min as indicated. Phosphorylation was detected by western-blot analysis using a phospho-specific antibody recognizing the phosphorylated TEY motif in MAP kinases (α-p44/p42). (B) Western-blot analysis showing the phosphorylation of MAP kinase Kpp2 at different time points after *fuz7DD* induction. The upper band represents the cell wall integrity protein kinase Mpk1which is also detected with the phospho-specific antibody p44/p42**.**

2.3 Phospho-peptide enrichment after *fuz7DD* induction in the strains FB1fuz7DD and FB1Δkpp2Δkpp6fuz7DD

A phospho-peptide enrichment approach was used to find potential substrates/targets of Kpp2 and/or Kpp6. This approach was successfully used to identify numerous potential *in*

vivo targets of *Arabidopsis* MAP kinases (Hoehenwarter *et al*., 2013). Phospho-peptide enrichment allows the isolation of phospho-peptides in complex protein samples. In this work, phospho-peptides were isolated by using a modified protocol, previously established for *Arabidopsis* phospho-peptide isolation (Hoehenwarter *et al*., 2013). Based on phosphorylation of Kpp2 at 90 min after induction of Fuz7DD in the strain FB1fuz7DD, *fuz7DD* was induced in parallel for 90 min in CM-arabinose medium in strains FB1Δkpp6Δkpp2fuz7DD and FB1fuz7DD. In total, three biological replicates were generated for this experiment. In parallel conjugation tube formation was assayed for the same cultures after induction for 5 hrs. This revealed that Fuz7DD was functionally activated; intern activating the Map kinases Kpp2 and Kpp6.

Phospho-peptide enrichment was performed by following the protocols used by Hoehenwarter *et al*., 2013 (Figure 8) (details in Material and Methods section) (Chen *et* al., 2010; Colby *et al*., 2011; Hoehenwarter *et al*., 2013). This part of work was done in collaboration with Gerold J. M. Beckers at Plant Biochemistry and Molecular Biology Group, Department of Plant Physiology, RWTH Aachen University, Germany. Cells were harvested after been induced for *fuz7DD* in FB1Δkpp6Δkpp2fuz7DD and FB1fuz7DD. Total protein was isolated using ground cells by phenol-Tris-Cl method. Isolated proteins were subjected to metal oxide affinity chromatography (MOAC) using $Al(OH)_3$ to isolate phospho-proteins. Equal amount of phospho-protein from FB1Δkpp6Δkpp2fuz7DD and FB1fuz7DD was subjected to overnight trypsin digestion. The trypsin beads and insoluble material were removed and samples were concentrated for phosphopeptide enrichment with titanium dioxide column. Finally, bound peptides were eluted from column using 200 µl NH_4OH in 30% acetonitrile (pH > 10). Eluates were dried and sent for mass spec analysis using LC-MS/MS. Mass spec analysis was done by Wolfgang Hoehenwarter at Department of Molecular Systems Biology, Faculty of Life Sciences, University of Vienna, Austria (Figure 8).

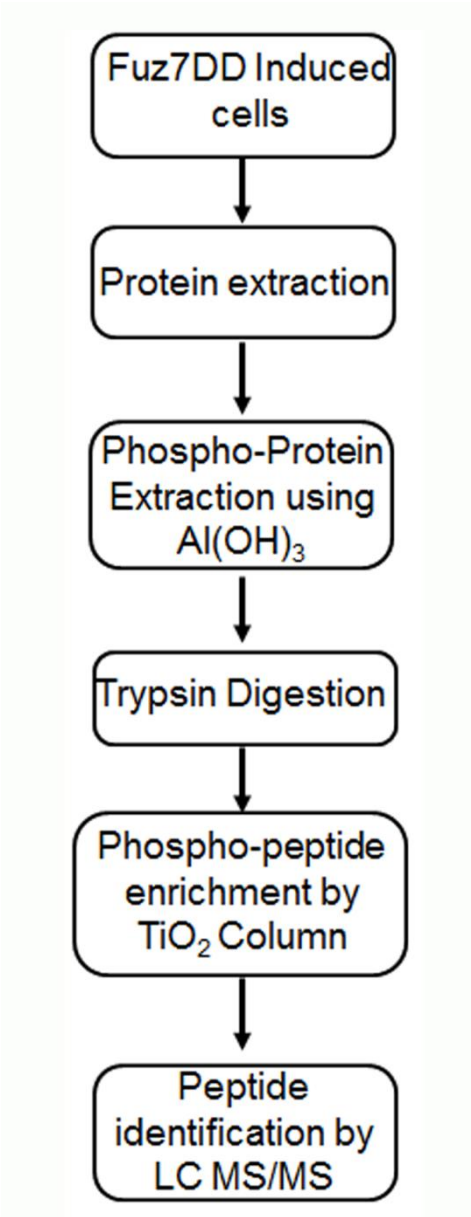

Figure 8: Schematic overview of the experimental approach. Phospho-protein and phospho-peptide enrichment strategy are shown. For further details, see description in the text**.**

Table 1: List of identified potential MAP kinase Kpp2and/or Kpp6 substrates. Capital letters in the peptide sequence column indicate amino acids and lower case ph indicates phosphorylation of the preceding Ser or Thr residue.

Gene name and predicted function	Peptide Sequence	Intensity of phosphorylation of WT[a]	Intensity of phosphorylation in kpp2 kpp6 mutant[b]	Ratio of WT /Mutant
>um12335 related to nuclear distribution protein RO11	_ADGPS(ph)PIPIHEFMDHDPASTIPHAAR_	7998500	0	7998500
>um00099 related to choline-phosphate cytidylyltransferase	_IQYQIKPTAIVDDKT(ph)PASSS(ph)PPR_	6223800	0	6223800
>um00082 putative protein	_KVTVSGIWNDQSASSSADAS(ph)PAR_	4115200	0	4115200
>um10462 conserved hypothetical protein	_STNISPPGTATSTGSGRIS(ph)PGESPSR_	1497900	0	1497900
>um04887 conserved hypothetical Ustilago-specific protein;>um06513 conserved hypothetical Ustilago-specific protein	_AIIPTIADS(ph)PR_	1017100	0	1017100
>um10368 related to Heat shock factor protein	_FTQIGS(ph)PPSSSSAADFGR_	988330	0	988330
>um01626 conserved hypothetical protein	_KAVHTSGIVS(ph)PSTTSGDSWTK_	530010	0	530010
>um02659.2 conserved hypothetical protein	_SKS(ph)PDSPTPAPSIDGVIHAGR_	519600	0	519600
>um00152 related to tandem ph domain-containing protein-2 (tapp2)	_YGISYTSSTGQSISGS(ph)PSTR_	488180	0	488180
>um10785 related to RPC34 - DNA-directed RNA polymerase III, 34 KD subunit	_RS(ph)PAASGGDIVPFVYR_	483770	0	483770
>um02102 related to HDA1 - histone deacetylase A	_SPIS(ph)PSQFVSR_	139810	0	139810
>um06304.2 conserved hypothetical protein	_AS(ph)PISSTTPPIR_	134930	0	134930
>um04849 hypothetical protein	_S(ph)PVVVGAAEPPIPPAAR_	10202000	2394400	4,260775
>um10343 conserved hypothetical protein	_SSNISTGFQQQQQQQQPGKNDDIS(ph)PIGSGR_	9323800	2880000	3,237431
>um04901 related to CKI1 - choline kinase	_HITGPTDKDAVS(ph)PHIYGIDNR_	5861200	3450400	1,698702

>um06195 related to EMG1 - Protein required for ribosome biogenesis	_PIAPIPHS(ph)PR_	775020	463970	1,67041
>um04022.2 conserved hypothetical protein	_GDPGS(ph)PSVGAASAITNASR_	1716600	1054100	1,628498
>um05337 related to SLA1 - cytoskeleton assembly control protein	_RGDSVS(ph)PAPPQIFSGPDGTIK_	7894300	4920700	1,604304
>um15076 hypothetical protein	_IHSPIQAPAQDATSQASQSNS(ph)PPR_	577450	397360	1,453216
>um05747 related to SEC31 - component of the COPII coat of ER-golgi vesicles	_GMMS(ph)PPPQGPPSGPGIAQQR_	518090	422390	1,226568
>um03437 related to BDF1 - sporulation protein	_STGS(ph)PSAAAAEYVPAKK_	1635500	1391800	1,175097
>um03437 related to BDF1 - sporulation protein	_DVPAVTS(ph)PSAQASDIAAVR_	6548200	3760100	1,741496
>um02618.2 probable transcriptional coregulator Snw1	_T(ph)AAGPPSPPPPVIRS(ph)PPR_	18245000	16741000	1,089839
>um03368 putative protein	_SFTAGPPSIVTPPS(ph)PPK_	1576600	1513500	1,041691
>um11494 related to SHP1 - potential regulatory subunit for Glc7p	_IGS(ph)PAPASFASSSASSSR_	32668000	31797000	1,027393
>um04462 putative protein	_MAS(ph)PAPSVGAISNR_	1361200	1429500	0,952221
>um11967 conserved hypothetical protein	_ADHESDSAHPISAASTPAPTAPAS(ph)PPADDIASSQEISR_	9151500	9797100	0,934103
>um00099 related to choline-phosphate cytidylyltransferase	_VAAAQTVAPIASARPGQPAVQHGFVS(ph)PSSVQQQSSTTAER_	24557000	26742000	0,918293
>um05552 conserved hypothetical protein	_IVADPIDSTDAFAPQPKPM( )S(ph)PVER_	16030000	17459000	0,918151
>um00532 putative protein	_AM S(ph)PAIGASIIPATDVPPAVSEIK_	57274000	70454000	0,812928
>um02587 related to SamB protein	_VIAPISGPDS(ph)PPR_	258430	337070	0,766695
>um05934 putative protein	_AQS(ph)PPIVTQPSGIIAR_	1218900	1697200	0,718183
>um10393 conserved hypothetical protein	_AVS(ph)PTIPPNVPSGPR_	12638000	17611000	0,71762
>um03276 related to SRP40 - serine-rich protein with a role in pre-ribosome assembly or transport	_VVS(ph)PPATPTPAPR_	764770	1069700	0,714939
>um02618.2 probable transcriptional coregulator Snw1	_T(ph)AAGPPSPPPPVIRS(ph)PPR_	2170800	3052500	0,711155
>um01134 related to HEM3 - porphobilinogen deaminase	_MS(ph)PVQDFTDATVPIQHK_	870170	1302700	0,667974

>um01009 probable glycogen synthase	_M PPPISMPGS(ph)PR_	8532400	13247000	0,644101
>um00168 related to Cell division control protein 15	_S(ph)PGAAFMQAPAR_	175490	276850	0,633881
>um11055 conserved hypothetical protein	_VSAAAATASDTPDS(ph)PQIVQR_	1591400	2678000	0,594249
>um06013 related to Intersectin 1;>um11804 related to PAN1 - actin-cytoskeleton assembly protein	_YVPPPS(ph)PPAAIEASSAVAER_	29873000	50724000	0,588932
>um05518 hypothetical protein	_FSGM GGVRS(ph)PPSSSAYITSSSER_	3297200	1580200	2,086571
>um05518 hypothetical protein	_NHPIM( )TTEQMS(ph)PPPSIAYGHSGPPR_	7790800	14123000	0,551639
>um05501 TPR-containing protein Mql1	_SQHGGSNAPS(ph)PAFGRPPVYGR_	1173400	2398200	0,489284
>um02066 conserved hypothetical protein	_ARS(ph)PAPQHDHDVTQAQQQAGEHIDEIHK_	1825200	3895000	0,468601
>um03017 putative protein	_TPAFRPHSPGEASVISVAVQPPAS(ph)PK_	2433700	5699900	0,426972
>um04609 conserved hypothetical protein	_IAPTIPAISS(ph)PR_	1452500	3960900	0,36671
>um11825 conserved hypothetical protein	_MAS(ph)PGVAPMGAHTGAR_	286130	790030	0,362176
>um03784 related to STRIATIN	_YISSSGAVQSSSS(ph)PISSQAPQVK_	909460	2752300	0,330436
>um00494 conserved hypothetical protein	_IAS(ph)PPPVPTSPPPKPISPPPPTR_	725570	2200100	0,32979
>um03796 related to dis1-suppressing protein kinase dsk1	_ISAQQQTPQGNSANRPGS(ph)PSPQGIPRPVATTVQ_	3742700	11524000	0,324774
>um02688 putative protein	_AAEKHS(ph)PPKESVIDIIER_	1160900	4629000	0,250789
>um00545 conserved hypothetical protein	_GDTSIHATPHS(ph)PVKVESPIITSHVK_	774420	3273600	0,236565
>um11301 probable SNF2 - component of SWI/SNF global transcription activator complex	_IVEIPRPPS(ph)PK_	671150	2864100	0,234332
>um00415 conserved hypothetical protein	_HSVAITTSAPS(ph)PSSAR_	298420	1328500	0,224629
>um10162 related to Transformer-2 protein homolog	_YGPPAGGRPFS(ph)PPPMR_	171640	3873100	0,044316
>um00342 hypothetical protein	_IGGASFSSASHAPIRS(ph)PNR_	0	777820	0
>um00429 probable TPS1 - alpha,alpha-trehalose-phosphate synthase, 56 KD subunit	_IKVEGEAES(ph)PSAGVPSIPSRP_	0	2762000	0
>um00551 related to putative C2H2 zinc finger protein flbC	_EAHFSQGEPPRHS(ph)PEQHISIISR_	0	628880	0

>um00607 related to phosducin homolog, likely to be involved in regulation of pheromone response	_AHGIIPPKPPS(ph)RS(ph)PS(ph)PEIASVR_	0	1262000	0
>um00770 probable URA7 - CTP synthase 1	_IPNDIPAAS(ph)PPFTSPR_	0	2857300	0
>um00890 putative protein	_STIDGAGRYS(ph)PPR_	0	252010	0
>um01267 putative protein	_IPSPIPITS(ph)PAR_	0	489340	0
>um02260 putative protein	_S(ph)PGIAPTIAMTR_	0	159220	0
>um02483 conserved hypothetical protein	_YPS(ph)PPIGAVHGQR_	0	545840	0
>um03037 related to BOI1 - BEM1 protein-binding protein	_SPTSNIHEIIENQAS(ph)PSQPAIQVK_	0	7135200	0
>um03280 probable TUP1 - general transcription repressor	_MRVEGPASHYSGPPS(ph)PGPER_	0	373930	0
>um03346.2 related to SKN7 - transcription factor (C-terminal fragment)	_M( )SGITTAPSTAAPIS(ph)PK_	0	293780	0
>um03608 related to RRP14 - protein involved in Ribosomal RNA Processing	_VAAASASTSSITNATS(ph)PSIK_	0	8148600	0
>um03783 conserved hypothetical protein	_VQSMSAFQTPQHS(ph)PR_	0	578280	0
>um03942 conserved hypothetical protein	_GAS(ph)PSPSTPHSPIPPTTPSK_	0	501910	0
>um03944 conserved hypothetical protein	_VNPTQDDTINDDAIAAYSFIEQPPS(ph)PIVR_	0	18587000	0
>um03944 conserved hypothetical protein	_GGAGTES(ph)PVNIADSVGSIGR_	1614500	5247900	0,307647
>um04381 related to SNF5 - component of SWI/SNF transcription activator complex	_VYGNSAPPAVAAGGGS(ph)PGAAAGSPHK_	0	354020	0
>um04517.2 putative protein	_HGFININPSS(ph)PGAIK_	0	1061700	0
>um04832 putative protein	_NEHGVEVRS(ph)PVAYQQQQYQHQR_	0	2310600	0
>um05287 related to Vacuolar protein sorting-associated protein VPS5	_NHQVSFASTAEPGS(ph)PTPTGR_	0	1131600	0
>um05373 related to REG1 - regulatory subunit for protein phosphatase Glc7p	_SINEYDSDGQGSYGIASPHFPAS(ph)PHIDAK_	0	4372500	0
>um05447 conserved hypothetical protein	_VAS(ph)PPSSTTIANK_	0	170780	0
>um06269 conserved hypothetical protein	_VVGGASSNPVIS(ph)PSR_	0	273960	0
>um10056 related to serine/threonine-protein kinase	_IDHIGNPIVDGAHAAGVVPGS(ph)PM( )RVD_	0	1503700	0
>um10161 conserved hypothetical protein	_TPGSSIS(ph)PKPAQSFVQPQEK_	0	4392300	0

>um10496 related to KIC1 - ser/thr protein kinase that interacts with Cdc31p	_S(ph)PTYEQRPSHAQIPHSPR_	0	3655300	0
>um10570 conserved hypothetical protein	_TPDRETVAHTSQEIESSTEPMS(ph)PPPIK_	0	1392700	0
>um11652 related to PSF2 - part of GINS, replication multiprotein complex	_HHSASIPHSDS(ph)PTIIHPPR_	0	1419000	0
>um11957 related to histidine kinase	_RPGGGIEITIPGPGEPGS(ph)PPR_	0	509570	0
>um12074 probable NMA2 - nicotinate-nucleotide adenylyltransferase	_QASSASIATIS(ph)PDKPIMR_	0	770970	0
>um00603 putative protein	_QSFAASAASAAVKPTVPASSANAAEGSQS(ph)PK_	0	0	
>um00668 related to SIP2 - subunit of the Snf1 serine/threonine protein kinase complex	_IPTAIPSSHVS(ph)PSSPPTSIYSQHSDR_	0	0	
>um00735 conserved hypothetical protein	_APS(ph)PPIIDIR_	0	0	
>um02280 putative protein	_YSTIHGSSISSGPTSITSSNWS(ph)PSR_	0	0	
>um02450 probable HYP2 - translation initiation factor eIF5A.1	_KYEDIS(ph)PSTHNMDVPNVR_	0	0	
>um02478 conserved hypothetical protein	_AYIPASESAQANQSSDSHPFASTSTTAQDTS(ph)PSSR_	0	0	
>um03544 related to SEC14 - phosphatidylinositol/phosphatidylcholine transfer protein	_NVSGSISAGATS(ph)PSVTPIQDSSQR_	0	0	
>um03866 related to UTP6 - U3 snoRNP protein	_YGS(ph)PETAHNVAEQTQYAASGPATIK_	0	0	
>um04849 hypothetical protein	_HQS(ph)PQPPPIPASSSGER_	0	0	
>um04989 related to RAD52 - recombination and DNA repair protein	_FVS(ph)PPPIPR_	0	0	
>um05364 related to Formin binding protein 3	_GAGFNS(ph)PNQIHRPGAEPASGS(ph)NTPIPNPHTASR_	0	0	
>um05533 related to EDE1 protein involved in endocytosis	_MQS(ph)PAPTGAAGAAPAIAISPVER_	0	0	
>um06271 conserved hypothetical protein	_PTIPTTPRPTNPDGADSSWIIDQQIS(ph)PTIAQSSIR_	0	0	
>um06278 conserved hypothetical protein	_IPPIS(ph)PSISR_	0	0	
>um06395 related to NOT3 - general negative regulator of transcription, subunit 3	_APASSQSAVIS(ph)PPKVPSAAPIPPIR_	0	0	

>um06491 related to RNA (guanine-N7-) methyltransferase	_GNS(ph)PTYAVGPQQPSISTINR_	0	0	
>um10147 probable 60S ribosomal protein L12	_IGPIGIS(ph)PK_	0	0	
>um10188 l-ornithine N5-oxygenase	_MNQAVSYGQDVISIEPIAIASAS(ph)PDAK_	0	0	
>um10905 conserved hypothetical protein	_EANIFIES(ph)PEIPSQGADSHSADGTYDGPNVPVVDESTIVHR_	0	0	
>um11132 related to NTG1 - DNA repair protein	_AASSPFSIS(ph)PR_	0	0	
>um11213 related to RRP6 - Exonuclease component of the nuclear exosome	_TGNIPSWVINAPIS(ph)PPQR_	0	0	
>um11224 putative protein	_DSTKPSSAISNSAAAS(ph)PSSSISASR_	0	0	
>um11960 conserved hypothetical protein	_MIVISS(ph)PVIESFFK_	0	0	
>um04849 hypothetical protein	_GTS(ph)PPIT(ph)ARSPVVVGAAEPPIPPAAR_	0	0	
>um06013 related to Intersectin 1;>um11804 related to PAN1 - actin-cytoskeleton assembly protein	_AAPAPAAAAAAPPAPPSTITPPEVPAAPAAPAQPS(ph)PTHSAGSSTNPFHR_	0	0	
>um06491 related to RNA (guanine-N7-) methyltransferase	_GNS(ph)PTYAVGPQQPSISTINR_	0	0	
>um11652 related to PSF2 - part of GINS, replication multiprotein complex	_HHSASIPHSDS(ph)PTIIHPPR_	0	0	

With [a] being WT strain FB1fuz7DD and [b] is mutated strain FB1Δkpp6Δkpp2 fuz7DD

2.4 LC/LC-MS analysis of phosphorylated substrates of *U. maydis* MAP kinases

Phospho-peptide enriched samples were analyzed by LC-MS/MS to enable detection of low abundant phosphorylated peptides. By these means, it was possible to do direct site-specific identification and quantification of phosphorylated peptides that were differentially accumulated after MAP kinase activation in wild type (FB1fuz7DD) and mutant cells (FB1Δkpp6Δkpp2fuz7DD). LC-MS/MS analysis of the phospho-peptide fraction obtained after the two-step metal oxide affinity chromatography (MOAC) yielded about 400 peptides, in which 111 putative substrates had (pSer/pThr) Prolin motif (Table 1). In 111 putative substrates, 24 showed phosphorylation intensity/phosphopeptide abundance higher in FB1fuz7DD in comparison to FB1Δkpp6Δkpp2fuz7DD, in that 13 genes were found only in FB1fuz7DD. Twenty-nine genes were conserved hypothetic proteins (conserved proteins whose functions are still unknown) with *um04887* as a conserved hypothetical Ustilago-specific protein. Five hypothetical proteins (share sequence similarity to an extent with characterized proteins) were also found. Through bioinformatics analysis, 16 genes were predicted to be transcription factors: *um11825, um11055, um10343, um06278, um05518, um05501, um04609, um04381, um03437, um03346.2, um03280, um02618.2, um02587, um02478, um02280, um00551*, Six kinase proteins: *um10056, um00668, um10496, um11957,um03796, um04901* and four zinc figure domains containing proteins: *um02478*, *um02587*, *um05518*, *um10343*.

Peptide and phosphopeptide abundance /intensity was determined by the ion count with the ProtMAX 2012 software version as described in Hoehenwarter *et al*., 2013 and was averaged from three biological replicates. Ion count is the number of times that a certain peptide ion signal, as defined by its mass to charge ratio (m/z) and retention time, is recorded at the MS level throughout the shotgun proteomics LC-MS analysis (Hoehenwarter *et al*., 2013).

Out of these substrates, 15 substrates which differentially phosphorylated proteins were chosen for subsequent functional analysis based on two criteria 1) ratio (from 1 to 7.9 and 0.36, 0.30) of phosphorylation intensity between wild type (FB1fuz7DD) and mutant

(FB1Δkpp6Δkpp2fuz7DD) and 2) the presence of protein or DNA binding domains in these potential MAP kinase substrates (Table 2).

Table 2: Potential MAP kinase substrates selected for more detailed analysis.

Gene	Predicted Functions	Intensity of phosphorylation WT[a]	Intensity of phosphorylation in kpp2 kpp6 mutant[b]	Ratio WT/Mutant
um12335	Related to nuclear distribution protein RO11	7998500	0	7998500
um04887	Conserved hypothetical *Ustilago*-specific protein	1017100	0	1017100
um01626	Conserved hypothetical protein	530010	0	530010
um02659.2	Conserved hypothetical protein	519600	0	519600
um10343	Conserved hypothetical protein	9323800	2880000	3.23743
um05364	Related to Formin binding protein3	16611000	7293500	2.27751
um05518	Hypothetical protein	3297200	1580200	2.08657
um05337	Related to SLA1 - cytoskeleton assembly control protein	7894300	4920700	1.6043
um03437	Related to BDF1 - sporulation protein	6548200	3760100	1,741496
um06278	conserved hypothetical protein	-	-	-
um02618.2	Probable transcriptional coregulator of Snw1	18245000	16741000	1.08984
um00890	Hypothetical protein	35857000	33437000	1.07237
um03944	Conserved hypothetical protein	1614500	5247900	0,307647
um11960	Conserved hypothetical protein	-	-	-
um11825	conserved hypothetical protein	286130	790030	0.36217

With [a] being WT strain FB1fuz7DD and [b] is mutated strain FB1Δkpp6Δkpp2 fuz7DD.

Um05518 was chosen based on phosphorylation intensity ratio which was higher in FB1fuz7DD strain (Table 2). Bioinformatics analysis showed the presence of functional domains including zinc finger and GATA transcription factor domain, which gave an indication that *um05518* could be a transcription factor (Figure 9). *Um11825* was chosen for deletion studies as it was one of the hints from the mass spec analysis of enriched peptide (Table 2). It was predicted to contain a homeo-box domain and therefore could act as a

putative transcription factor (Figure 9**)**. This gene belongs to *b* mating type locus cluster, Bioinformatics analysis also indicated homology in closely related fungi *Sporisorium reilianum* with unknown function.

Um10343 was studied because it was also one of the hints from the mass spec analysis in enriched peptide (Table 2). Bioinformatics analysis showed the presence of leucine-rich repeat and zinc finger domain that could be a potential transcription factor (Figure 9**)**. The *um06278* was studied because it was one of the hints found in the mass spec analysis of enriched peptide (Table 2). Bioinformatics analysis showed the presence Zn-C6 fungal-type DNA-binding domain and PAS domains. These PAS domains are involved in many signaling proteins where they are used as a signal sensor domain (Taylor and Zhulin, 1999). *Um01626* was studied because it was also one of the hints from the mass spec analysis in enriched peptide (Table 2). Bioinformatics analysis showed the presence of WD40-repeat-containing domain. WD40 motifs act as a site for protein-protein interaction, and proteins containing WD40 repeats are known to serve as platforms for the assembly of protein complexes or mediators of transient interplay among other proteins (http://www.ebi.ac.uk/interpro/entry/IPR017986) (Figure 9**)**.

Um11960 was studied because it was one of the hints found in the mass spec analysis of enriched peptide (Table 2). Bioinformatics analysis showed the presence of OHCU decarbox (2-oxo-4-hydroxy-4-carboxy-5-ureidoimidazoline decarboxylase) domain structure. It shows homology to GTPase-activating protein in *Cryptococcus gattii* (27% homology at protein level), in *A. niger* (28% homology at protein level) (Figure 9**)**. *Um12335* was selected based on phospho-proteomics approach. This gene was peptide enriched only in FB1fuz7DD strains and in FB1Δkpp2Δkpp6 fuz7DD was not present (Table 2). Um12335 is highly conserved and homologous to NudE in *A. nidulans* and Ro11 of *N. crassa*, both of which functions in the dynein/dynactin pathway and are required for the distribution of nuclei along the hyphae (Efimov, 2000; Hoffmann *et al*., 2001; Minke *et al*., 1999). The mammalian NudE homologues directly interact with Lis1 (mutation in this gene causes lissencephaly) and dynein (Morris *et al*., 1998, Feng *et al*., 2000) (Figure 9**)**.

Um05364 was studied because it was one of the hints from the mass spec analysis of enriched peptide (Table 2). Bioinformatics analysis showed the presence FF domain; these

domains are involved in protein-protein interactions (Bedford and Leder, 1999) (Figure 9**)**. Predicted function is related to formin binding protein 3. *Um04887* was chosen on basis of phosphorylation intensity ratio which was higher in FB1fuz7DD strain (Table 2). Bioinformatics analysis showed it has similarity to STE50 of *S. cerevisiae.* Ste50p is adaptor protein for various signaling pathways; involved in mating response, invasive/filamentous growth, osmotolerance; acts as an adaptor that links G protein-associated Cdc42p-Ste20p complex to the effector Ste11p to modulate signal transduction (Ramezani-Rad *et al*., 2003; Wu *et al*., 2006).

Um05337 was chosen on basis of phosphorylation intensity ratio which was higher in FB1fuz7DD strain (Table 2). Bioinformatics analysis showed it is related to SLA1 cytoskeleton assembly control protein (Figure 9**)**. *Um03437* was also chosen on basis of phosphorylation intensity ratio which was higher in FB1fuz7DD strain (Table 2). Bioinformatics analysis showed it is related to BDF1 sporulation protein (Figure 9**)**. Gene *um02618.2* was chosen on basis of phosphorylation intensity ratio which was higher in FB1fuz7DD strain (Table 2). Bioinformatics analysis showed it is a probable transcriptional coregulator of Snw1 (Folk *et al*., 2004) (Figure 9**)**. *Um03944* was chosen based phosphorylation intensity ratio (Table 2). Bioinformatics analysis showed it has pleckstrin homology (PH) domains, which bind to phosphoinositides with high affinity and specificity, (Lemmon *et al.*, 2007) (Figure 9**)**.

Figure 9: Schematic representation of potential MAP kinase substrates studied in this work. Showing conserved domain and phosphorylation site predicted in LC/MS analysis.

2.5 Functional analysis of potential MAP kinase targets

The selected genes (Table 2) were assessed for a possible contribution to mating and virulence. The eight genes were deleted in the solopathogenic strain SG200 and for six of the genes; they were also deleted in a pair of compatible haploid strains. For some of the genes *um05364, um05337, um03437, um02618.2, um00890, um04887*, it was not possible to produce deletion strains because they might be essential genes. For each of these genes minimum of 10 transformants were checked for deletion. Functional analysis of eight genes is described in detail in the following paragraphs.

2.5.1 Functional analysis of *um05518*

To find out the potential role of *um05518* in pathogenicity, mating and pheromone response the gene was deleted in the solopathogenic strain SG200 and in the compatible haploid strains FB1 and FB2 following the method of Kämper (2004). Haploid strains were tested for mating by co-spotting on a PD-charcoal plate. After 24 hours, all combinations of compatible strains developed a fuzzy phenotype, comparable to the cross of FB1XFB2 (Figure 10). This indicates that *um05518* does not influence the formation of dikaryotic filaments, and is thus not contributing to cell fusion in haploid strains. In a preliminary plant infection assay of SG200Δum05518 and SG200, no significant reduction in tumors was detected in maize plants, of the three mutants checked two behaved similar to SG200 (Figure 10). Also, in a plant infection assay using compatible haploid strains *um05518* deletion strains showed no significant reduction in tumor formation in maize plants in comparison to the cross FB1XFB2. These results indicated that *um05518* was not important for virulence and mating of *U. maydis* under the assayed conditions (Figure 10).

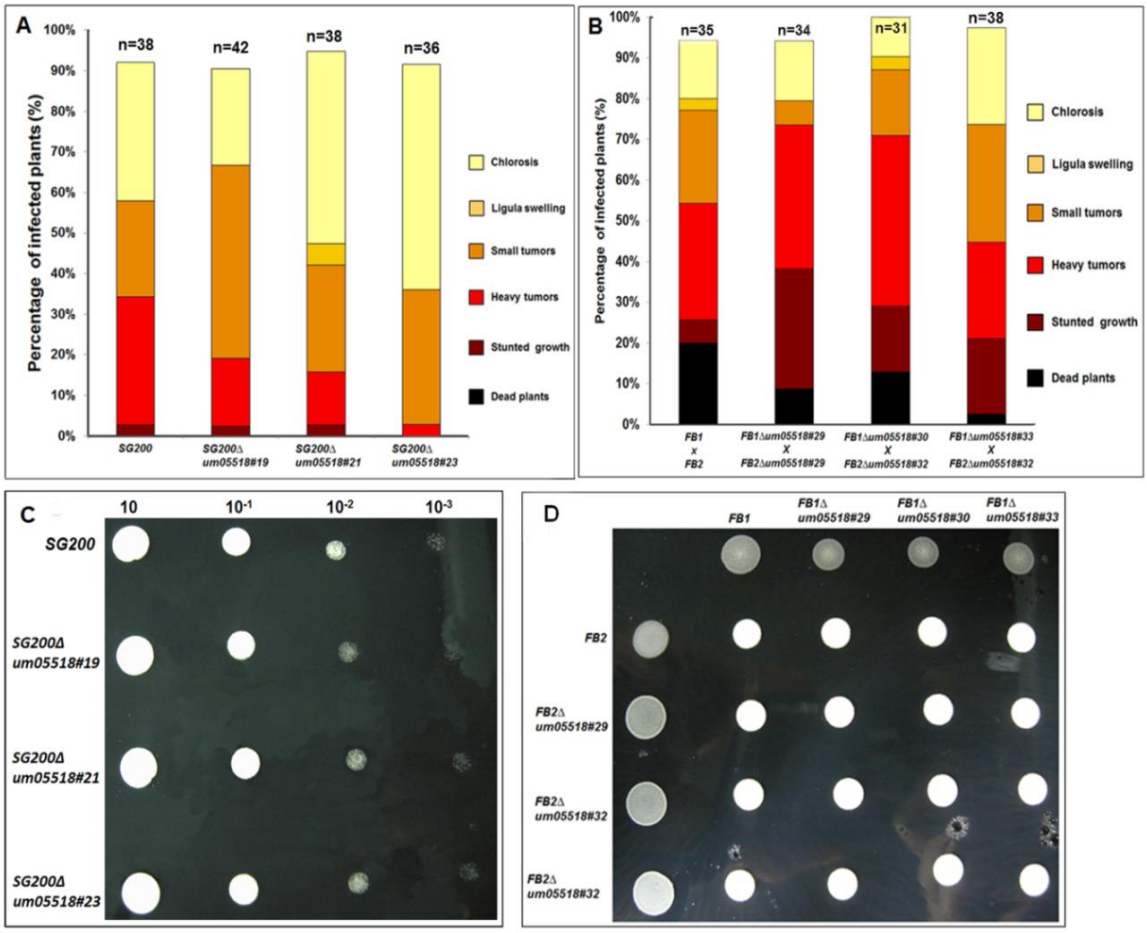

Figure 10: Influence of *um05518* on mating, filament formation and plant pathogenicity. (A) and (B) disease symptoms on maize plant caused by the indicated strains. Strains were injected into 7 day old maize seedlings and the disease symptoms were scored 12 days post infection. Disease symptoms were scored according to categories described in Kämper *et al* (2006). For each strain, the total number of infected plants is given above each column. Scoring pattern is indicated on the left side of graph. (C) The indicated strains were spotted on a PD-charcoal plate and incubated at room temperature for 24 h. Strains showed white fuzzy morphology due to the formation of filaments. (D) Mating between compatible strains. The strains indicated on top were spotted alone and in combination with the strains indicated on the left on charcoal-containing PD plates. Dikaryotic filaments display white fuzziness.

2.5.2 Functional analysis of *um11825*

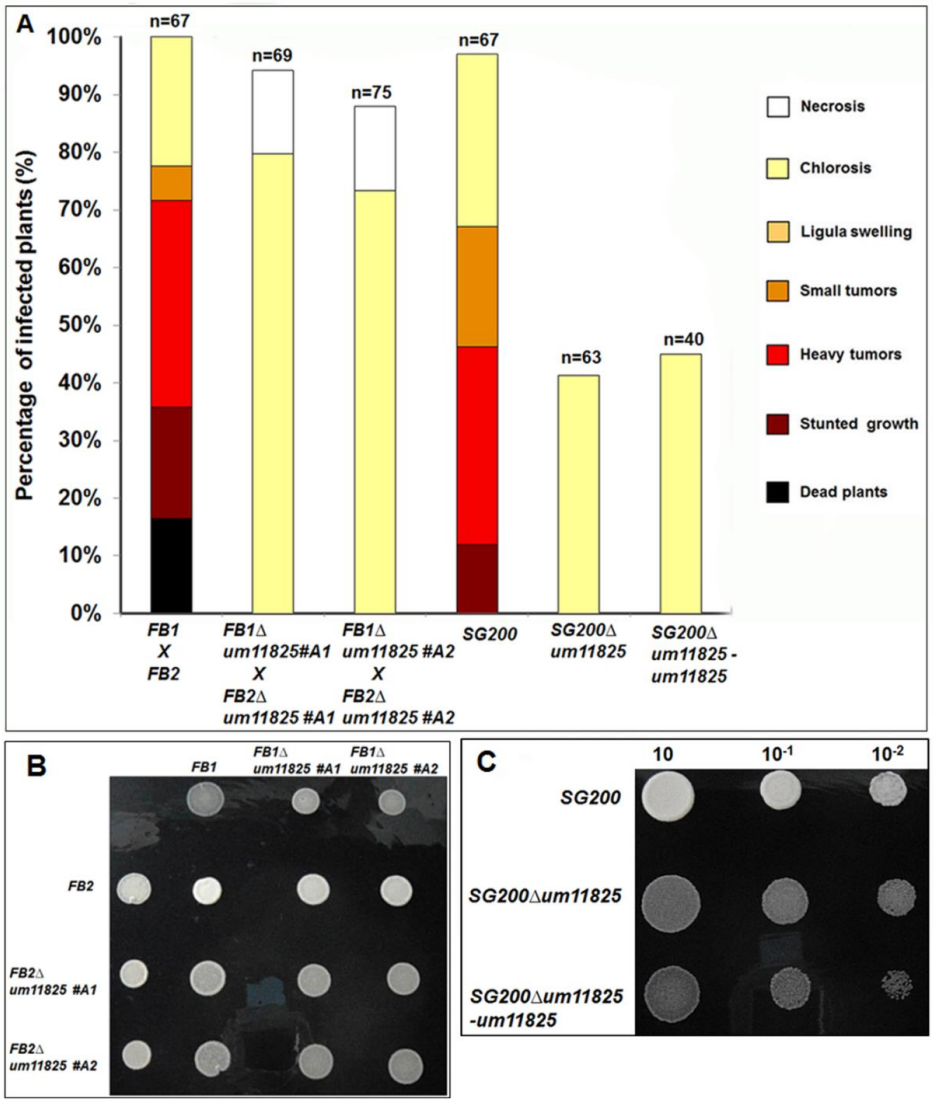

Figure 11: Pathogenicity assay of *um11825* mutant strains on maize plant showed there were no tumors. (A) Disease symptoms on maize plant caused by the indicated strains. Strains were injected into 7 day old maize seedlings and the disease symptoms were scored 12 days post infection. Disease symptoms were scored according to categories described in Kämper *et al* (2006). Two independent replicates were used for each strain. Total number of infected plants is given above each column; scoring pattern is indicated on the left side of graph. (B) Mating between compatible strains. The strains indicated on top were spotted alone and in combination with the strains indicated on the left on charcoal-containing PD plates. Dikaryotic filaments display white fuzziness. (C) Filamentation assay of solopathogenic strains. The strains indicated on top were spotted on charcoal containing PD plates, white fuzziness indicates the filament formation. Plates were incubated at room temperature for 24 h.

To find out the potential role of *um11825* in pathogenicity, mating and pheromone response the gene was deleted in the solopathogenic strain SG200 and in the compatible haploid strains FB1 and FB2 following the method of Kämper (2004). Haploid strains were tested for mating by co-spotting on PD-charcoal plate. After 24 hours, all deletion strains displayed a reduction in the dikaryon formation when compatible deletion strains were co-spotted with the strain combination (Figure 11). This shows that *um11825* is involved in mating and cell fusion. In solopathogenic deletion strain only one mutant was generated and when this single strain was spotted on charcoal plate, the deletion strain showed a strong reduction in filamentation compared to SG200, indicating that *um11825* plays a role in post fusion development. In a plant infection assay using compatible haploid strains *um11825* deletion strains showed significant reduction in tumor formation in maize plants in comparison to the cross FB1XFB2. To exclude that the reduction in tumor formation is caused by the cell fusion defect of compatible *um11825* deletion strains, plant infections were performed with the solopathogenic strain SG200 and its derivative SG200Δum11825. Upon infection with SG200Δum11825, no tumors could be observed in infected plants as compared to SG200. Complementation of SG200Δum11825 by introduction of a single copy of *um11825* ORF into the *ip* locus using one kb of promoter region was not successful (Figure 11). As there was only one SG200Δum11825 strain was tested for virulence assay, it is crucial to complement the virulence phenotype using appropriate size of promoter region.

2.5.3 Functional analysis of *um10343*

To ascertain the potential role of *um10343* in pathogenicity on maize plant and its effect on mating, the gene was deleted in both the compatible haploid strains FB1, FB2 and in the solopathogenic strain SG200 following the method of Kämper (2004). In a plant infection assay using compatible haploid strains *um10343* deletion strains showed no significant reduction in tumor formation in maize plants in comparison to the cross FB1XFB2. Moreover, in plant infections performed with the solopathogenic strain SG200 and its derivative SG200Δum10343, there was also no significant reduction in tumor formation in the deletion strains. Haploid strains were also tested for mating by co-spotting on PD-charcoal plate. After 48 h, all deletion strains displayed filament formation which was comparable to the mixture of FB1XFB2. The solopathogenic deletion strain spotted on charcoal plate showed white fuzzy

phenotype similar to SG200. These results indicated that *um10343* does not play a significant role in dikaryon formation or pathogenicity and thus appears unaffected by *um10343* in pre- and post-fusion events (Figure 12).

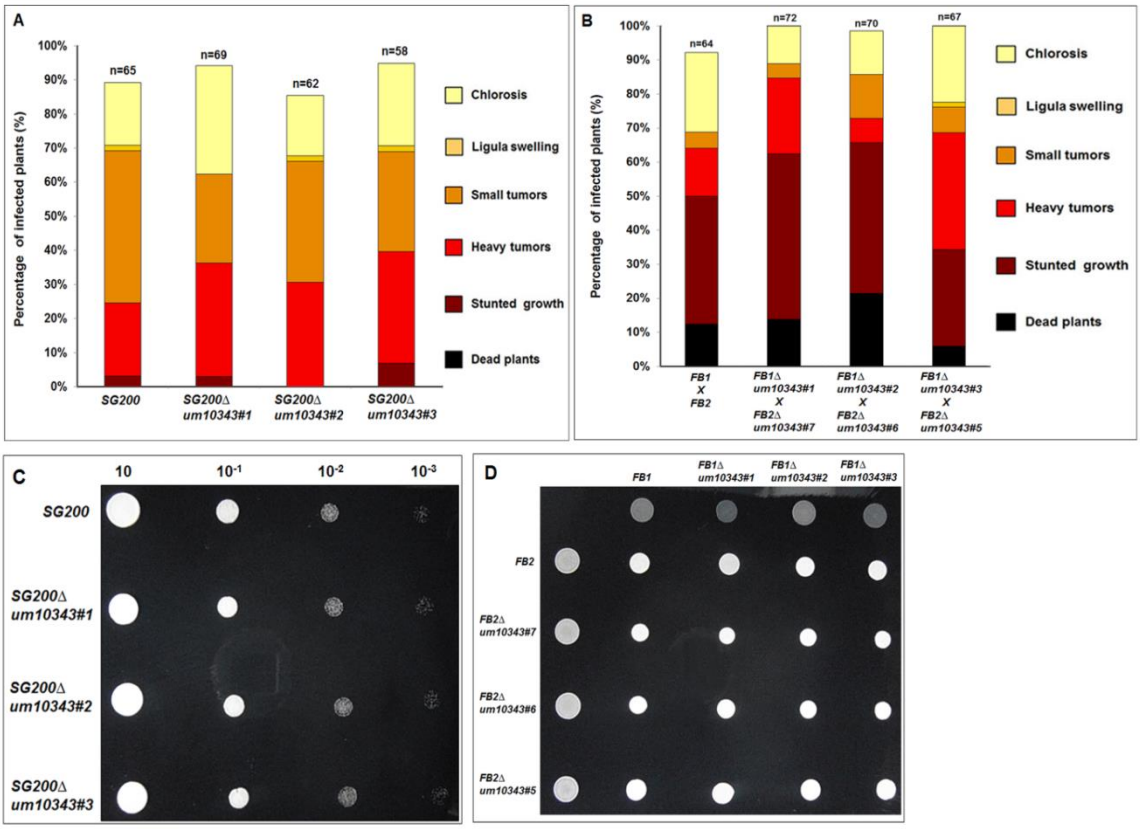

Figure 12: Influence of *um10343* on mating, filament formation and plant pathogenicity. (A) and (B) disease symptoms on maize plant caused by the indicated strains. Strains were injected into 7 day old maize seedlings and the disease symptoms were scored 12 days post infection. Disease symptoms were scored according to categories described in Kämper *et al* (2006), scoring pattern is indicated on the left side of graph. (C) Filamentation assay of solopathogenic strains. The strains indicated on left were spotted on charcoal containing PD plates, white fuzziness indicate the filament formation. (D) Mating between compatible strains. The strains indicated on top were spotted alone and in combination with the strains indicated on the left on charcoal-containing PD plates. Dikaryotic filaments display white fuzziness. Plates were incubated at room temperature for 24 or 48 h.

2.5.4 Functional analysis of *um01626*

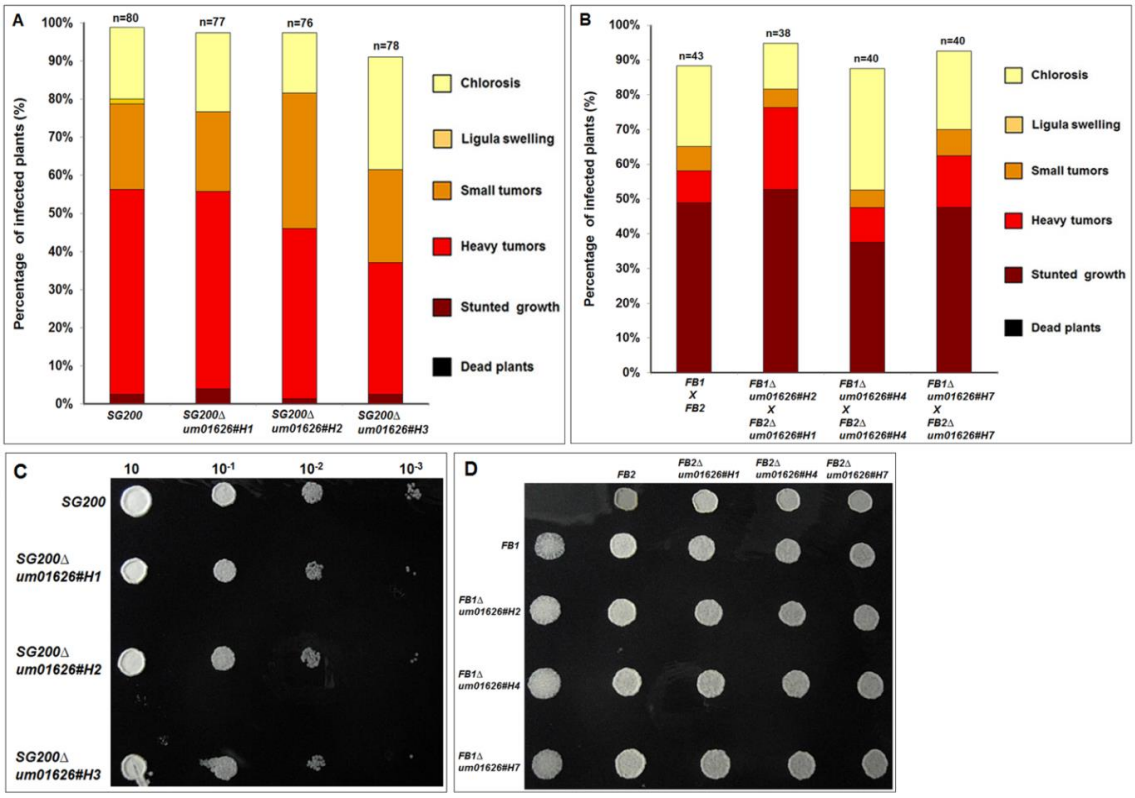

Figure 13: Influence of *um01626* on mating, filament formation and plant pathogenicity. (A) and (B) disease symptoms on maize plant caused by the indicated strains. Strains were injected into 7 day old maize seedlings and the disease symptoms were scored 12 days post infection. Disease symptoms were scored according to categories described in Kämper *et al* (2006), scoring pattern is indicated on the left side of the graph. (C) Filamentation assay of solopathogenic strains. The strains indicated on left were spotted on charcoal containing PD plates, white fuzziness indicate the filament formation. (D) Mating between compatible strains. The strains indicated on top were spotted alone and in combination with the strains indicated on the left on charcoal-containing PD plates. Dikaryotic filaments display white fuzziness. Plates were incubated at room temperature for 24 or 48 h.

To ascertain the potential role of *um01626* in pathogenicity on maize plant and its effect on mating, the gene was deleted in both the compatible haploid strains FB1, FB2 and in the solopathogenic strain SG200 following the method of Kämper (2004). In a plant infection assay with the three independent *um01626* deletion in compatible haploid strains did not show significant deviations in tumor formation in maize plants in comparison to wild type strains. Also, in plant infection assays performed with the solopathogenic strain SG200 and its

derivative SG200Δum01626, there were no significant differences detected in virulence. Haploid strains were also tested for mating by co-spotting on PD-charcoal plate. After 48 h, all deletion strains displayed a dikaryon filament formation when compatible deletion strains were co-spotted with the strain combination. When the solopathogenic deletion strain was spotted on charcoal plate, deletion strain showed white fuzzy phenotype similar to SG200. These results indicate that *um01626* does not play a significant role in filament/dikaryon formation or pathogenicity (Figure 13).

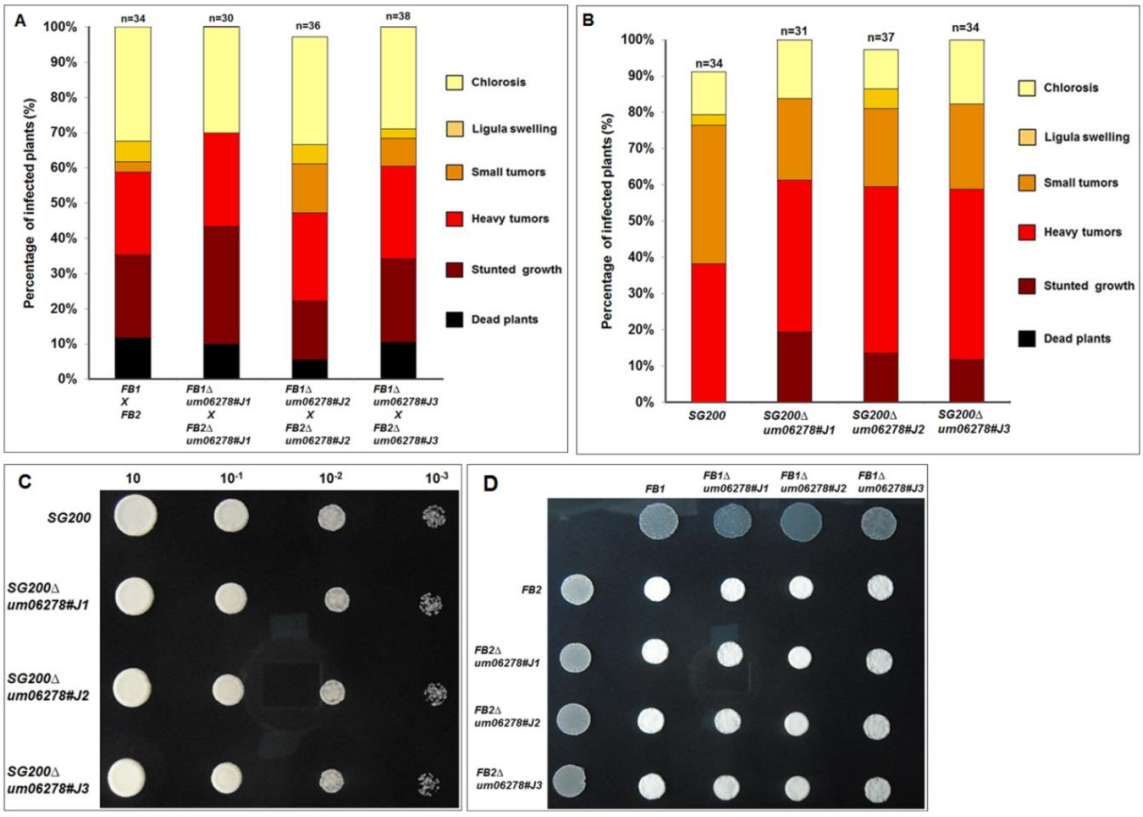

Figure 14: Influence of *um06278* on mating, filament formation and plant pathogenicity. (A) And (B) disease symptoms on maize plant caused by the strains indicated were scored after 12 days of post infection as described in Kämper *et al* (2006), scoring pattern is indicated on the left side of the graph. (C) Filamentation assay of solopathogenic strains. The strains indicated on left were spotted on charcoal containing PD plates, white fuzziness indicate the filament formation. (D) Mating between compatible strains. The strains indicated on top were spotted alone and in combination with the strains indicated on the left on charcoal-containing PD plates. Dikaryotic filaments display white fuzziness. Plates were incubated at room temperature for 24 or 48 h.

2.5.5 Functional analysis of *um06278*

To ascertain the potential role of *um06278* in pathogenicity and its effect on mating, the gene was deleted in both the compatible haploid strains FB1, FB2 and in solopathogenic strain SG200 following the method of Kämper (2004). In a plant infection assay with the three independent *um06278* deletions in haploid strains in comparison to wild type FB1XFB2 did not show significant deviations in virulence. And in plant infections performed with the solopathogenic strain SG200 and its derivative SG200Δum06278, there was no significant change in tumor formation in the deletion strain in comparison to SG200. Haploid strains were also tested for mating by co-spotting on PD-charcoal plate. After 48 h, all deletion strains displayed a dikaryon formation when compatible deletion strains were co-spotted with the strain combination. When the solopathogenic deletion strain was spotted on charcoal plate, deletion strain showed white fuzzy phenotype similar to SG200. These results indicated that *um06278* does not contribute significantly to filament/dikaryon formation or play a significant role in pathogenicity (Figure 14).

2.5.6 Functional analysis of *um11960*

To assay the effect on pathogenicity on plant I deleted *um11960* in solopathogenic strain SG200 following the method of Kämper (2004). In plant infection assay with SG200 and its three independent derivatives SG200Δum11960, there was no significant reduction in tumor formation in deletion strains. Solopathogenic haploid strain SG200 exhibits white fuzziness on charcoal-containing plates without prior cell fusion (Bolker *et al.*, 1995). On PD-charcoal plate assay SG200Δum11960 showed attenuated filament formation in comparison to the SG200, it might play role during post-fusion development. The results indicated that *um11960* does not play significant role in pathogenicity (Figure 15).

2.5.7 Functional analysis of *um05364*

To find out the potential role of *um05364* in pathogenicity on maize plant and its effect on filament formation, the gene was deleted in the solopathogenic strain SG200 following the method of Kämper (2004). In a plant infection assay with the SG200 and its three independent

derivatives SG200Δum05364, there was no significant reduction in tumor formation in deletion strains. These strains were also tested for the filament formation by spotting on the PD-charcoal plate, after 48 h, all the deletion strains showed white fuzzy phenotype indicating that there was no defect in filament formation. These results indicated that *um05364* does not play significant role in post fusion filament formation or pathogenicity (Figure 16).

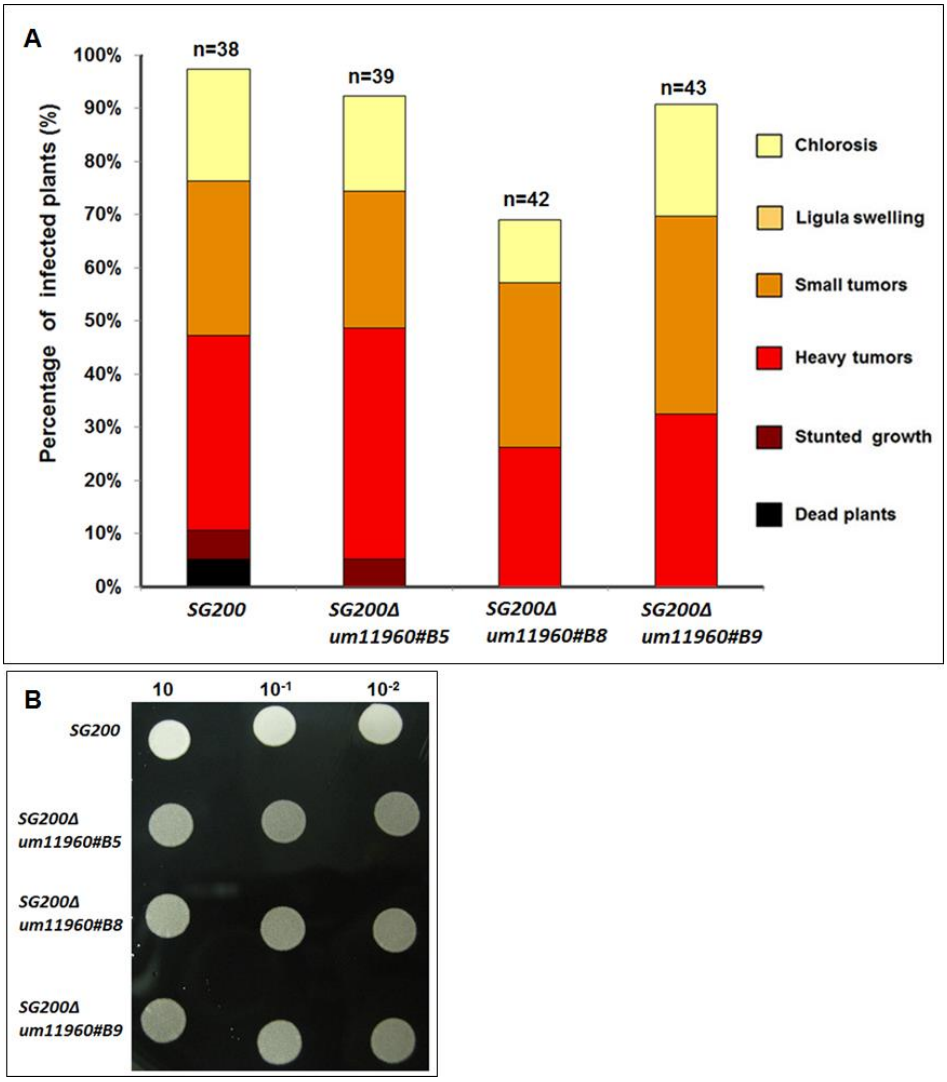

Figure 15: Pathogenicity of *um11960* mutant strains in SG200. (A) Disease symptoms on maize plant caused by the strains indicated were scored after 12 days of post infection as described in Kämper *et al* (2006), scoring pattern is indicated on the left side of the graph. (B) Solopathogenic SG200 and three independent deletion strains were spotted on PD-charcoal plates and incubated for 24hours at room temperature. Formation of filament was reflected in white fuzzy appearance of colonies.

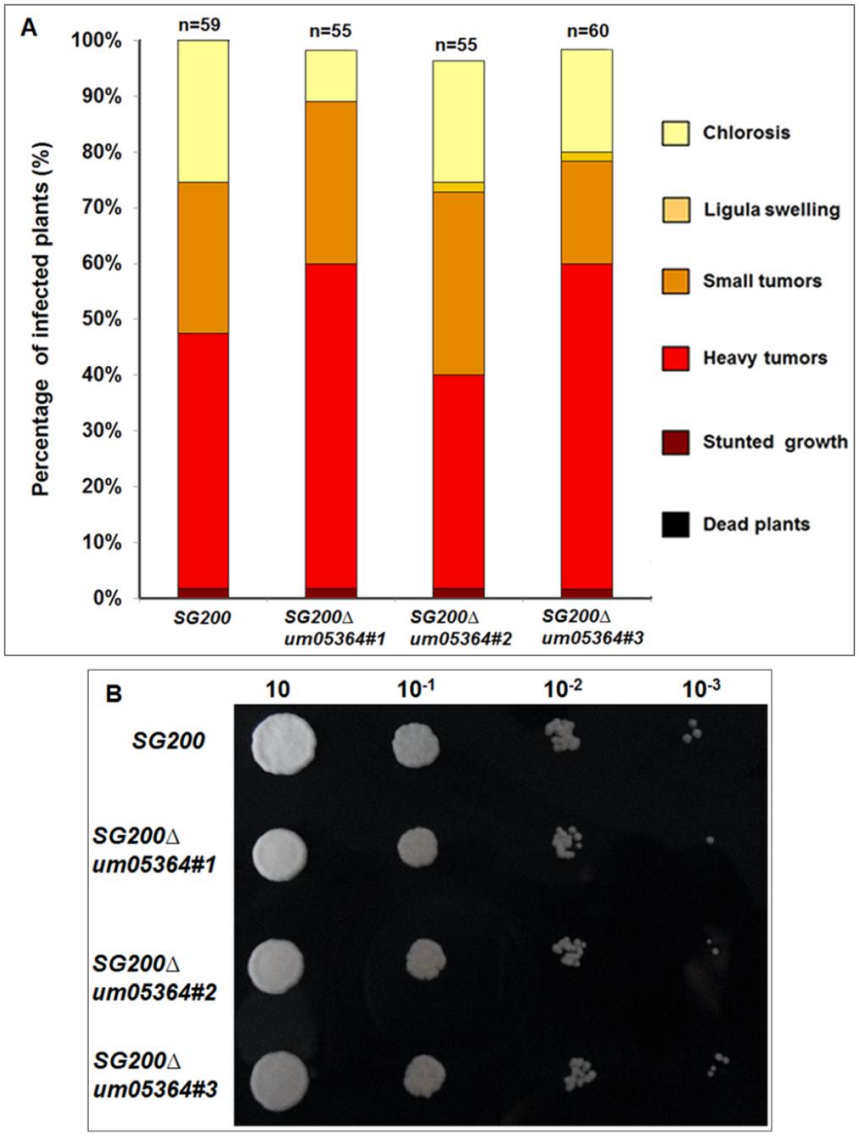

Figure 16: Pathogenicity and filamentation assay for um05364. (A) Disease symptoms on maize plant caused by the strains indicated were scored after 12 days of post infection as described in Kämper *et al* (2006), scoring pattern is indicated on the left side of the graph. (C) Filamentation assay of solopathogenic strains. The strains indicated on left were spotted on charcoal containing PD plates, white fuzziness indicate the filament formation. Plates were incubated at room temperature for 48 h.

2.5.8 Functional analysis of *um12335*

In order to study the function of *um12335* in *U. maydis,* deletion mutants were generated in the compatible strains FB1 and FB2 as well as in the haploid solopathogenic strain SG200 by replacing the entire *um12335 ORF* region with a hygromycin resistance

cassette following the method of Kämper (2004). To investigate the role of *um12335* in pathogenicity development, maize seedlings were infected with mixtures of compatible *um12335* deletion strains or with wild type strains. The plants infected by *um12335* deletion strains formed no tumors compared to the plants infected by wild type FB1XFB2 strains. To exclude that the reduction in tumor formation is caused by the cell fusion defect of compatible *um12335* deletion strains, plant infections were performed with the solopathogenic strain SG200 and its derivative SG200Δum12335. Upon infection with SG200, 84 % of plants showed tumor formation, while in SG200Δum12335 only small tumors less than 1mm could be observed on the plants (Figure 17). Introduction of single copy of *um12335*ORF into the *ip* locus of SG200Δum12335 could restore tumor formation, indicating successful complementation (Figure 17). These results clearly showed the significance of *um12335* as a pathogenic factor in *U. maydis* infection.

In mating assays on charcoal-containing plates, *um12335* deletion strains displayed no significant reduction in the dikaryon formation when compatible *um12335* deletion strains were co-spotted, however there appears to be problem in forming complete fuzziness (Figure 17), this could be due to the role of *um12335* in nuclear distribution or in microtubule stabilization (Figure 18 and 22). Solopathogenic haploid strain SG200 exhibits white fuzziness on charcoal-containing plates without prior cell fusion (Bolker *et al*., 1995). SG200Δum12335 did not show a significant reduction in filamentation compared to SG200. These findings indicate that *um12335* is not involved in cell fusion and might have relatively minor role during post-fusion development.

Um12335 is a homologue of NudE in *A. nidulans* and Ro11 protein of *N. crassa,* both are shown to be required for the distribution of nuclei along the hyphae (Efimov, 2000; Hoffmann *et al*., 2001; Minke *et al*., 1999). To check the function of *um12335* in nuclear distribution, nuclear envelope marker Nup1GFP (kindly given by Marie Tollot, from this lab) was introduced into FB1Δum12335, this allows for the visualization of nuclear movement under the microscope (Theisen *et al*., 2008). FB1Nup1GFP also has nuclear marker Nup1GFP (kindly given by Marie Tollot, from this lab).

When FB1 cells are treated with a2 pheromone they form conjugation tubes (Mendoza-Mendoza *et al*., 2009). An interesting morphological observation was found, when the FB1Δ-

um12335Nup1GFP strains, which has nuclear envelope marker Nup1GFP, were treated with synthetic a2 pheromone for 5 h. In FB1Δum12335- Nup1GFP after treatment with pheromone, about 12% cells (needs further investigation) showed polar filaments (Figure 18) compared to control strain FB1Nup1GFP. And about 10% ±1% of filamentous cells contained more than one nucleus in each cell, FB1Nup1GFP control strains always showed single nucleus in each filament (Figure 18). It is known that in *A. nidulans*, NudE impairs the distribution of nuclei along the filamentous hyphae (Efimov and Morris, 2000). Therefore, *um12335* might play a role in nuclei localization or distribution in *U. maydis*.

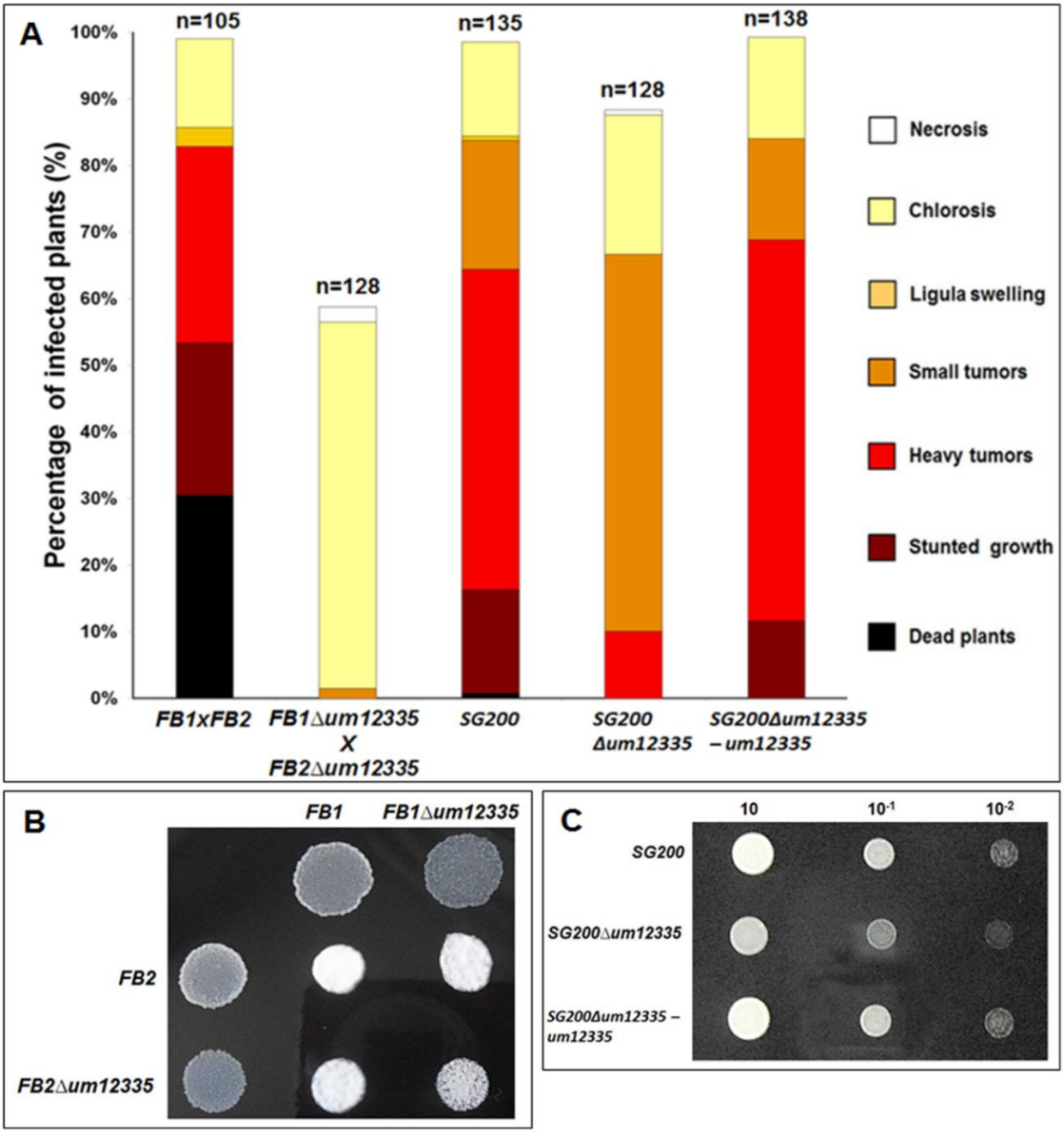

Figure 17: Deletion of *um12335* results in reduction in pathogenicity. (A) Disease symptoms caused by indicated strains were scored 12 days after infection of 7 day old maize seedlings. Based on the severity of symptoms observed on each plant, symptoms were grouped into color coded categories according to Kamper *et al* (2006), depicted on the right side. Total number of maize plants tested was given above each column. (B) Mating between compatible strains. The strains indicated on top were spotted alone and in combination with the strains indicated on the left on charcoal-containing PD plates. Dikaryotic filaments display white fuzziness. (C) Filamentation assay of solopathogenic strains. The strains indicated on the side were spotted on charcoal containing PD plates. White fuzziness indicates the formation of filaments. PD plates were incubated at room temperature for 24 h.

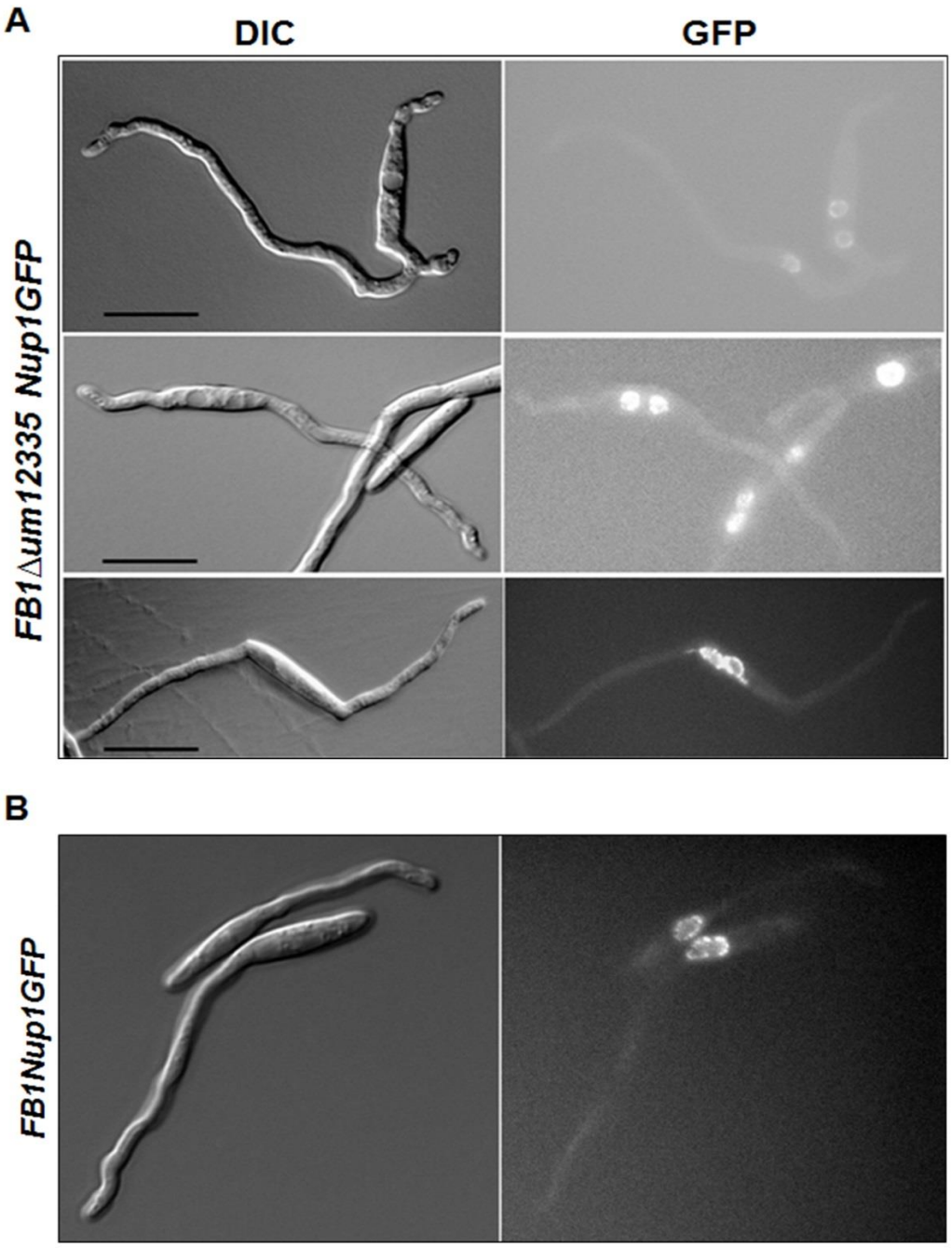

Figure 18: Analysis of nuclear distribution after pheromone treatment. (A) FB1Δum12335Nup1GFP cells showing bipolar filaments and (B) FB1Nup1GFP were treated with synthetic a2 pheromone dissolved in DMSO for 5 h. In the FB1Δum12335Nup1GFP strain about 10% ±1% filaments showed more than one nucleus. However, FB1Nup1GFP always showed one nucleus. Images were taken by DIC (left panel) and GFP channels (right panel). Nuclei are revealed through GFP fluorescence. Scale bars indicate 10 µm.

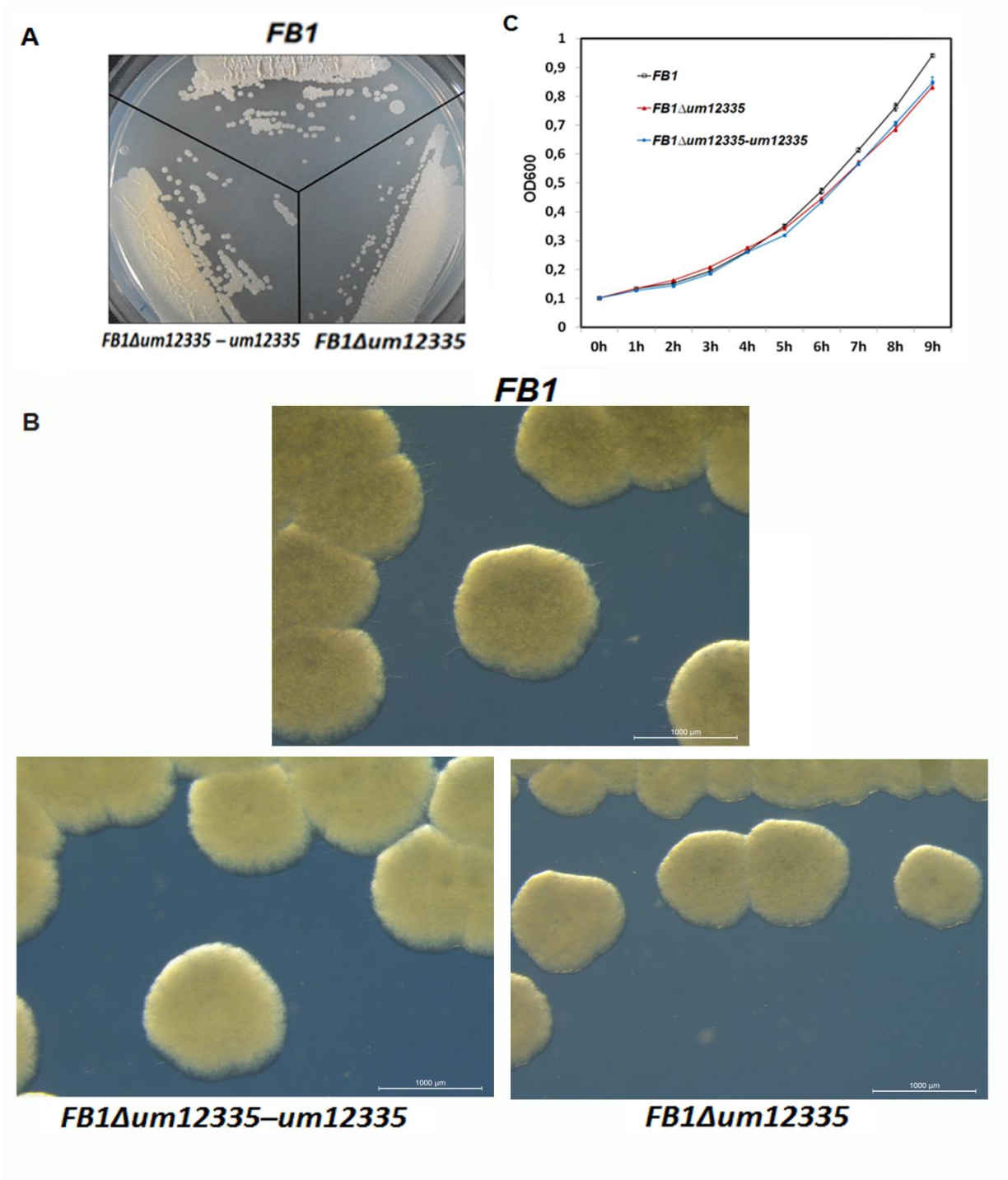

Figure 19: Effect of *um12335* deletion on growth phenotype. (A) and (C), strains streaked on CM plates and incubated at 28°C for 2 d. FB1 and FB1Δum12335–um12335 colonies show filaments radiating from colonies, while FB1Δum12335 colonies are smaller and irregular and smoother in appearance. (B) Strains grown in CM medium with 2% glucose and OD600 measured at different time points at 28°C. Error bars represent the standard deviation. Scale bar, 1 mm.

2.6 Um12335 is involved in cell growth and stress responses

In order to study the role of *um12335* in growth of *U. maydis*, FB1Δum1233 strains were grown on CM-glucose agar plates and compared with wild type FB1 cells. The colonies of FB1Δum12335 were comparatively smaller and smoother in texture than FB1 cells, which showed filaments radiating from the colonies (Figure 19). In liquid medium, the doubling time of FB1Δum12335 was 2.8±0.8 h compared to FB1 with a doubling time of 2.4 ±0.8 h (Figure 19). These data indicates that *um12335* play a role in the growth of *U. maydis.* In the strain FB1Δum12335–um12335, reintroduction of *um12335* partially complements the filamentation and the growth phenotype (Figure 19).

To find out whether *um12335* plays a role in stress environments, SG200Δum12335 was exposed to the osmotic stressors sorbitol and sodium chloride, cell wall stressing agentss calcofluor white and congo red and, to the peroxide stressor H_2O_2. Compared to SG200, SG200Δum12335 showed increased sensitivity to the cell wall stressors calcofluor white, congo red and to the saline stressor NaCl (Figure 20). These defects can be rescued by the introduction of a single copy of *um12335* ORF. Deletion of *um12335* did not affect the sensitivity towards the osmotic stressor sorbitol and oxidative stressor H_2O_2 (Figure 20). These findings suggest that *um12335* is involved in cell wall stress and saline stress response.

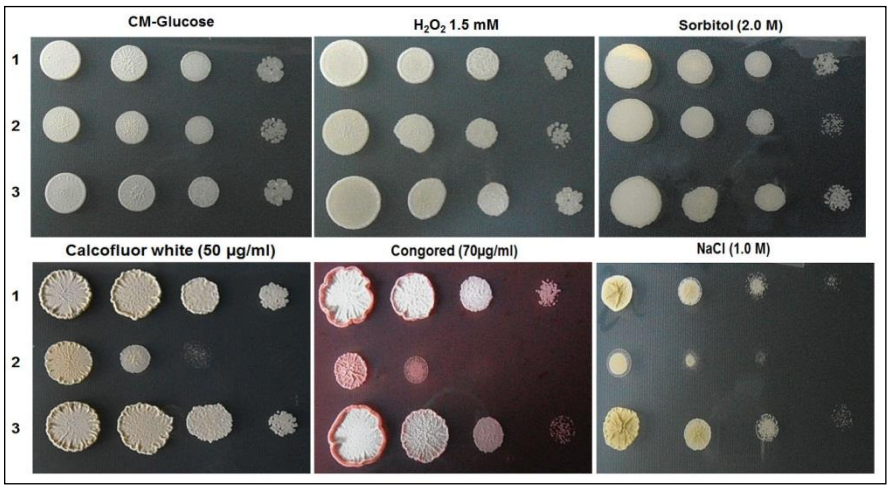

Figure 20: *um12335* is involved in cell wall stress responses and saline stress responses. Serial dilution of strains (1) SG200, (2) SG200Δum12335 and (3) SG200Δum12335-um12335 were plated on CM agar plates with different stressors, H_2O_2, sorbitol, calcofluor white, congo red and NaCl. Plates were incubated at 28°C for 2 to 3 days.

2.7 Um12335 is associated with microtubules

Based on studies in *A. nidulans* where NudE is shown to be localized to microtubules (Efimov 2003). I attempted to visualize whether Um12335 is associated with microtubules. To this end an Um12335-fusion protein was generated where mCherry is fused to the C-terminus of Um12335 and expression is driven by the native promoter. This construct was introduced in the *ip* locus of SG200Δum12335 in single copy. Introduction of *um12335-mCherry* complemented the stress related phenotypes of the deletion strain SG200Δum12335 (Figure 21). Um12335 contains a conserved NudE domain, this domain was shown to interact with cytoplasmic dynein/dynactin pathway of *A. nidulans* (Hoffmann *et al*., 2001). Visualization of the Um12335-mCherry fusion protein in SG200Δum12335-um12335mCherry strains revealed rapidly moving comet-like structures (Figure 22), similar to the structures found for NudE in *A. nidulans*, (Efimov, 2003). In order to examine whether Um12335 is associated with microtubules (MTs), cell were treated with 20 µM benomyl for 30 min. Benomyl is a fungicide that reversibly disrupts the MTs also in *U. maydis* (Straube *et al*., 2003; Fuchs *et al*., 2005). Upon benomyl treatment, comment like structures was observed, but the rapid movement was abrogated. This indicated that Um12335 is associated with MTs (Figure 22).

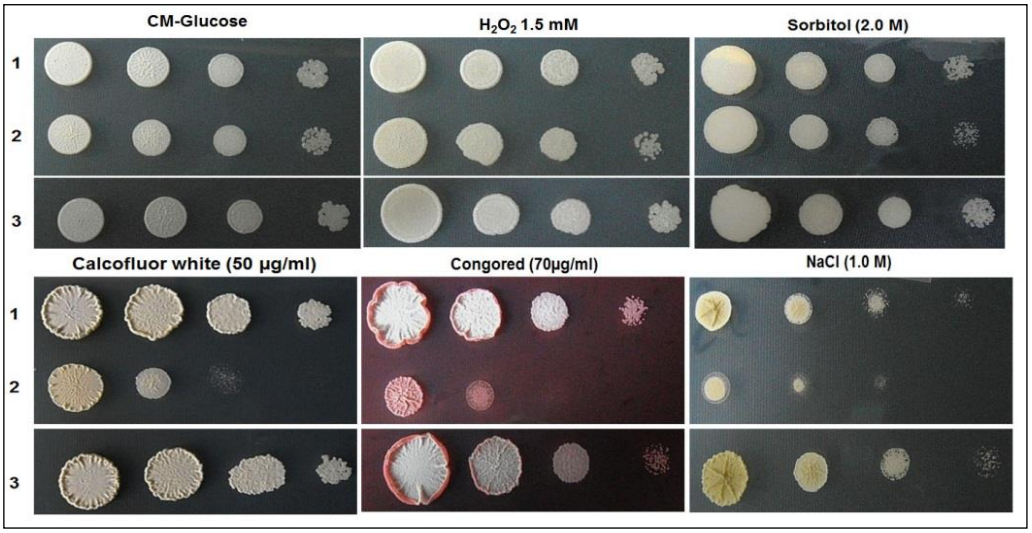

Figure 21: SG200Δum12335-um12335mCherry complements the stress associated phenotype of SG200Δum12335. Serial dilution of strains (1) SG200, (2) SG200Δum12335 and (3) SG200Δum12335-um12335mCherry were plated on CM agar plates with different stressors indicated on the top of each plate. Photos were taken after incubation for 2 to 3 days at 28°C.

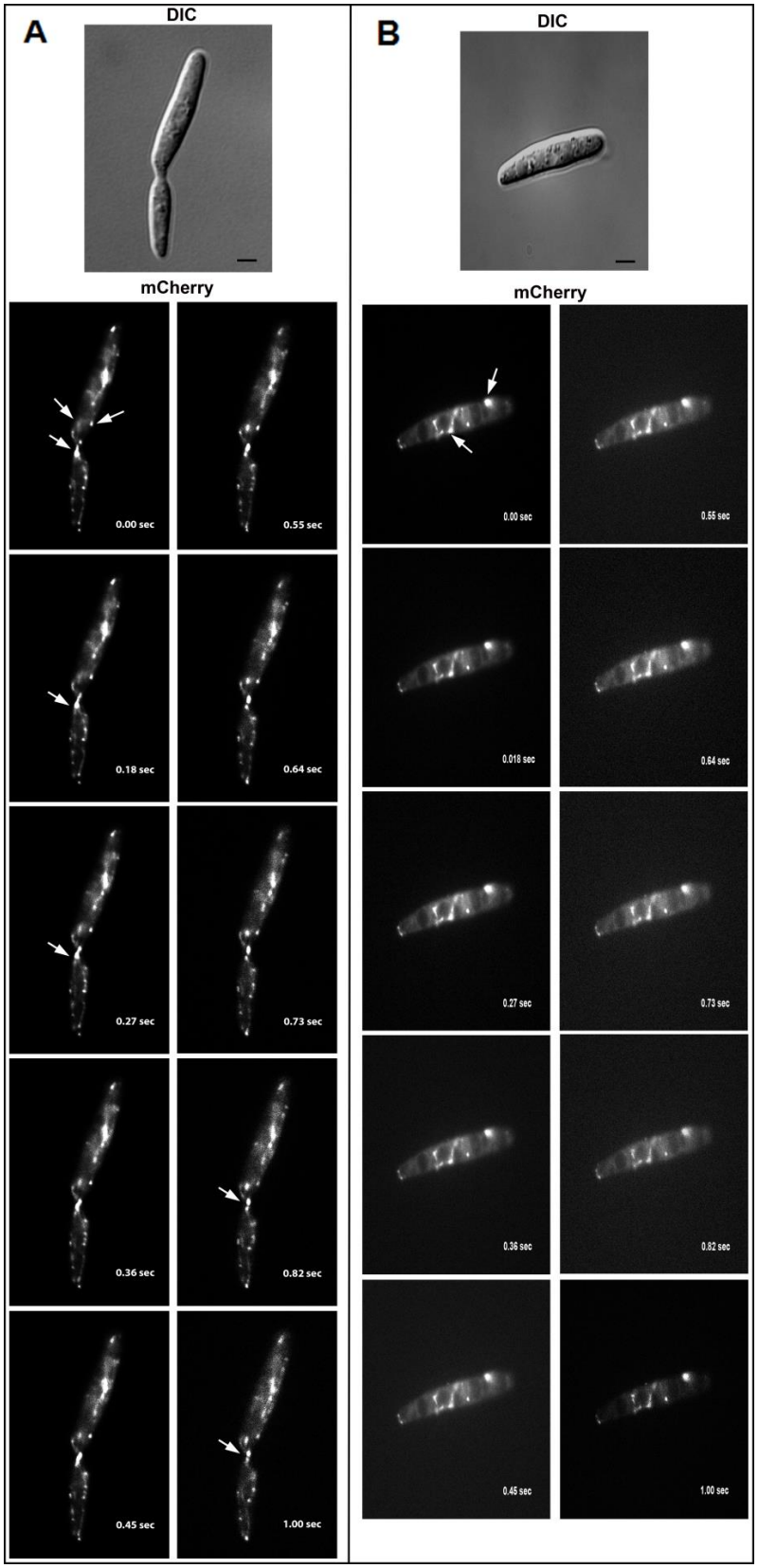

Figure 22: Localization of *um12335-mCherry* in SG200Δum12335-um12335-mCherry. (A) SG200Δum12335-um12335-mCherry was grown in YEPS light medium to an OD600 of 0.6. Arrows indicate fluorescence dots (Comets), which showed movement along the cells axis, this is observable by following fluorescence dots in successive image (B) Cells were treated with 20µM benomyl, for 20 min and checked for the localization of *um12335-mCherry*. Arrows indicate fluorescence dots (Comets), movement of these dots was abrogated.

In each case movies of 100 millisecond were made and processed using Image-J software to show 10 still images showing the movement/abrogation of fluorescence dots. Picture was taken using Texas Red filter.

2.8 Detection of phosphorylation in Um12335 on SDS-PAGE using Phos tag™

The phosphorylation detection experiment was done to investigate whether Um12335 is phosphorylated by MAP kinase Kpp2 and/or Kpp6. As the Um12335 was isolated in mass spec analysis after the induction of *fuz7DD* in FB1fuz7DD strain but it was not detected in phosphorylated form in the FB1Δkpp6Δkpp2fuz7DD induced strain (Table2). This result gave an indication that it could be a downstream target of Kpp2 and/or Kpp6 MAP kinases. In order to investigate whether Um12335 is phosphorylated after induction of the MAPK kinase Fuz7DD, I introduced the *um12335-HA* under the control of the constitutive *otef* promoter into the FB1fuz7DD and FB1Δkpp6Δkpp2fuz7DD strains. After inducing Fuz7DD for 0 to 120 min, a western-blot with and anti-HA antibody was performed. This blot revealed that Um12335-HA was expressed at all-time points (Figure 23).

To determine whether Um12335-HA is phosphorylated after the Fuz7DD induction in presence or absence of the MAP kinase Kpp2 and/or Kpp6. I induced *fuz7DD* in the Um12335-HA expressing strains for 0 to 120 min. The western blot analysis with anti-HA antibody showed that Um12335-HA was expressed in both FB1fuz7DD and FB1Δkpp6Δkpp2fuz7DD (Figure 23). In order to identify that Um12335 is indeed phosphorylated by Kpp2 and/or Kpp6, I used Phos-tag ligand which provides a phosphate affinity SDS-PAGE for mobility shift detection of phosphorylated proteins (Kinoshita *et al*., 2006). High-resolution detection of phosphorylation events can be achieved by incorporating the phosphate binding molecule (Phos-tag) into the polyacrylamide gels (Kinoshita *et al*., 2006; Kinoshita *et al*., 2012; Dunn *et al*., 2010). In the western blot analysis with anti-HA antibody, Um12335-HA showed a mobility shift in the strain possessing the MAP kinases *kpp2* and *kpp6* and the shift was most prominent in the 120 min time point. In strain FB1Δkpp6Δkpp2fuz7DD where kpp6 and kpp2 are deleted there was no mobility shift of the Um12335-HA protein detectable (Figure 23, Supplementary figure 3). Of note, the Um12335-HA bands and presumed phosphorylated forms appeared as doublets and this has also been observed for the presumed orthologue of Um12335 (NudE) in *A. nidulans* (Efimov and Morris, 2000). To demonstrate that the observed mobility shift result from phosphorylation (Peck, 2006). Comparisons of protein migration before and after phosphatase treatments were

used to demonstrate phosphorylation-dependent band shifts of Um12335-HA. Dephophorylation assay was done using the 120 min *fuz7DD* induced strains. Mobility shift of dephosphorylated Um12335-HA was abrogated in FB1fuz7DD (Figure 23). These preliminary results indicated that Um12335 could be potentially phosphorylated by either the MAP kinase Kpp2 and/or Kpp6.

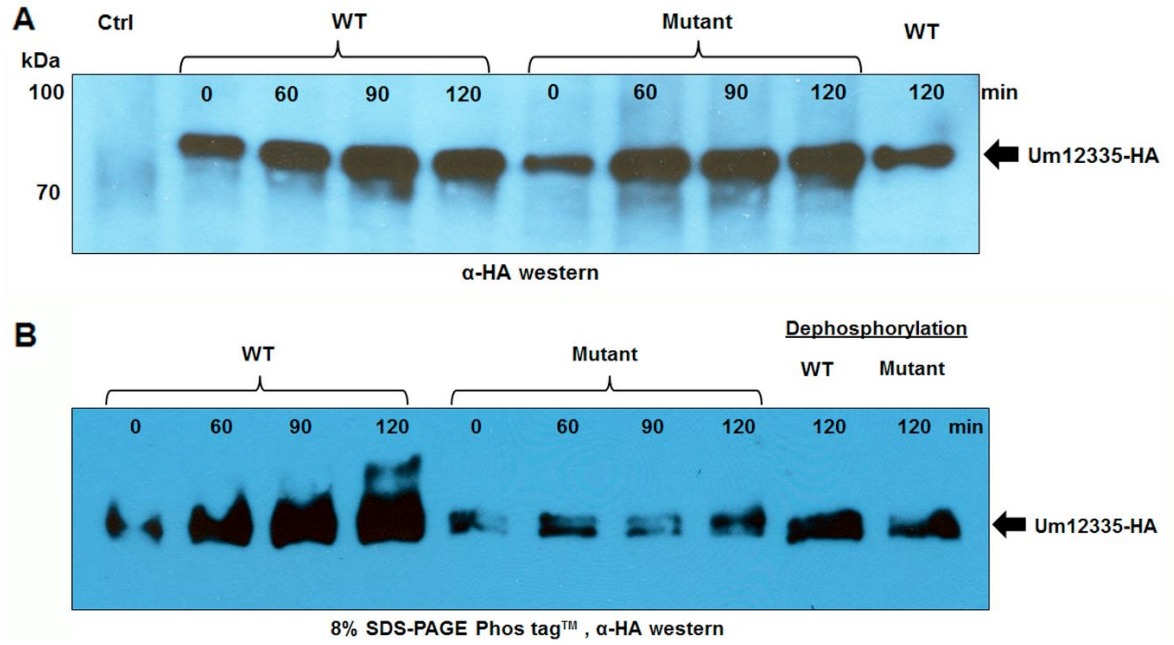

Figure 23: Phosphorylation of Um12335-HA after induction of fuz7DD. (A) Strain FB1fuz7DD (Ctrl), FB1fuz7DDPotef-um12335HA (WT) and FB1Δkpp6Δkpp2fuz7DD-Potef-um12335HA (Mutant) were induced for *fuz7dd* at the different time points indicated, western showed that Um12235-HA was induced in all the strains except in control strain (Ctrl). (B) Strains (WT) and (Mutant) were induced for *fuz7DD* at different time points indicated on the western blot, 50mM Phos-tag SDS-PAGE was used for detecting the mobility shift in Um12335HA after induction. Also dephosphorylation of 120 min induced cell extract of both strains (WT) and (Mutant) were included as control. Bands were detected using anti-HA antibodies.

3 Discussion

In this study I made a strain in which MAP kinase signaling can be induced in the presence or absence of *kpp2* and *kpp6*, by expressing a constitutively active version of the MAP kinase-kinase Fuz7 (Fuz7DD), which is under control of an inducible promoter. By using a phospho-peptide enrichment approach 111 potential MAP kinase substrates that were differentially phosphorylated in strains FB1fuz7DD and FB1Δkpp6Δkpp2fuz7DD were detected in mass spec analysis. Fifteen of these differentially phosphorylated proteins, that could possibly be targets of Kpp2 and Kpp6, were selected for further studies based on extensive bioinformatics analysis. To assess a possible contribution of the selected genes to mating and virulence, eight of the genes were deleted in a solopathogenic strain and for six of respective genes also in compatible haploid strains. Analysis of the respective deletions strains showed that, *um12335* was required for virulence. Subsequent studies suggest that Um12235 is a microtubule-associated protein that is a direct substrate of the MAP kinase Kpp2 and/or Kpp6.

3.1 Do the constructed strains, where MAP kinase signaling can be induced, mimic functionally activated situations?

In the pheromone signaling cascade, MAP kinase Kpp2 was shown to be essential for the formation of filaments and pathogenesis, while a partially redundant second MAP kinase Kpp6, is specifically required for penetration of plant cells (Brachmann *et al*., 2003; Müller *et al*., 2003b). I analyzed the FB1fuz7DD, FB1Δkpp2Δkpp6fuz7DD and FB1Δkpp6fuz7DD strains, in which the inducible allele *fuz7DD* is integrated into the *ip* locus, for the formation of filamentation. In natural conditions, pheromone stimulation leads to the formation of conjugation tubes and expression of pheromone responsive genes *mfa*, *pra1* and *b* (Müller *et al*., 2003). As expected, the strains FB1fuz7DD and FB1Δkpp6fuz7DD showed the formation of filaments, upon induction with artificial a2 pheromone. However, filamentation for FB1Δkpp2Δkpp6fuz7DD did not occur since Kpp2 is required for the filament formation (Figure 4; Müller *et al*., 2003b). It is also shown that upon expression of the constitutively

active allele of the MAPK kinase Fuz7 under control of the arabinose inducible *crg1* promoter FB1fuz7DD efficiently formed structures that morphologically resemble conjugation tubes (Müller *et al*., 2003; Di Stasio *et al*., 2009). FB1fuz7DD and FB1Δkpp6fuz7DD were able to form filaments upon induction of *crg1* promoter, while FB1Δkpp2Δkpp6fuz7DD was unable to react with the morphological response (Figure 5).This showed the suitability of these strains for the induction of MAP kinase signaling.

Analysis of the pheromone responsive gene *mfa1* revealed that all the three strains express elevated *mfa1* levels upon induction of *fuz7DD* thus, indicating that the MAP kinase cascade downstream of the MAP kinases is functionally activated (Figure 6). Nevertheless, FB1Δkpp2Δkpp6fuz7DD showed the induction of *mfa1* due to fact that expression of *mfa1* is regulated by both the cAMP pathway and pheromone signaling pathway (Hartmannet *et al*., 1996; Kaffarnik *et al*., 2003; Müller *et al*., 2003). The *mfa1* expression is dependent on the *Prf1* transcription factor. Prf1 transcription is regulated by the MAP kinase Kpp2 as well as the MAP kinase Crk1 and cAMP pathway (Hartmannet *et al*., 1996; Kaffarnik *et al*., 2003; Müller *et al*., 2003b). In *U. maydis*, the MAPK kinase Fuz7 phosphorylates both Kpp2 and Kpp6 (Müller *et al*., 2003; Di Stasio *et al*., 2009). Phosphorylation of Kpp2 in the strains constructed was analyzed by using a phospho-specific antibody. Kpp2 is phosphorylated upon induction of *crg1* promoter in both FB1fuz7DD and FB1Δkpp6fuz7DD strains at 90 min and continues until 180 min. These results demonstrate that in the *fuz7DD* integrated strains, MAP kinase signaling cascade is successfully induced which should coincide with the phosphorylation of Kpp2 and/or Kpp6 substrates/targets. Based on these evidences, in order to identify the downstream targets of MAP kinase, 90 min *fuz7DD* induced strains were considered for isolation of phospho-peptide using double metal oxide affinity chromatography.

In *U. maydis* the MAP kinases Kpp2 and Kpp6 have partially redundant functions and respective single mutants show attenuated pathogenicity and only when both genes are deleted simultaneously does one observe a complete loss of virulence (Brachmann *et al*., 2003; Müller *et al*., 2003). Kpp2 is required for mating and filamentous growth and Kpp6, which is related to Kpp2, has a partially redundant function with Kpp2 in mating and plays a specific role in appressoria function (Brachmann *et al*., 2003; Mayorga and Gold, 1999; Müller *et al*., 1999;

2003b). By isolating phospho-peptides from FB1fuz7DD and FB1Δkpp2Δkpp6fuz7DD, it was possible to isolate potential substrates/targets of Kpp2 and/or Kpp6. However, it is not possible to discriminate between the Kpp2 and Kpp6 targets using these strains.

3.2 Is phospho-peptide enrichment a suitable approach to identify MAP kinase targets in *U. maydis*?

Number of protein kinase substrates has been identified through interaction screens, most commonly yeast two- hybrid screens, with the kinase of interest as bait. By using two-hybrid screening MAP kinase 4, a substrate of MKS1 (MAP kinase substrate 1) was identified in *Arabidopsis* (Andreasson, *et al*., 2005). Far1p was isolated as a multicopy suppressor of a non-arresting *fus3* mutant and interacts with Fus3 in a two hybrid system (Elion *et al*., 1993). In an analog-sensitive kinase approach, a kinase of interest is mutated by a single amino acid substitution, allowing it to accommodate the bulky sulfur-containing ATP analog *N*6-(benzyl) ATP-γ-S (Blethrow *et al*., 2008). This approach has been used to identify substrates of CDK1/cyclin B in human cultured cells and Cdk1 substrates in budding yeast (Blethrow *et al*., 2008; Holt, *et al*., 2009). Ste12, a substrate of Fus3 was identified using in-vitro kinase assay in *S .cerevisiae* (Elion *et al*., 1993).

Proteomic approach that combines stable isotope labeling by amino acids in cell culture (SILAC) for quantitation with IMAC (immobilized metal affinity chromatography) for phosphopeptide enrichment and three stages of mass spectrometry (MS/MS/MS) was used for successful confirmation and identification of yeast pheromone signaling pathway substrates, for example Fus3 substrates Bni1p and Sst2p were isolated by this way (Gruhler *et al*., 2005). Many of the successful phosphoproteomics studies applied selective phosphoprotein and phosphopeptide enrichment techniques in combination with sensitive mass spectrometric peptide sequencing methods (Jensen, 2004). In a phosphoproteomic study of transgenic *A. thaliana* plants harboring a gene encoding a constitutively active *MEKDD* from *Nicotiana tabacum* (NtMEK2*DD*) expressed under the control of the dexamethasone (DEX)-inducible GVG promoter identified 141 putative MAPK substrates with the help of complementary enrichment of phosphoproteins and consecutive phosphopeptide enrichment (Hoehenwarter *et al*., 2013). In a similar approach, early and late putative substrates of MPK3 and MPK6 were

identified by phosphoproteomics performed on *A. thaliana* plants transformed with a constitutively-active variant of *MKK5* from *Petroselinum crispum*, expressed under the control of a DEX- inducible promoter (Lassowskat *et al*., 2014). Screening of databases for proteins with known consensus motifs for particular kinases has also been applied, for example p38-regulated/activated protein kinase (PRAK), a substrate of p38 MAP kinase, has been detected by this screening method (New *et al*., 1998). However, bioinformatics tools for the prediction of phosphorylation site still lack precise algorithms (Morandell *et al*., 2006).

Progress in tracing signaling pathways has been limited by the lack of reagents (Site-specific phosphoserine/threonine antibodies) and methods required to identify substrates of particular protein kinases. Although proteomics approaches are highly informative, they carry some serious drawbacks. Proteins expressed in artificial systems might not fold appropriately or carry the necessary posttranslational modifications (e.g. phosphorylation sites might not be primed) (Berwick and Tavaré, 2004). There are concerns about data quality and potential biases in the enrichment and identification procedures (Amoutzias *et* al., 2012). Another challenge in phosphorylation analysis by mass spectrometry is the fact that phosphorylation is generally a labile modification (Amoutzias *et* al., 2012). Finally, in vivo the subcellular compartmentalization of proteins might preclude a protein substrate from becoming effectively exposed to the kinase, even though that protein might be an excellent substrate in vitro (Berwick and Tavaré, 2004).

In *U. maydis*, transcription factor *prf1* was isolated using the conserved sequence of HMG (high mobility group) domain (Hartmann *et al*., 1996). The dual specificity phosphatase Rok1 was identified while searching for orthologues of dual specificity phosphatases in *U. maydis* genome (Di Stasio *et al*., 2009).The HMG domain proteins Rop1 (Brefort *et al*., 2005) has been identified while screening for highly conserved HMG DNA-binding domains in the *U. maydis* genome sequence, The CCAAT-box binding-protein Hap2 was initially identified as a potential interaction partner of Kpp6 in a two-hybrid screen (Mendoza-Mendoza *et al*., 2009a). Even after using these approaches, there still remain many unknown factors to be elucidated in the MAP kinase pathway of *U. maydis*. In particular, downstream targets of MAP kinase Kpp2 and Kpp6, which are significant for mating and virulence in *U. maydis.*

This highlighted our interest in applying the phospho-proteomics approach to find the potential substrates of the main MAP kinases Kpp2 and Kpp6.

By using the phospho-peptide enrichment approach on two strains harboring *kpp1* and *kpp6* and lacking both genes, respectively and restricting the analysis to early time point of MAP kinase activation, identified the potential MAP kinase substrates of *U. maydis*. The three biological replicates produced 111 potential substrates for the MAP kinases Kpp2 and/or Kpp6. Similar phosphoproteomics approach was used in identification of *A. thaliana* MAP kinase substrates (Hoehenwarter *et al*., 2013; Lassowskat *et al*., 2014). Here, both known as well as new kinase substrates were identified by using three biological experiments (Hoehenwarter *et al*., 2013; Lassowskat *et al*., 2014). In our phosphopeptide analysis there were 16 potential transcription factors, six kinase domain containing genes, four zinc finger domain containing proteins (Table 1). Also Tup1 (*um03280*), a general transcription repressor in *U. maydis* was present, which regulates the *prf1* transcription factor (Elías-Villalobos *et al*., 2011). But there were no homologues of known phosphorylation targets of *S. cerevisia* MAP kinases in isolated potential substrates.

3.3 Deletion mutants of putative MAP kinase target genes - are they affected in mating and/or virulence?

In *U. maydis*, deletion of the MAP kinase Kpp2 affects conjugation tube formation, shows a severe mating defect, inability to form appressoria and the abolishment of pathogenicity (MendozaMendoza *et al.*, 2009; Muller *et al.*, 2003b) and Kpp6 has a specific function during penetration of the plant cuticle (Brachmann *et al*., 2003). Kpp2 and Kpp6 have partially redundant functions and respective single mutants show attenuated pathogenicicty and only when both genes are deleted simultaneously does one observe a complete loss of virulence (Brachmann *et al*., 2003; Müller *et al*., 2003). Based on these previous findings, phenotypes expected from downstream targets of Kpp2 are defect in mating, inability to form approssoria and reduced virulence on maize plant. Kpp6 targets might show attenuated pathogenicity and inability to penetrate plant surface. Substrates of both Kpp2 and Kpp6 might show complete loss of pathogenicity.

In this study eight of the potential phosphorylation targets of Kpp2/Kpp6 have been deleted in solopathogenic strain. Six of these were deleted in haploid FB1 and FB2 strains and for these six mutants the mating reaction could be analyzed. In virulence assay only two genes *um12335* and *um11825* showed the expected phenotype for MAP kinase targets regarding tumor formation (Table 3).

The *um11825* was predicted to contain a homeo-box domain. Homeo-box containing proteins function as transcription factors and are found associated with chromatin (Levine *et al*., 1998). Bioinformatics analysis showed that this gene might act as sequence-specific DNA binding transcription factor. It shows homology in closely related fungi *Sporisorium reilianum* with unknown function. *Um11825* showed reduction in tumor formation and is required for mating and conjugation tube formation. *Um11825* is also required for both mating and conjugation tube formation. *Um11825* showed the expected phenotype for the MAP kinase substrates in *U. maydis* (Figure 11). However, construction of a complemention strain, by introduction of single copy of a *um11825* ORF into the *ip* locus including one kb of promoter region, was not successful. This is likely a technical problem since the promoter could be too short for complementation. As there was only one independent SG200Δum11825 strain and two independent Δum11825 strains in haploid FB1 and FB2 background were used for functional analysis, it is necessary to have complementation of *um11825* to prove that the phenotype is due to the introduced mutation.

Um12335 is predicted to be microtubule associated protein and has a role in nuclear distribution. It was possible to show that deletion of *um12335* in haploid and solopathogenic *U. maydis* strains leads to a drastic reduction in tumor formation on plants. Formation of conjugation tubes are not affected in *um12335* deleted haploid compatible strains, indicating that the *um12335* acts post fusion during pathogenic development (Figure 17). Pheromone treatment also leads to the formation of filaments in FB1Δum12335, thus *um12335* could also be regulated independently of the pheromone pathway or it could be only target of MAP kinase Kpp6 (Figure 18). *Um12335* was also involved in cell wall stress regulation and saline stress response, this might be due to the role of um12335 in stabilizing microtubules. These outcomes indicated that Um12335 might be target of MAP kinase Kpp2 and/or Kpp6.

Table 3: Potential MAP kinase substrate mutation analysis for pathogenicity.

Gene	Probable functions	Mutation Introduced	Pathogenicity
um05518	hypothetical protein	SG200, , FB1,FB2	Pathogenic
um10343	conserved hypothetical protein	SG200, FB1,FB2	Pathogenic
um01626	conserved hypothetical protein	SG200, FB1,FB2	Pathogenic
um06278	putative protein	SG200, FB1,FB2	Pathogenic
um11960	conserved hypothetical protein	SG200	Pathogenic
um05364	related to Formin binding protein 3	SG200	Pathogenic
um11825	conserved hypothetical protein	SG200, FB1,FB2	Reduced
um12335	related to nuclear distribution protein RO11 of *N. crassa*	SG200, FB1,FB2	Reduced

3.4 Is Um12335 a genuine MAP kinase target?

Using the phospho-proteomics approach a single phosphorylated peptide of Um12335 was detected only after fuz7DD induction in FB1fuz7DD and not in FB1Δkpp2Δkpp6fuz7DD (Table 2). This peptide was isolated using three biological replicates. This indicated that Um12335 might be a substrate of the MAP kinases Kpp2 and/or Kpp6.

Performing the phosphate affinity electrophoresis assay using Phos-tag SDS-PAGE on Um12335 isolated protein, I could observe a change in mobility of Um12335 only in the strain FB1fuz7DD and not in strain FB1Δkpp2Δkpp6fuz7DD where *kpp2* and *kpp6* were deleted (Figure 23). This phos-tag approach permits the simultaneous detection of phosphorylated protein and their non-phosphorylated counterpart on a SDS-PAGE system **(**Kinoshita *et al*., 2014). The reduced mobility of presumably phoshorylated Um12335 could be reversed by incubation with phosphatase, providing strong indications that the mobility shift is resulting from phosphorylation. These preliminary results indicate that Um12335 could be phosphorylated by the MAP kinase Kpp2 and/or Kpp6. But, this result should be further confirmed using other phosphorylation detection techniques for example immunoprecipitation

followed by mass spectroscopic analysis and also to check whether the potential phosphorylation sites in *um12335* are functionally important (Figure 24).

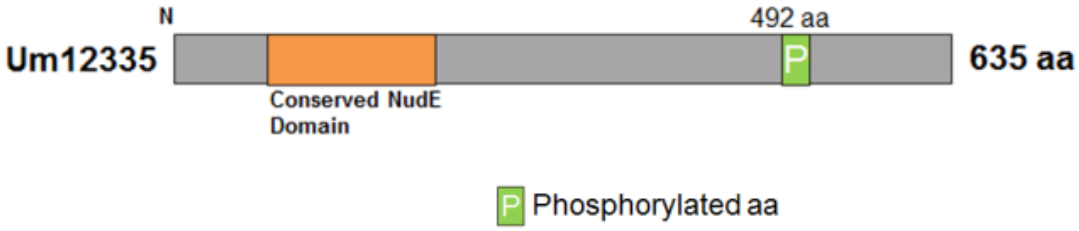

Figure 24: Domain structure of Um12335. Showing conserved domain and phosphorylation site predicted in LC/MS analysis.

3.5 Proposed model for the function of *um12335*

Bioinformatic analysis demonstrated that *um12335* is a homologue of NudE in *A. nidulans* and Ro11 protein of *N. crassa*, both with functions in the dynein/dynactin pathway and required for the distribution of nuclei along the hyphae (Efimov, 2000, 2003; Hoffmann *et al*., 2001; Minke *et al*., 1999). In *A. nidulans*, NudE interacts with the Lis1-related NudF protein (Efimov, 2000). In *U. maydis* Lis1 is essential for cell viability and is necessary for cell morphogenesis, cell wall deposition and integrity, positioning of the septum and organization of the microtubule cytoskeleton (Valinluck *et al*., 2010). In Δum12335 strains nuclei in haploid filamentous cells fail to migrate, there was no effect on the growth of the filamentous cells (Figure 18). I also observed that the virulence phenotype of *Δum12335* is much stronger when 2 haploid strains are mated compared to infections of the solopathogenic SG200Δum12335 strain, this could be because of the role of um12335 in nuclear migration. In haploid strains *um12335* deletion might interfere with the nuclear fusion post mating leading to the stronger phenotype observed for the tumor formation.

Also, the mammalian NudE homologues (Nde1 and NudeL1) directly interact with the Lis1 and dynein (Derewenda *et al*., 2007; Li *et al*., 2005; Niethammer *et al*., 2000). Lis1 is required for proper neuronal migration during brain development and mutation in this gene causes lissencephaly (Morris *et al*., 1998, Feng *et al*., 2000). Interestingly, NudeL and Nde1 are phosphorylated in M phase by Cdc2 and probably by the MAP kinase Erk1/2 (Niethammer

et al., 2000; Yan *et al*., 2003). Especially NudeL has been experimentally shown to serve as a substrate for Cdk5, Cdc2, Cdk1 and Aurora-A kinase (Mori *et al*., 2007; Niethammer *et al*., 2000; Toyo-Oka *et al*., 2005; Toyo-Oka *et al*., 2003; Yan *et al*., 2003). Aurora-A-mediated phosphorylation of NdeL1 is essential for centrosomal separation and centrosomal maturation and for mitotic entry (Mori *et al*., 2007). Phosphorylation of NdeL1 by Cdk5 facilitates interaction between NdeL1 and katanin p60 and is essential for mitotic cell division and neuronal migration (Toyo-Oka *et al*., 2005). Phosphorylation of Nudel by Cdc2 regulates the cell cycle-dependent distribution of microtubule-organizing center (Yan *et al*., 2003). MAP kinases have been shown to be spatially regulated by Nde1-Lis1-Brap complex patterns in mammalian central nervous system (Lanctot *et al*., 2013). Lis1, Nde1 and NudeL have also been implicated in many dynein mediated activities (Barbar, 2012; Vergnolle and Taylor, 2007; Yan *et al*., 2003). As *U. maydis* shows certain similarities to animal cells for many functions (Steinberg and Perez-Martin, 2008). Um12335 activity could also have similarity with mammalian NudE homologues and might function as MAP kinase substrate.

A working model is proposed based on current results (Figure 25). After phosphorylation by Kpp2 and/or Kpp6, Um12335 binds to dynein/dynactin complex. Um12335 may interact with nuclear migration protein Lis1 and this molecular complex composed of Um12335-Lis1 may controls microtubule dynamics and thus the regulated delivery of vesicles to growth sites and other cell domains that govern nuclear movements. Role of Um12335 in movement of nucleus may play major role in reduction of virulence.

Several key challenges still need to be addressed to substantiate this preliminary model. First of all, phosphorylation of Um12335 needs further confirmation using immunopreciation followed by mass spec analysis. Interaction between Um12335 and nuclear migration protein Lis1 also needs to be investigated. How Um12335 is involved in nuclear distribution, whether its role is in post mating needs to be confirmed. Finally, whether Um12335 phosphorylation is regulated by either by Kpp2 or Kpp6 or both of these MAP kinases are involved also needs to be investigated.

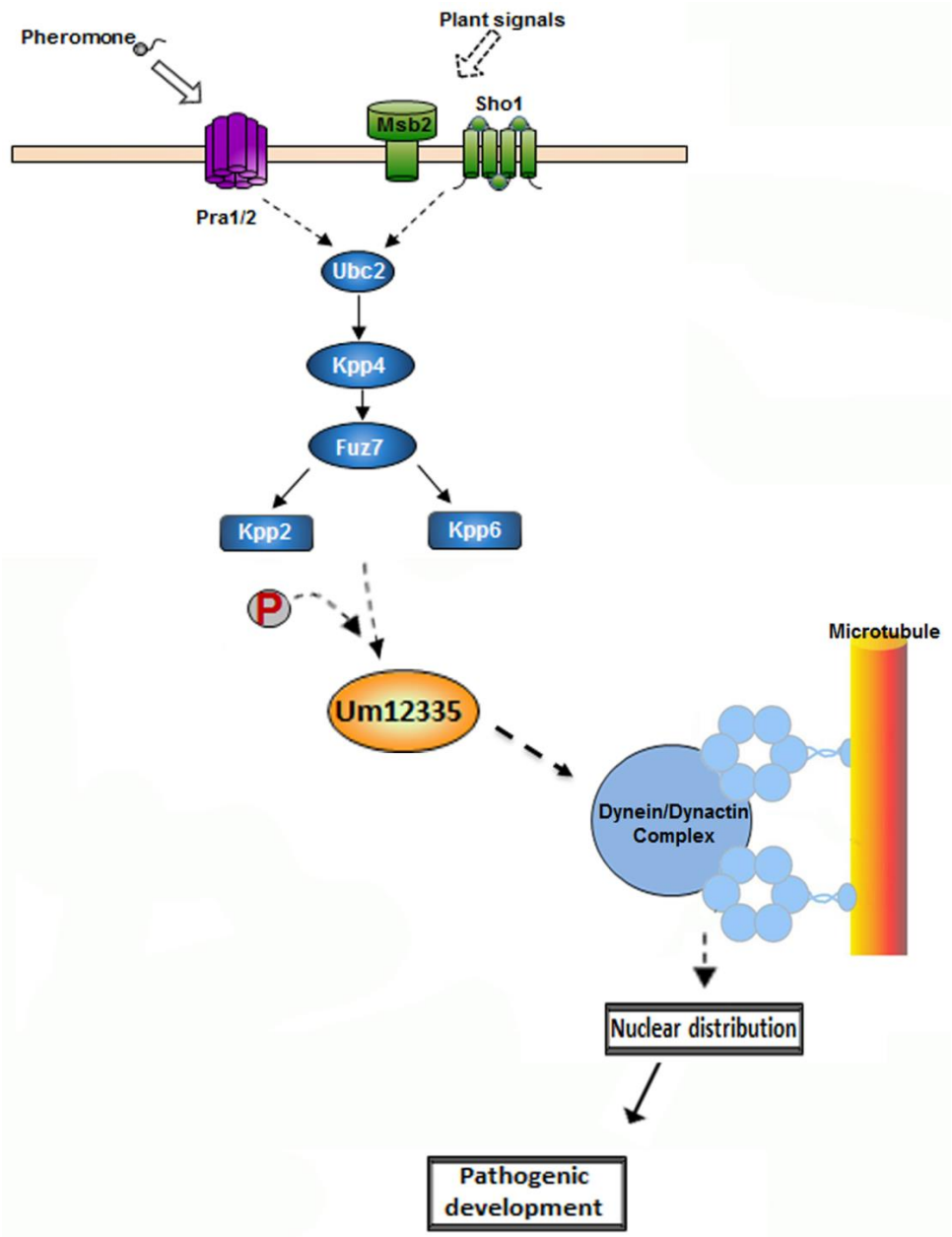

Figure 25: Proposed model for the function of Um12335. The main components of MAP kinase (green) are indicated. Um12335 is phosphorylated by MAP kinases Kpp2 and/or Kpp6 and it interacts with microtubule via Dynein/Dynactin complex. Phosphorylated Um12235 has a role in nuclear distribution. Therefor Um12335 influences pathogenic development on plant.

4 Materials and Methods

4.1 Chemicals, Enzymes, Buffers and Solutions

4.1.1 Chemicals and enzymes

All chemicals used in this study were purchased from Sigma, Fluka, Merck, Roche and Invitrogen, Difco, Life Technologies, QIAGEN, Roth, Clontech.

Restriction enzymes and Phusion™ High-Fidelity DNA Polymerase were purchased from New England Biolabs (NEB) and were used as specified by the manufacturer. T4 ligase was obtained from Roche. *Taq* DNA Polymerase was purchased from Fermentas. KOD extreme polymerase was obtained from Merck

4.1.2 Buffers and solutions

Standard buffers and solutions were prepared according to Ausubel *et al.* (1987) and Sambrook *et al*. (1989). Specific buffers and solutions are listed with the corresponding methods.

4.1.3 Kits used in this study

The following kits were used following protocols recommended by the suppliers: TA Cloning Kit (Invitrogen) for direct cloning of PCR products, Wizard SV Gel and PCR clean-up system (Promega) for DNA extraction from gels, QIAquick plasmid Purification Kit (QIAGEN) for plasmid isolation and purification, Western Blotting Detection Kit (GE Healthcare and Promega) for chemiluminescene detection.

4.2 Microbiological and cell biology methods

4.2.1 Media for *E.* coli growth

E. coli was grown in liquid dYT medium and on YT agar or LB agar plates (Ausubel *et al*., 1987; Sambrook *et al*., 1989). The media was supplemented with appropriate antibiotics (Ampicillin (Amp) - 100 µg/ml; Kanamycin (Kan) - 50 µg/ml). dYT glycerol medium was use for preparation of frozen stocks.

dYT:20 g Trypton, 10 g Yeast-Extract, 5 g NaCl, ddH_2O was added to 1 liter following autoclaving at 121°C for 5 min.

YT agar:10 g Trypton, 5 g Yeast-Extract, 5 g NaCl, 20 g Bacto Agar (Difco), ddH_2O was added to 1 liter following autoclaving at 121°C for 5 min.

dYT glycerol medium: 1.6 % (w/v) Trypton-Pepton, 1.0 % (w/v) Yeast Extract, 0.5 % (w/v) NaCl, 800 ml (v/v) 87 % Glycerol (f.c.69.6 %), Add ddH_2O and autoclave at 121°C for 5 min.

4.2.2 Media for *U. maydis* growth

YEPS light medium modified from Tsukuda *et al*., 1988: 10 g Yeast extract, 10 g Peptone, 10 g Saccharose, and ddH_2O was added to 960 ml following autoclaving at 121°C for 5 min.

CM Complete Medium (Holliday, 1974): 1.5 g NH_4NO_3, 2.5 g casamino Acids, 0.5 g DNA, 1.0 g yeast extract, 10 ml vitamin solution (see below), 62.5 ml salt solution (see below), ddH_2O was added to 980 ml and adjust pH to 7.0 with 5 M NaOH following autoclaving at 121°C for 5 min. 20 ml of 50% (w/v) glucose was added for *U. maydis* growth. For media with arabinose as sole carbon source, 40 ml of 25% arabinose solution was added to 960 ml medium after autoclaving. For solid media, agar was added to a final concentration of 2%.

Vitamin solution(Holliday, 1974): 100 mg Thiamine, 50 mg Riboflavin, 50 mg Pyridoxine, 200 mg Calcium pantothenate, 500 mg p-Amino benzo acid, 200 mg Nicotinic acid, 200 mg Choline chloride, 1000 mg myo-inositol, ddH_2O was added to 1 liter, following solution was filter sterilized.

Salt solution (Holliday, 1974): 16 g KH2PO4, 4 g Na_2SO_4, 8 g KCl, 4 g $MgSO_4X7H_2O$, 1.32 g $CaCl_2X2H_2O$, 8 ml trace elements solution (see below), ddH_2O was added to 1 liter following filter sterilization.

Trace elements solution (Holliday, 1974): 60 mg H_3BO_3, 140 mg $MnCl_2X$ $4H_2O$, 400mg $ZnCl_2$, 40 mg $NaMoO_4X$ $2H_2O$, 100 mg $FeCl_3X$ $6H_2O$, 40 mg $CuSO_4X$ $5H_2O$, ddH_2O was added to 1 liter following filter sterilization.

Potato dextrose agar with activated charcoal: 24 g Potato dextrose broth, 10 g charcoal, 20 g Bacto Agar, ddH_2O was added to 1 liter following autoclaving at 121°C for 5 min.

Regeneration agar (Schulz *et al*., 1990): 10 g yeast extract (Difco), 20 Bacto Pepton(Difco), 20 g sucrose, 182.2 g sorbitol, 15 g Bacto Agar, ddH_2O was added to 1 liter following autoclaving at 121°C for 5 min. For the bottom layer, 10 ml Regeneration agar was poured in a petri dish containing double concentrated antibiotics. After solidification, 10 ml of Regeneration agar medium without antibiotics was added. Antibiotics in the bottom layer were used in the following concentrations: carboxine (4 µg/ml), ClonNAT (300 µg/ml), hygromycin (400 µg/ml).

NSY-Glycerol: 8 g Bacto nutrient broth, 1 g Yeast extract, 5 g Sucrose, 800 ml of 87% glycerol, ddH_2O was added to 1 liter following autoclaving at 121°C for 5 min.

4.2.3 *Escherichia coli* strains

E. coli strains TOP10 (Invitrogen) and DH5α were used as host strains for plasmid constructions and amplifications.

4.2.4 *U. maydis* strains

Following strains were used in this study

Table 4: Strain tables showing all the strains used in this study.

Strains	Genotype	Resistance[1]	Reference
FB1	*a1b1*		Banuett and Herskowitz, 1989
FB2	*a2b2*		Banuett and Herskowitz, 1989
SG200	*a1mfa2b,E1bW2,ble*	Phleomycin	Bolker *et al.*, 1995
FB1fuz7DD	*a1b1ip^{r}[Pcrg1:fuz7DD]ip^{S}*	Cbx	Muller *et al.*, 2003b
FB1Δkpp2Δkpp6fuz7DD	*a1b1ipr[Pcrg1:fuz7DD]ipS, kpp6::hyg,kpp2::Nat*	Hyg, Nat, Cbx	Supple figure 1
FB1Δkpp6fuz7DD	*a1b1ip^{r}[Pcrg1:fuz7DD]ipS, kpp6::hyg*		Supple figure 1
SG200Δum05518	*a1mfa2b,E1bW2,ble; um05518::hyg*	Hyg	Supple figure 12
FB1Δum05518	*a1b1,um05518::hyg*	Hyg	Supple figure 12
FB2Δum05518	*a2b2,um05518::hyg*	Hyg	Supple figure 12
SG200Δum10343	*a1mfa2b,E1bW2,ble; um10343::hyg*	Hyg	Supple figure 11
FB1Δum10343	*a1b1,um10343::hyg*	Hyg	Supple figure 11
FB2Δum10343	*a2b2,um10343::hyg*	Hyg	Supple figure 11
SG200Δum01626	*a1mfa2b,E1bW2,ble; um01626::hyg*	Hyg	Supple figure 7
FB1Δum01626	*a1b1,um01626::hyg*	Hyg	Supple figure 7
FB2Δum01626	*a2b2,um01626::hyg*	Hyg	Supple figure 7
SG200Δum06278	*a1mfa2b,E1bW2,ble; um06278::hyg*	Hyg	Supple figure 6
FB1Δum06278	*a1b1,um06278::hyg*	Hyg	Supple figure 6
FB2Δum06278	*a2b2,um06278::hyg*	Hyg	Supple figure 6
SG200Δum11960	*a1mfa2b,E1bW2,ble; um11960::hyg*	Hyg	Supple figure 5
SG200Δum11825	*a1mfa2b,E1bW2,ble; um11825::hyg*	Hyg	Supple figure 13
FB1Δum11825	*a1b1,um11825::hyg*	Hyg	Supple figure 13
FB2Δum11825	*a2b2,um11825::hyg*	Hyg	Supple figure 13
SG200Δum12335	*a1mfa2b,E1bW2,ble; um12335::hyg*	Hyg	Supple figure 8
FB1Δum12335	*a1b1,um12335::hyg*	Hyg	Supple figure 8
FB2Δum12335	*a2b2,um12335::hyg*	Hyg	Supple figure 8
SG200Δum05364	*a1mfa2b,E1bW2,ble; um05364::hyg*	Hyg	Supple figure 4
FB1Δum12335P$_{um12335}$um12335	*a1b1ip^{r}[P$_{um12335}$:um12335-]ip^{S}*	Cbx, Hyg	This lab
FB1Nup1GFP	*a1b1,nup1-gfp::nat*	Nat	Marie Tollot (This lab)
FB1Δum12335:Nup1GFP	*a1b1,um12335::hyg, nup1-gfp::nat*	Hyg, Phleomycin	This lab
SG200Δum12335P$_{um12335}$	*a1mfa2bE1bW2,ble;*	Cbx,	Supple figure 10

um12335-mCherry	*um12335::hyg,ip^r [P$_{um12335}$:um12335-mCherry]ip^S*	Phleomycin	
FB1fuz7DDP$_{otef}$ um12335HA	*a1b1ip^r[Pcrg1:fuz7DD]ip^S ip^r[POtef:um12335-HA]*	Cbx, Neo	Supple figure 9
FB1Δkpp6Δkpp2fuz7DDP$_{otef}$um12335HA	*a1b1ip^r[Pcrg1:fuz7DD]ip^S ip^r[POtef:um12335-HA]*	Cbx, Neo	Supple figure 9
SG200Δum12335P$_{um12335}$um12335	*a1mfa2bE1bW2ip^r [P$_{um12335}$:um12335]ip^S*	Hyg, Cbx	This lab

[1] Hygromycin (Hyg), Nourseothricin (Nat), Carboxin (Cbx), Geneticin (Neo)

4.2.5 Competent cell preparation and transformation of *E. coli*

The chemical competent cells were prepared following the protocol of Hanahan (Hanahan, 1985). To transform the *E. coli*, an aliquot of competent cells was thawed on ice. Afterwards, 1-10 µl plasmid or ligation mixture was added, gently mixed and incubated on ice for 15-30 min. The mixture was then heat shocked at 42 °C for 1 min and immediately cooled on ice for 30 sec. For the recovery of the *E. coli* cells, 300 µl dYT medium was added and the cells were incubated at 600 rpm for 30-60 min at 37 °C. Finally, the entire *E. coli* cell suspension was plated on YT-agar containing appropriate antibiotics and incubated at 37 °C overnight.

4.2.6 Protoplast preparation and transformation of *U. maydis*

U. maydis strains were grown at 28°C in liquid medium with shaking at 200 rpm to a density of OD600 =0.5-0.6. The cell density of culture was determined using a Novosec II Photometer (Pharmacia Biotech) at an optical density of 600 nm (OD600). The corresponding culture medium was used as a reference. A culture density of OD600 ~1.0 corresponds to about 1-5 X10^7 cells ml^{-1}. Glycerol stocks were prepared from exponentially growing cultures, mixed with NSY-Glycerol at a 1:1 ratio and stored at -80°C. To grow strains from glycerol stocks, cells were streaked onto agar plates and incubated at 28°C.

Transformation of *U. maydis*

Transformation of *U. maydis* was performed as described previously (Schulz *et al*., 1990). In brief, *U. maydis* cells were grown in YEPS light medium at 28°C to an OD600 =0.5-0.8. 50 ml cultures were harvested by centrifugation for 5 min at 3,500 rpm, washed with 25 ml of SCS (20 mM sodium citrate, 1 M sorbitol, pH 5.8) and centrifuged again for 5 min at

3,500 rpm. The cells were resuspended in 2 ml filter sterilized SCS containing 2.5 mg ml^{-1} Novozyme. Cells were incubated for 5-10 min at room temperature for the digestion of cell wall. This process was checked under the microscope until about 50% of the cells started to protoplast. 20 ml of SCS was added following centrifugation at 2,300 rpm for 10 min. Cells were carefully resuspended in 20 ml of SCS, centrifuged at 2,300 rpm for 10 min. Cells were carefully resuspended in 10 ml of SCS, centrifuged at 2,300 rpm for 10 min. Afterwards, cells were carefully resuspended in 20 ml of STC (10 mM Tris-HCl, 100 mM CaCl2, 1 M sorbitol), centrifuged at 2,400 rpm for 10 min. Finally, the protoplast pellet was resuspended in 0.5 ml ice cold STC and aliquots of 70 µl were used immediately or stored at -80°C. For transformation of protoplasts, 5 µg linearized DNA (in a volume of 1-10 µl) and 1 µl heparin (15 mg ml^{-1}) were added to the protoplasts and incubated on ice for 10 min. Subsequently, 500 µl of STC/40% PEG was added and incubated for 15 min on ice. In the end, the transformation mixture was plated on Regeneration agar and incubated at 28°C for 4-7 days. Transformants appeared after 4-7 days were singled out and grown on PD-agar plates containing no antibiotics. Single colonies were picked and correct transformants were determined by southern blotting.

4.2.7 Mating, pheromone stimulation and pathogenicity assays

For mating assays, compatible strains were grown in YEPS light medium to an OD600 of 0.8 and adjusted to an OD600 of 1.0. After mixing in 1:1 (v/v) and 8 µl of culture was spotted on charcoal-containing PD plate (Holliday, 1974). The plate was sealed with Parafilm and incubated at room temperature for 24 to 48 h.

For pheromone stimulation, strains were grown in CM medium with 2% glucose to an OD600 of 0.6. Synthetic a2 pheromone (Bachem AG Weil am Rhein, Germany) was dissolved in dimethyl sulfoxide (DMSO) and added to a final concentration of 2.5 gml^{-1}. Cells were incubated at 28°C with shaking. After 5 h incubation, quantification of conjugation tubes was performed with photomicrographs by manual counting. After harvesting, RNA was prepared for Northern blotting analysis.

4.2.8 Induction of the *crg1* promoter

The *crg1* promoter is a carbon-regulated promoter, which can be repressed by glucose and induced by arabinose (Bottin *et al.*, 1996). Cells were incubated in CM medium with 2% glucose to an OD600 of 0.5 at 28°C and collected by centrifugation at 3,500 rpm for 5 min at room temperature. The supernatant was discarded; the cells were washed twice with ddH_2O and resuspended in CM medium with 2% glucose or with 2% arabinose. Cultures were incubated at 28°C with shaking at 200 rpm for 5 h. Cells were subjected to microscopy or collected for RNA preparation. For the isolation of proteins, cells were isolated at different time point after addition of 2% arabinose and washed with ddH_2O and snap freezing was done using liquid nitrogen before proceeding to protein isolation.

4.2.9 Pathogenicity assays

Plant infections of the corn variety Early Golden Bantam (Olds Seeds, Madison, Wis.) were performed as described previously (Muller *et al*., 1999). Strains were grown in YEPS light medium to an OD600 of 0.8, washed twice with ddH_2O and resuspended in ddH_2O to a final OD600 of 1.0. This suspension was used to inoculate seven-day-old maize seedlings. Compatible haploid strains were mixed (1:1) prior to infection. Twelve days after infection, disease symptoms were scored according to the disease rating criteria reported by Kämper *et al.* (2006). Experiments were repeated three times and each replicate involved at least 30 to 40 infected plants.

4.2.10 Staining and microscopy

For the microscopy Zeiss Axioplan II microscope with differential interference contrast optics was used. For DIC (differential interference contrast) and Fluorescene microscopy 40-, 63-, 100-mangification Plan- Apochromat Objective (Zeiss) with 1.4 numerical aperture was used. GFP fluorescence was detected with a specific filter set for GFP (ET470/40BP, ET495LP and ET525/50BP). Fluorescence of mCherry and calcofluor white was observed using Texas Red filter (HC562/40BP, HC593LP, HC624/40BP). Image processing was done using, Adobe Photoshop and Image J.

4.2.11 Benomyl treatment for microtubule de-polymerization

Benomyl-induced depolymerization was monitored by treating the logarithmically growing *U. maydis* cells with 20 µM benomyl. Prepare 500µl of CM-glucose grown cells in 2 ml tubes. Add benomyl (Sigma Chemie, Taufkirchen, Germany) to get the final concentration of 20 µM. Incubate in vertical rotator on 15 rotation per minute at room temperature for 20 min. Depolymerization of MTs was immediately observed in the microscope. Observation was done either by directly or on a 2% agar with 10 or 20 µM benomyl cushion that was generated by flattening 100 µl of hot agar solution between two microscope slides. DMSO was used as control.

4.3 Molecular biological methods

Standard molecular biology methods are performed following protocols as described by Ausubel and Sambrook (Ausubel *et al.*, 1987, Sambrook *et al.*, 1989).

4.3.1 Plasmids used in this study

pBS-hhn (Kamper *et al*., 2004) This plasmid contains the hygromycin phosphotransferase gene (*hph*) fused to the *hsp70* promoter and *tnos* terminator. The cassette is flanked by two incompatible SfiI sites upstream of the hsp70promoter and downstream of of the nos terminator.

p123 (Aichinger *et al.*, 2003). It is a plasmid containing the carboxin resistance gene and an eGFP gene which is fused to the *otef* promoter and *nos* terminator**.**

pJet1 (Lanver, 2011). This plasmid is derivative of pJet1 (Fermentas, St. Leon-Rot). This linearized pJet1 plasmid is used for cloning of blunt end DNA fragments. Re-circularization of pJet1 and its transformation into the *E. coli* leads to the production of lethal restriction enzymes (Eco47IR). The derivative used in this work contains 0.6 kb sequence in the ORF of *eco47IR,* which protects the lethality of this gene and therefore, can be used for the propagation in *E. coli.* The Cloning of desired DNA fragment was done using the EcoRV blunt end restriction enzyme site.

p123crg1fuz7DD (Müller *et al*., 2003b). This plasmid is derivative of p123. It contains constitutively active *fuz7DD* allele under the control of *crg1* promoter. This plasmid can be linearized with Ssp1 and integrated into the *ip*- locus of *U. maydis*.

p123 Neo is derivative of p123 plasmid. It has an additional resistance *neo* gene, which confers resistance to G418 (Geneticin). This plasmid can be linearized with Ssp1 can be used to integrate into the *ip*- locus of *U. maydis*.

Table 5: Plasmids used in this study

No	Plasmid	gene
1	p123crg1fuz7DD	*fuz7*
2	pum11825hyg	*um11825*
3	pum11960hyg	*um11960*
4	pum05518hyg	*um05518*
5	pum10343hyg	*um10343*
6	pum01626hyg	*um01626*
7	pum06278hyg	*um06278*
8	pum05364hyg	*um05364*
9	pum05337hyg	*um05337*
10	pum12335hyg	*um12335*
11	p123-native-um12335	*um12335*
12	p123 native-um11825	*um11825*
13	p123-um12335-mCherryHA	*um12335*
14	p123Neo-Otef-um12335HA	*um12335*

pum11825hyg is plasmid used for the deletion of gene *um11825*. Two approximately 1 kb fragments flanking the 3'- and 5'- side of the gene were amplified using the genomic DNA from FB1 as template with the primer pairs um11825LB1 (CAGAAG GAGACCGAGGTGAAATC) and um11825LB2 (GTATGGCCATCTAGGCCGCTCGTCTG CATACATGATCTC) for left border and um11825RB3 (CTATGGCCTGAGTGGCCCAAG TCGATCGGTTGACAAGTG) and um11825RB4(TGCTGCTGCTGCTGCTGTTGTTG) for

the right border. The PCR fragments were digested with SfiI and ligated to the hygromycin resistance cassette isolated as a 1.9 kb SfiI fragment from plasmid pBS-hhn (Kamper *et al*., 2004). The ligation product was cloned into pJet1 (Lanver, 2011) back bone plasmid by blunt end ligation. From this plasmid deletion cassette was amplified using primers um11825LB1 and um11825RB4.

pum11960hyg is a plasmid used for the deletion of gene um11960. Two approximately 1 kb fragments flanking the 3'- and 5'- side of the gene were amplified using the genomic DNA from FB1 as template with the primer pairs um11960LB-1 CTGATTGGCGAGCGAGCATTCGG and um11960LB-2 GTATGGCCATCTAGGCCTTC GTACGGCGCCTGCTCAATG for left border and um11960RB-3 (CTATGGCCTGAGTG GCCTCGCTTATCGGTCGCAGGATAG) and um11960RB-4 (GACGGATCTTCGAGGCT TCTTTC) for the right border. The PCR fragments were digested with SfiI and ligated to the hygromycin resistance cassette isolated as a 1.9 kb SfiI fragment from plasmid pBS-hhn (Kamper *et al*., 2004). The ligation product was cloned into pJet1 (Lanver, 2011) back bone plasmid by blunt end ligation. From this plasmid deletion cassette was amplified using primers um11960LB-1 and um11960RB-4.

pum05518hyg is a plasmid used for the deletion of gene *um05518*. Two approximately 1 kb fragments flanking the 3'- and 5'- side of the gene were amplified using the genomic DNA from FB1 as template with the primer pairs um05518LB-1 (CGTGTAGCGTCTCAGGTCTTAG) and um05518LB-2 (GTATGGCCATCTAGGCC GCTCAAGAAATAGTGGCTGTAG) for left border and um05518RB-3 (CTAT GGCCTG AGTGGCCATCCAATTGTATAGCCGACACC) and um05518RB-4 (ATCGAACACTG CTACAGCAATG) for right border. The PCR fragments were digested with SfiI and ligated to the hygromycin resistance cassette isolated as a 1.9 kb SfiI fragment from plasmid pBS-hhn (Kamper *et al*., 2004). The ligation product was cloned into pJet1 (Lanver, 2011) back bone plasmid by blunt end ligation. From this plasmid deletion cassette was amplified using primers um05518LB-1 and um05518RB-4.

pum10343hyg is a plasmid used for the deletion of gene *um10343*. Two approximately 1 kb fragments flanking the 3'- and 5'- side of the gene were amplified using the genomic DNA from FB1 as template with the primer pairs um10343 LB-1 (CATCCGGTG

CAACTCGACATTC) and um10343LB-2 (GTAT GGCCATCTAGGCCGCACCACGAACA GAGATCAAG) for left border and um10343RB-3 (CTATGGCCTGAGTGGCCTGGTGA GACGGAGTGTAGAAG) and um10343RB-4 (TATCGATCTCAACGGT AGAGAC) for right border. The PCR fragments were digested with SfiI and ligated to the hygromycin resistance cassette isolated as a 1.9 kb SfiI fragment from plasmid pBS-hhn (Kamper *et al*., 2004). The ligation product was cloned into pJet1 (Lanver, 2011) back bone plasmid by blunt end ligation. From this plasmid deletion cassette was amplified using primers um10343LB-1 and um10343RB-4.

pum01626hyg is a plasmid used for the deletion of gene *um01626*. Two approximately 1 kb fragments flanking the 3'- and 5'- side of the gene were amplified using the genomic DNA from FB1 as template with the primer pairs um01626LB-1 (AGGTGGCAA GTCGAGTGAAAC) and um01626LB-2 (GTATGGCCATCTAGGCCAATCTTGGCTTC GCCCTTCTC) for left border and um01626RB-3 CTATGGCCTGAGTGGCCGAGTGC AGAGCGCGTGTTAAG and um01626RB-4 (CCTCTGGTCTACCCTCAAGTC) for right border. The PCR fragments were digested with SfiI and ligated to the hygromycin resistance cassette isolated as a 1.9 kb SfiI fragment from plasmid pBS-hhn (Kamper *et al*., 2004). The ligation product was cloned into pJet1 (Lanver, 2011) back bone plasmid by blunt end ligation. From this plasmid deletion cassette was amplified using primers um01626LB-1 and um01626RB-4.

pum06278hyg is a plasmid used for the deletion of gene *um06278*. Two approximately 1 kb fragments flanking the 3'- and 5'- side of the gene were amplified using the genomic DNA from FB1 as template with the primer pairs um06278LB-1 (GGAACGAAT CATCGTGAAGTC) and um06278LB-2 (GTATGGCCATCTAGGCCTGCTGATCGCATC GCTCTTCC) for left border and um06278RB-3 (CTATGGCCTGAGTGGCCATCGATTC AAGGCCACAGATG) and um06278RB-4 (TGTGGTGAGTCGTCAGTTTAG) for right border. The PCR fragments were digested with SfiI and ligated to the hygromycin resistance cassette isolated as a 1.9 kb SfiI fragment from plasmid pBS-hhn (Kamper *et al*., 2004). The ligation product was cloned into pJet1 (Lanver, 2011) back bone plasmid by blunt end ligation. From this plasmid deletion cassette was amplified using primers um06278LB-1 and um06278RB-4.

pum05364hyg is a plasmid used for the deletion of gene *um05364*. Two approximately 1 kb fragments flanking the 3'- and 5'- side of the gene were amplified using the genomic DNA from FB1 as template with the primer pairs um05364LB-1(CAAACAATC CCGTAGCTTTGG) and um05364LB-2 (GTATGGCCATCTAGGCCGCCAAAGTACCGA CTGAACTG) for left border and um05364RB-3 (CTATGGCCTGAGTGGCCGGCGAAGT GTAATCATGACTC) and um05364RB-4 (TATGGAAGAGCTCACTGAAGTC) for right border. The PCR fragments were digested with SfiI and ligated to the hygromycin resistance cassette isolated as a 1.9 kb SfiI fragment from plasmid pBS-hhn (Kamper *et al*., 2004). The ligation product was cloned into pJet1 (Lanver, 2011) back bone plasmid by blunt end ligation. From this plasmid deletion cassette was amplified using primers um05364LB-1 and um05364RB-4.

pum05337hyg is a plasmid used for the deletion of gene *um05337*. Two approximately 1 kb fragments flanking the 3'- and 5'- side of the gene were amplified using the genomic DNA from FB1 as template with the primer pairs um05337LB-1 (GAAATTATTTCCCGCTTCCTCC) and um05337LB-2 (GTATGGCCATCTAGGCCTTC GTCCTCCTTGCTAGACTG) for left border and um05337RB-3 (CTATGGCCTGAGTGG CCAGCATTGGTGGATGGTTGTTG) and um05337RB-4 (CGTGATTCGACTTTCCACTT AC) for right border. The PCR fragments were digested with SfiI and ligated to the hygromycin resistance cassette isolated as a 1.9 kb SfiI fragment from plasmid pBS-hhn (Kamper *et al*., 2004). The ligation product was cloned into pJet1 (Lanver, 2011) back bone plasmid by blunt end ligation. From this plasmid deletion cassette was amplified using primers um05337LB-1 and um05337RB-4.

pum12335hyg is a plasmid used for the deletion of gene *um12335*. Two approximately 1 kb fragments flanking the 3'- and 5'- side of the gene were amplified using the genomic DNA from FB1 as template with the primer pairs um12335LB-1 (CCTGTGA TTCCGATCTTGTTC) and um12335LB-2 (GTATGGCCATCTAGGCCCCTTCTAGGCCA TGAACATC) for left border and um12335RB-3 (CTATGGCCTGAGTGGCCATGATCGAA GTGCGACAGAAG) and um12335RB-4 (GAATCGAGCTCAACATGGAAG) for right border. The PCR fragments were digested with SfiI and ligated to the hygromycin resistance cassette isolated as a 1.9 kb SfiI fragment from plasmid pBS-hhn (Kamper *et al*., 2004). The

ligation product was cloned into pJet1 (Lanver, 2011) back bone plasmid by blunt end ligation. From this plasmid deletion cassette was amplified using primers um12335LB-1 and um12335RB-4.

p123-native-um12335 is a plasmid derived from the p123. This plasmid contains full length *um12335* gene with its promoter region. The 3.2 kb fragment was amplified using the genomic DNA from FB1 as template with the primer pair's um12335CM-1 (CCAGGTACCG AATCGAGCTCAACATGGAAG) and um12335CM-2 (GACTGCGGCCGCCCCGTCTCGG GATATCAATAC). The PCR fragments were digested with Acc65I and Not1 and ligated into Acc65I/Not1 double digest p123 plasmid. This plasmid is used for complementation of *um12335* deletion strains.

p123 native-um11825 is a plasmid derived from the p123. This plasmid contains full length *um11825* gene with 1 kb of promoter region. The 3.1 kb fragment was amplified using the genomic DNA from FB1 as template with the primer pair's um11825CM-1 (GACTGCG GCCGCATGAGACCGAGATCATGTATGC) and um11825CM-2 (CCAGGTACCTGCTGC TGCTGCTGCTGTTGTTG). The PCR fragments were digested with Acc65I and Not1 and ligated into Acc65I/Not1 double digest p123 plasmid. This plasmid was used for complementation of *um11825* deletion strains, which was un-successful.

p123-um12335-mCherryHA is a plasmid derived from the pPotef:msb2-mCherry ((Lanver, 2011). This plasmid contains full length *um12335* gene with its promoter region fused to C-terminal *m-Cherry-ha*. The 3.1 kb fragment was amplified using the genomic DNA from FB1 as template with the primer pair's um12335Mchery-2 (TCAT GGATCCGAAGGT TTCGGTCTCGGACCC) and um12335Mchery-1 (TCCAGGTACCGCGTCTCAAGGATG AGCTTC). The PCR fragments were digested with Acc65I and BamH1 and ligated into Acc65I/BamH1 double digest pPotef:msb2-mCherry plasmid. This plasmid was used to analyze the subcellular localization of *um12335.*

p123Neo-Otef-um12335HA is plasmid derived from p123Neo. This plasmid contains full length *um12335* gene with C-terminal *ha*-Epitope. The 2 kb fragment was amplified using the genomic DNA from FB1 as template with the primer pairs um12335HACter-1 (ACGGGA TCCATGAGCGAACATGGTGCCGACC) and um12335HACter-2 (AGTGCGGCCGC

CTAGCCCGAGGCATAGTCGGGGACGTCGTAGGGATAGCCGCCGAAGGTTTCGGTC TCGGACCC). The PCR fragments were digested with NotI and BamH1 and ligated into Not1/BamH1 double digest p123Neo plasmid. This plasmid was used to analyze the phosphorylation of Um12335.

4.3.2 Oligonucleotides

All oligonucleotides used in this study were ordered from Eurofins MWG Operon (Table 4)

Table 6: Oligonucleotides used in this study

Primer	Sequence (5'- 3')[1]	Cleavage site
um11825LB-1	CAGAAGGAGACCGAGGTGAAATC	
um11825LB-2	GTAT GGCCATCTAGGCCGCTCGTCTGCATACATGATCTC	SfiI
um11825RB-3	CTAT GGCCTGAGTGGCCCAAGTCGATCGGTTGACAAGTG	SfiI
um11825RB-4	TGCTGCTGCTGCTGCTGTTGTTG	
um11825ORF-1	CGTCTCTGAAAGCCGCCTTAACC	
um11825ORF-2	TTACCCGGATCGACGACTATAC	
um11825LB-5	TGACGTCCGAGCTGCTCAAATC	
um11825RB-6	TTACACTTGCGGCTGGGTCTC	
um11825CM-1	GACTGCGGCCGCATGAGACCGAGATCATGTATGC	Not1
um11825CM-2	CCA GGTACCTGCTGCTGCTGCTGTTGTTG	Acc65I
um11960LB-1	CTGATTGGCGAGCGAGCATTCGG	
um11960LB-2	GTAT GGCCATCTAGGCCTTCGTACGGCGCCTGCTCAATG	SfiI
um11960RB-3	CTAT GGCCTGAGTGGCCTCGCTTATCGGTCGCAGGATAG	SfiI
um11960RB-4	GACGGATCTTCGAGGCTTCTTTC	
um11960 ORF-1	CCACATCGCCGAGCTCTTCTAC	
um11960 ORF-2	CACAGGAGTTGCGAGATAAGGAG	
um11960LB-5	GCTCGACGTGCGGTAAGAATC	
um11960RB-6	AAACACGCAAGCTGCTTCTTC	
um05518 LB-1	CGTGTAGCGTCTCAGGTCTTAG	
um05518 LB-2	GTAT GGCCATCTAGGCCGCTCAAGAAATAGTGGCTGTAG	SfiI
um05518 RB-3	CTAT GGCCTGAGTGGCCATCCAATTGTATAGCCGACACC	SfiI
um05518 RB-4	ATCGAACACTGCTACAGCAATG	
um05518 CF-F	GCCTTGCCTTGCTTTGCCATTC	
um05518 ORF-1	GCTTCATACCCACTCATCAAC	
um05518 ORF-2	GAGGAGCGTTGTTCGTAATCG	
um10343 LB-1	CATCCGGTGCAACTCGACATTC	
um10343 LB-2	GTAT GGCCATCTAGGCCGCACCACGAACAGAGATCAAG	SfiI

um10343 RB-3	CTAT GGCCTGAGTGGCCTGGTGAGACGGAGTGTAGAAG	SfiI
um10343 RB-4	TATCGATCTCAACGGTAGAGAC	
um10343 CF-F	CAGCGTGCGAAGAGATTTCTG	
um10343 ORF-1	CTCCTCCTCACCCACCAAATC	
um10343 ORF-2	AAAGCTGTGAGGCCATTCTTG	
um01626LB-1	AGGTGGCAAGTCGAGTGAAAC	
um01626LB-2	GTAT GGCCATCTAGGCCAATCTTGGCTTCGCCCTTCTC	SfiI
um01626RB-3	CTAT GGCCTGAGTGGCCGAGTGCAGAGCGCGTGTTAAG	SfiI
um01626RB-4	CCTCTGGTCTACCCTCAAGTC	
um01626ORF-1	GGTTGCTGGTGTCAAACAAAG	
um01626ORF-2	ATTCTCGAGTCCACGCTCAAC	
um06278LB-1	GGAACGAATCATCGTGAAGTC	
um06278LB-2	GTATGGCCATCTAGGCCTGCTGATCGCATCGCTCTTCC	SfiI
um06278RB-3	CTAT GGCCTGAGTGGCCATCGATTCAAGGCCACAGATG	SfiI
um06278RB-4	TGTGGTGAGTCGTCAGTTTAG	
um06278ORF1	GTTGCGTGGTCGATCTGAAAG	
um06278ORF-2	ACCATCTTTGTGCAGGAAGAC	
um06278CF-F	TTGCCATGCTCTTGAGAAGTG	
um06278LB-ST	CCCACGACAATGACAATGACG	
um05364LB-1	CAAACAATCCCGTAGCTTTGG	
um05364LB-2	GTAT GGCCATCTAGGCCGCCAAAGTACCGACTGAACTG	SfiI
um05364RB-3	CTAT GGCCTGAGTGGCCGGCGAAGTGTAATCATGACTC	SfiI
um05364RB-4	TATGGAAGAGCTCACTGAAGTC	
um05364ORF-1	TGCTGTCGGTGTTTGAAGAG	
um05364ORF-2	TCGTGCATTTTCTGCTTGAC	
um05364CF-F	TTTACAGGTGGCATTCCAAC	
um12335LB-1	CCTGTGATTCCGATCTTGTTC	
um12335LB-2	GTATGGCCATCTAGGCCCCTTCTAGGCCATGAACATC	SfiI
um12335RB-3	CTATGGCCTGAGTGGCCATGATCGAAGTGCGACAGAAG	SfiI
um12335RB-4	GAATCGAGCTCAACATGGAAG	
um12335ORF-1	GCGTCTCAAGGATGAGCTTC	
um12335ORF-2	CATTGGCAGACAAGTTGGTG	
um12335OCF-F	CTTTGGACGCAATCAGAAAGC	
um12335CM-1	CCA GGTACCGAATCGAGCTCAACATGGAAG	Acc65I
um12335CM-2	GACTGCGGCCGCCCCGTCTCGGGATATCAATAC	Not1
um12335Mchery-2	TCAT GGATCCGAAGGTTTCGGTCTCGGACCC	BamH1
um12335Mchery-1	TCCA GGTACCGCGTCTCAAGGATGAGCTTC	Acc65I
um12335HACter-1	ACGGGATCCATGAGCGAACATGGTGCCGACC	BamH1
um12335HACter-2	AGT GCGGCCGCCTAGCCCGAGGCATAGTCGGGGACGTCGTA GGGATAGCCGCCGAAGGTTTCGGTCTCGGACCC	Not1

[1] Sequences are in 5' to 3' directions.

4.3.3 Isolation of nucleic acids

The concentration of isolated nucleic acids was determined by photometry (NanoDrop ND-1000 Spectrophotometer)

4.3.3.1 Isolation of *E. coli* plasmid DNA

The boiling preparation of *E. coli* plasmid was based on the protocol of Sambrook *et al*. (1989). The plasmid DNA purification was also performed using QIAprep spin miniprep kit (QIAGEN) following the manufacturer's instructions. DNA fragment was purified using Wizard® SVGel and PCR Clean-Up System (Promega) following the manufacturer' instructions

4.3.3.2 Isolation of genomic DNA from *U. maydis*

The preparation of genomic DNA from *U. maydis* was followed by the protocol of (Hoffman and Winston, 1987).

4.3.4 DNA blotting and hybridization (Southern analysis)

10 µl of genomic DNA was digested overnight with respective restriction enzymes (NdeI/BamHI for cbx locus) in 20 µl volume. Digestions were separated on a 1× TAE 0.8 % agarose gel for about 4 hours at 90 V. The gels were soaked in 0.25 M HCl solution with shaking for 20-30 min until bromothymol blue turns yellow. HCl solution was then replaced by 0.4 M NaOH and incubated for 20-30 min with shaking until the color turns blue again. Subsequently, DNA was transferred from the gel to nylon membrane in 0.4 M NaOH for 2 hours (change the tissue every 30 min). The membrane was UV cross-linked at 1200 µJoules (100×) (UV Stratalinker 1800, Stratagene). Dig-labeling probe was generated as described in the PCR DIG Labeling Mix protocol (Roche, Mannhein). The hybridization, wash and exposure steps were performed following the protocol of (Sambrook et al., 1989).

Southern blot analysis for all the strains generated in this study is shown in supplementary figures.

4.3.5 *U. maydis* total RNA isolation from axenic culture

RNA preparation with Trizol reagent

This procedure was performed as described by the manufacturer (Invitrogen). In brief, 50 ml of *U. maydis* culture with an OD600 ~0.5-1.0 was harvested by centrifugation at 3,500

rpm for 5 min. The pellet was resuspended in 1 ml Trizol reagent and transferred to a 2 ml centrifuge tube containing 100 mg of glass beads followed by homogenization on a Vibrax-VXR shaker (IKA) with shaking at 1,200 rpm. Afterwards, samples were incubated for 5 min at room temperature, 200 µl of chloroform was added, mixed for 15 sec and incubated for an additional 2-3 min. Samples were centrifuged at 4°C for 15 min at 11,500 rpm. The upper aqueous phase (500 µl) was transferred to a 1.5 ml RNase free centrifuge tube. RNA was precipitated by the addition of 500 µl isopropanol and incubated for 10 min at room temperature. After centrifugation at 4°C for 10 min at 11,500 rpm, the pellet was washed once with 1 ml of 70% ethanol and air dried. The RNA pellet was dissolved in 50 µl RNase-free water.

4.3.6 RNA blotting and hybridization (northern analysis)

5-15 µg of RNA sample was transferred to a 1.5 ml eppendorf tube and the volume of RNA was adjusted to 4.8 µl with DEPC-H_2O. 1.6 µl of 10X MOPS, 1.6 µl of 8 M glyoxal and 8 µl DMSO were individually added followed by incubation at 55°C for 15 min. 4 µl of 5X RNA loading buffer was added to the mixture of RNA sample followed by loading onto 1X MOPS gel. The gel was run at 80 V for 2 h in 1X MOPS buffer. The orientation of the gel in the chamber and the polarity of the chamber were inverted every 30 min. The gel was soaked in 20X SSC buffer for 15 min with gentle shaking. Afterwards, RNA was transferred from the gel to a nitrocellulose membrane with 20X SSC buffer overnight. The hybridization, wash and exposure steps were followed by the protocol of Sambrook *et al*. (1989).

Probes of Northern hybridization were prepared using a PCR DIG-labeling kit (Roche) following the specification of the manufacturer.

For *fuz7*, a 1.3 kb fragment was generated with primer pair's fuz7-for1 (5'-GATACTCA TATGCTTTCGTCCGGTGCGGGATCTTC-3') and fuz7-rev1 (5'-CGCATATGGATCC TTACTTCATCCCATCGGCCCATGCTTG-3') by PCR using FB1 genomic DNA as template (Wang, L. 2011). A 0.67 kb EcoRV fragment from pSP4.2EcoRV was used for detecting *mfa1* (Wang, L. 2011).

4.4 Protein biological methods

4.4.1 Protein preparation from *U. maydis*

U. maydis strains were grown in CM medium with 1% glucose to an OD600 of 0.5-1.0. Cultures were collected by centrifugation for 5 min at 3,500 rpm. The pellet was washed once with Tris-HCl (50 mM pH 7.5) following by centrifugation for 5 min at 3,500 rpm. The pellet was resuspended in cold lysis buffer (PBS buffer with Roche Complete Protease Inhibitor Cocktail and 1% Triton X-100) and 100 mg of lysing matrix B (MP Biomedicals) was added following lysis in a FastPrep homogenization system (MP Biomedicals) with 4.5 30 s, 5.5 30 s, 5.5 30 s and centrifugation at 13,000 rpm for 10 min at 4°C. The supernant was transferred to a 1.5 ml eppendorf tube. The sample loading buffer was added following by boiling at 95°C for 3 min and 15-20 µl of sample was subjected to SDS-PAGE.

PBS buffer (phosphate-buffered saline): 8 g NaCl, 0.2 g KCl, 1.44 g Na2HPO4, 0.24 g KH2PO4 and ddH2O was added to 1 liter and pH was adjusted to 7.4 with HCl following autoclaving at 121°C for 5 min.

4.4.2 Western blotting

Protein extracts were separated by SDS-PAGE and transferred to a PVDF (polyvinylidene difluoride) membrane. Membrane was blocked with TBST buffer (50 mM Tris-HCl, 150 mM NaCl, 0.1% Tween-20, pH 7.4) containing 5% non-fat dry milk at room temperature for 1 h. The membrane was washed three times with TBST buffer each time for 5 min. Thereafter, the membrane was incubated with respective antibody as the primary antibody diluted in TBST buffer with 3% non-fat dry milk with shaking at 4oC overnight. The membrane was washed with TBST buffer three times each time for 5 min. Next the membrane was incubated with respective secondary antibody in TBST buffer containing 3% non-fat dry milk and incubated for 1 h with shaking at room temperature. Finally, the membrane was washed with TBST buffer three times each time for 5 min. Chemiluminescent detection was performed using an ECL kit (Amersham Biosciences, cat. no. RPN-2106). Immunodetection was carried out using related antibodies (Table 7)

Table 7: Antibodies used in this study

Antibody	Source	Company	Working solution
α-HA	Mouse	Sigma H9658	1:10,000
α-Tubulin	Mouse	Calbiochem	1:3,000
α-Phospho-p44/42 MAPK	Rabbit	Cell Signaling Technology- 9101	1:10,000
α-rabbit IgG, HRP-linked	Rabbit	Cell Signaling Technology - 7074	1:10,000
α-mouse IgG, HRP-linked	Horse	Cell Signaling Technology - 7076	1:10,000

4.4.3 Protein preparation from *U. maydis* for isolation of phosphoproteins

Proteins were extracted from ground cells. The powdered cells were incubated in 2.5 ml of protein extraction buffer (50 mM HEPES/KOH,40% w/v sucrose, 1% ß-mercaptoethanol, 50 mM NaF, 0.1% proteinase inhibitor cocktail, 0.1% phosphatase inhibitor cocktail 1 and 0.1% phosphatase inhibitor cocktail 2, pH 7.5) per mg in a 50 ml reaction falcon tube. Three volumes of chilled water-saturated phenol were added, and the mixture was shaken for 30 min at 4°C. After centrifugation at 4000 g, 4°C for 8 min, the soluble proteins were in the upper phenolic phase. The phenolic phase was removed and the proteins were precipitated overnight in five volumes of ice-cold acetone. After centrifugation at 4000 g, 4°C for 10 min, the pellets were briefly washed three times with ice-cold methanol. The dried protein pellets were then resolved in 8 M urea, 100 mM NH_4HCO_3 by gently shaking at room temperature for 5 min and then stored at -80°C. Protein concentration in extracts was determined with the Bio-Rad protein assay kit using BSA as a standard.

4.4.4 Isolation of phospho-protein using $Al(OH)_3$ Metal Oxide Affinity Chromatography (MOAC)

The following protocol was tailored for total protein batches of 36 mg protein (based on the Bradford assay using Bio-Rad protein assay kit performed at the end of the total protein extraction). For the following steps, the incubation and washing buffers were kept at cold temperatures (at 10°C), and the elution buffer equilibrated at room temperature. Protein pellets

(~36 mg) were dissolved in 10 ml incubation buffer Part A (IB/A; 30 mM 2-(N-morpholino) ethanesulfonic acid (MES), pH 6.1, 0.25% (w/v) 3-[(3-cholamidopropyl)dimethyl ammonio]-1-propanesulfonate(CHAPS), 7 M urea, 2 M thiourea, and 30 mM imidazole) by using sonication and by agitating the sample to assure that the pellet was mechanically disrupted. Incubation continued overnight at 10°C by slow-mixing on a rotator. The sample concentration was adjusted to approximately 1 mg/ml by adding 16 ml of buffer IB/B (30 mM MES, pH 6.1, 0.23 M sodium glutamate, 0.23 M potassium aspartate, 0.25% CHAPS, 8 M urea, and 30 mM imidazole) to the completely dissolved protein pellet. Meanwhile, 2.88 $Al(OH)_3$ was washed twice with IB150 buffer and after discarding the supernatant from the tubes, 36 ml of soluble protein supernatant was transferred to each of these tubes containing the $Al(OH)_3$ and incubated for 60 min at 10°C in a rotator. Once the phospho-protein was bound to the $Al(OH)_3$, the supernatant containing un-phosphorylated protein was discarded and washed six times with washing buffer. The $Al(OH)_3$ pellet was carefully ressuspended after each addition of washing buffer, agitating gently each time. Then, phospho-proteins were eluted by adding 24 ml of elution buffer (300 mM potassium pyrophosphate and 8 M urea, pH adjusted to 9.0 with phosphoric acid) and agitating for 30 min at room temperature in a rotator.

Eluted phospho-protein was precipitated using a modified protocol from the DOC-TCA precipitation (Colby *et al*., 2011). The phospho-protein solution was transferred into Amicon Ultracel-10K centrifugal concentrators (Millipore) and concentrated to get about 250 µl. Phospho-protein was precipitated using 2% DOC (Sodium deoxycolate) and 100% TCA (Trichloroacetic acid) solutions. The precipitated pellet was given a series of wash with washing buffers (first wash with 1ml of 25% TCA solutions, second wash with 1ml of 80% Acetone-20% TrisHCl(50mM, pH7.5), final wash with 1 ml of 100% Acetone) to remove all of the residual aluminum from the phospho-protein as aluminum interferes with trypsin digestion. The phospho-protein pellet was re-dissolved in elution buffer (200 mM of Potassium pyrophosphate pH-9.8, 8M Urea)

4.4.5 In-solution tryptic phospho-protein digestion

For in-solution digestion, 500 µg of protein were diluted four-fold with 10% acetonitrile and 25 mM NH_4HCO_3; samples were digested overnight with Poroszyme

immobilized trypsin (1/100 v/w) at 37°C. Digestion was then stopped by adding trifluoroacetic acid (TFA) to 2% (pH 3). The trypsin beads and insoluble material were removed by centrifugation at 15000 g for 20 min. Samples were concentrated in a vacuum centrifuge for phospho-peptide enrichment with titanium dioxide.

4.4.6 Phospho-peptide enrichment with TiO_2 Metal Oxide Affinity Chromatography (MOAC)

Titanium dioxide tips were supplied by Glygen Inc and the phosphopeptide enrichment procedures used were essentially those described by Larsen et al. (2005) with some modifications. TiO_2 beads were equilibrated prior to binding of phospho-peptides by aspirating/ expelling 200 µl of 30 mg/ml 2,5-dihydroxybenzoic acid (DHB) in 80% acetonitrile and 0.1% TFA. Before binding, the trypsin-digested peptide lysate was adjusted to pH 1.9 by adding 1% TFA. Each peptide mixture was then added to a 2 ml reaction tube containing 12.5 mg of the TiO_2 beads and incubated batch wise with end-over-end rotation for 30 min. After incubation, the beads were spun down at 500 g and briefly washed once with 80% acetonitrile, 0.1% TFA and again once with 10% acetonitrile, 0.1% TFA. Finally, bound peptides were eluted from the beads using 200 µl of 0.3 M NH_4OH in 30% acetonitrile (pH > 10). Eluates were immediately neutralized in 5% TFA solvent and dried and sent for mass spec analysis using LC-MS/MS. Mass spec analysis was done by Wolfgang Hoehenwarter at department of molecular systems biology, faculty of life sciences, University of Vienna, Vienna, Austria.

4.4.7 Immuno-precipitation using magnetic beads

U. maydis cells were incubated in CM medium with 2% glucose/arabinose to an OD600 of 0.8-1.0 and collected by centrifugation at 4,000 rpm for 5 min. The pellet was washed once with 1 ml of ddH_2O followed by centrifugation at 4,000 rpm for 5 min. The pellet was resuspended in 800 µl cold lysis buffer (PBS buffer with Roche Complete Protease Inhibitor Cocktail and 1% Triton X-100 and Protease inhibitor cocktail 2 and 3 from Sigma-

Aldrich) and aliqouted to two 2 ml screw cap centrifuge tubes. 100 mg of lysing matrix C (MP Biomedicals) was added followed by lysis in a FastPrep homogenization system (MP Biomedicals) 5 to 6 times with 6.5 speed 60 s. After centrifugation at 13,000 rpm for 10 min at 4°C, the supernant was transferred to a 1.5 ml eppendorf tube and centrifuged again until the protein lysate was clear. About 750 µl protein lysate was aliquoted into a spin column with a closed bottom.

The anti-HA antibody magnetic beads was prepared by following the supplied protocol from Life technologies (Dynabeads® Protein G; catalogue # 10003D). For the anti-HA antibody conjugation around 300 – 800 µl protein lysate was added and incubated at 4° C with rotation overnight following by washing 5 times with 500 µl cold lysis buffer. Resuspend in 60-70µl µl of 1xSDS loading buffer with DTT l (use 100 µl of 1M DTT in 400µl of 1x SDS loading buffer). Non-denaturing elution was done using the buffer containing 50 mM Glycine pH 2.8. The sample was subjected to SDS-PAGE or to dephosphorylation assay.

To avoid co-elution of anti-HA antibody, crosslink of antibody to the magnetic beads before continuing with immunoprecipitation was performed. Crosslinking reagent BS^3 (Thermo scientific 21585) was use, following the provided protocol.

PBS (pH 7.4)	8mM Na_2PO_4
	1.5 mM KH_2PO_4
	2.7 mM KCl
	137 mM NaCl
	in dd H_2O

4.4.8 Protocol for de-phosphorylation of proteins

Anti-HA immunoprecipitated protein was eluted using non-denaturing buffer. Dephosphorylation of protein was done as described in Peck, 2006. After eluting the protein bound to magnetic beads, the tubes were given a spin for 3min and the protein concentration was measured using Nanodrop (50 µg used). Phosphatase reaction was set up using Lambda Protein Phosphatase (Lambda PP) from NEB (Catalogue # P0753S). The reaction mix was

incubated for 30 min and the reaction was stopped by adding 2x SDS sampler buffer with DTT. This sample was subjected to SDS-PAGE Phos tag analysis.

4.4.9 SDS-PAGE Phos Tag™

The acrylamide-pendant Phos-tag ligand (Wako chemicals # AAL-107) provides a phosphate affinity SDS-PAGE for mobility shift detection of phosphorylated proteins. The 8% mini-slab PAGE was cast using the protocol provided by Wako chemicals. 50 µM Phos-tag acrylamide concentrations were used. After loading the protein into each well of the SDS-PAGE Phos-tag, electrophoresis was done for 5-6 hours at constant voltage of 100 V. After the electrophoresis transfer the gel to new clean tray to remove all of the Manganese ions in SDS_PAGE. Take 100 ml of 1x running buffer (Running Buffer, pH 8.3（10x soln) 0.25 mol/L Tris base, 0.5% SDS, 1.92 mol/L Glycine) to this add 1ml for 0,5 M EDTA (5 mM/L concentration) for one SDS-PAGE. Gently agitate for 10 minute, repeat this for 2 to 3 times. For thicker 1.5 mm gel increased the agitation time by 20 min was used. For the analysis of the anti-HA immunoprecipitated protein was done following the general western blots procedure.

8%SDS-PAGE with Phos-tag	
Acryl amide	4.005 ml
1,5 M Tris-HCl pH 8,8	3,750 ml
Water	6,795 ml
50 mmol Phos-Tag	150 µl
10 mmol $MnCl_2$	150 µl
10% SDS	150 µL
TEMED	20 µl
10% APS	75 µl
Total	15 ml

4.5 Bioinformatics

Several bioinformatic analysis were performed within the MPI Bioinformatics Toolkit at http://toolkit.tuebingen.mpg.de/ (Biegert *et al*., 2006). *U. maydis* genome was accessed using MUMDB database http://www.helmholtz-muenchen.de/en/ibis/institute/groups/fungal-microbial-genomics/resources/ustilaginaceae/index.html. For cloning of plasmids and sequence analysis Clone manager tools was used. For the protein domain analysis SMART (Simple Modular Architecture Research Tool; Schultz *et al.*, 1998; http://smart.embl-heidelberg.de/).

5 References

Adamczyk, M., Gebler, J.C., and Wu, J. (2001). Selective analysis of phosphopeptides within a protein mixture by chemical modification, reversible biotinylation and mass spectrometry. Rapid communications in mass spectrometry **15,** 1481–1488.

Aichinger, C., Hansson, K., Eichhorn, H., Lessing, F., Mannhaupt, G., Mewes, W., and Kahmann, R. (2003). Identification of plant-regulated genes in *Ustilago maydis* by enhancer-trapping mutagenesis. Mol Genet Genomics **270,** 303–314.

Alaimo, P.J., Shogren-Knaak, M.A., and Shokat, K.M. (2001). Chemical genetic approaches for the elucidation of signaling pathways. Current Opinion in Chemical Biology **5,** 360–367.

Amoutzias, G.D., He, Y., Lilley, K.S., Van de Peer, Y., and Oliver, S.G. (2012). Evaluation and properties of the budding yeast phosphoproteome. Molecular & cellular proteomics : MCP **11,** M111.009555.

Andersson, L., and Porath, J. (1986). Isolation of phosphoproteins by immobilized metal (Fe3+) affinity chromatography. Analytical Biochemistry **154,** 250–254.

Andreasson, E., Jenkins, T., Brodersen, P., Thorgrimsen, S., Petersen, N.H., Zhu, S., Qiu, J.L., Micheelsen, P., Rocher, A., Petersen, M., Newman, M.A., Bjorn Nielsen, H., Hirt, H., Somssich, I., Mattsson, O., and Mundy, J. (2005). The MAP kinase substrate MKS1 is a regulator of plant defense responses. EMBO J **24,** 2579-2589.

Andrews, D.L., Egan, J.D., Mayorga, M.E., and Gold, S.E. (2000). The *Ustilago maydis* ubc4 and ubc5 genes encode members of a MAP kinase cascade required for filamentous growth. Molecular plant-microbe interactions: MPMI **13,** 781–786.

Banuett, F. (1995). Genetics of *Ustilago maydis*, A Fungal Pathogen that Induces Tumors in Maize. Annual Review of Genetics **29,** 179–208.

Banuett, F. (2007). History of the Mating Types in *Ustilago maydis*. In Sex in Fungi (American Society of Microbiology), pp. 351–375.

Banuett, F., and Herskowitz, I. (1994). Identification of fuz7, a *Ustilago maydis* MEK/MAPKK homolog required for a-locus-dependent and -independent steps in the fungal life cycle. Genes & Development **8,** 1367–1378.

Barbar, E. (2012). Native disorder mediates binding of dynein to NudE and dynactin. Biochem Soc Trans **40,** 1009-1013.

Barbieri, C.M., and Stock, A.M. (2008). Universally applicable methods for monitoring response regulator aspartate phosphorylation both in vitro and in vivo using Phos-tag-based reagents. Analytical Biochemistry **376,** 73–82.

Bedford, M.T., and Leder, P. (1999). The FF domain: a novel motif that often accompanies WW domains. Trends in Biochemical Sciences **24,** 264–265.

Berwick, D.C., and Tavaré, J.M. (2004). Identifying protein kinase substrates: hunting for the organ-grinder's monkeys. Trends in Biochemical Sciences **29,** 227–232.

Blethrow, J.D., Glavy, J.S., Morgan, D.O., and Shokat, K.M. (2008). Covalent capture of kinase-specific phosphopeptides reveals Cdk1-cyclin B substrates. Proceedings of the National Academy of Sciences **105,** 1442–1447.

Bluhm, B.H., Zhao, X., Flaherty, J.E., Xu, J.R., and Dunkle, L.D. (2007). RAS2 Regulates Growth and Pathogenesis in *Fusarium graminearum*. Molecular Plant-Microbe Interactions **20,** 627–636.

Bodenmiller, B., Mueller, L.N., Pedrioli, P.G.A., Pflieger, D., Junger, M.A., Eng, J.K., Aebersold, R., and Tao, W.A. (2007). An integrated chemical, mass spectrometric and computational strategy for (quantitative) phosphoproteomics: application to Drosophila melanogaster Kc167 cells Molecular BioSystems **3,** 275–286.

Boisnard, S., Ruprich-Robert, G., Florent, M., Da Silva, B., Chapeland-Leclerc, F., and Papon, N. (2008). Role of Sho1p adaptor in the pseudohyphal development, drugs sensitivity, osmotolerance and oxidant stress adaptation in the opportunistic yeast *Candida lusitaniae*. Yeast **25,** 849–859.

Bolker, M. (2001). *Ustilago maydis*-a valuable model system for the study of fungal dimorphism and virulence. Microbiology (Reading, England) **147,** 1395–1401.

Bolker, M., Urban, M., and Kahmann, R. (1992). The a mating type locus of *U. maydis* specifies cell signaling components. Cell **68,** 441–450.

Bölker, M., Genin, S., Lehmler, C., and Kahmann, R. (1995). Genetic regulation of mating and dimorphism in *Ustilago maydis*. Can. J. Bot. **73,** 320–325.

Bottin, A., Kamper, J., and Kahmann, R. (1996). Isolation of a carbon source-regulated gene from *Ustilago maydis*. Mol Gen Genet **253,** 342–352.

Brachmann, A., Schirawski, J., Muller, P., and Kahmann, R. (2003). An unusual MAP kinase is required for efficient penetration of the plant surface by *Ustilago maydis*. EMBO J **22,** 2199–2210.

Brefort, T., Muller, P., and Kahmann, R. (2005). The high-mobility-group domain transcription factor Rop1 is a direct regulator of prf1 in *Ustilago maydis*. Eukaryot Cell **4,** 379–391.

Brefort, T., Doehlemann, G., Mendoza-Mendoza, A., Reissmann, S., Djamei, A., and Kahmann, R. (2009). *Ustilago maydis* as a Pathogen. Annual Review of Phytopathology **47,** 423–445.

Carbó, N., and Pérez-Martín, J. (2010). Activation of the Cell Wall Integrity Pathway Promotes Escape from G2 in the Fungus *Ustilago maydis*. PLoS Genet **6,** e1001009.

Cargnello, M., and Roux, P.P. (2011). Activation and function of the MAPKs and their substrates, the MAPK-activated protein kinases. Microbiol Mol Biol Rev **75,** 50–83.

Chacko, N., and Gold, S. (2012). Deletion of the *Ustilago maydis* ortholog of the *Aspergillus* sporulation regulator medA affects mating and virulence through pheromone response. Fungal Genetics and Biology **49,** 426–432.

Chang, L., and Karin, M. (2001). Mammalian MAP kinase signalling cascades. Nature **410,** 37–40.

Chen, R.E., and Thorner, J. (2007). Function and regulation in MAPK signaling pathways: Lessons learned from the yeast *Saccharomyces cerevisiae*. Biochimica et Biophysica Acta (BBA) - Molecular Cell Research **1773,** 1311–1340.

Chen, Y., Hoehenwarter, W., and Weckwerth, W. (2010). Comparative analysis of phytohormone-responsive phosphoproteins in *Arabidopsis thaliana* using TiO2-phosphopeptide enrichment and mass accuracy precursor alignment. The Plant Journal **63,** 1–17.

Cho, Y., Cramer Jr, R.A., Kim, K.-H., Davis, J., Mitchell, T.K., Figuli, P., Pryor, B.M., Lemasters, E., and Lawrence, C.B. (2007). The Fus3/Kss1 MAP kinase homolog Amk1 regulates the expression of genes encoding hydrolytic enzymes in *Alternaria brassicicola*. Fungal Genetics and Biology **44,** 543–553.

Colby, T., Rohrig, H., Harzen, A., and Schmidt, J. (2011). Modified metal-oxide affinity enrichment combined with 2D-PAGE and analysis of phosphoproteomes. Methods Mol Biol **779,** 273–286.

Cook, J.G., Bardwell, L., and Thorner, J. (1997). Inhibitory and activating functions for MAPK Kss1 in the *S. cerevisiae* filamentous-growth signalling pathway. Nature **390,** 85–88.

Cook, J.G., Bardwell, L., Kron, S.J., and Thorner, J. (1996). Two novel targets of the MAP kinase Kss1 are negative regulators of invasive growth in the yeast *Saccharomyces cerevisiae*. Genes & Development **10,** 2831–2848.

Correia, I., Alonso-Monge, R., and Pla, J. (2010). MAPK cell-cycle regulation in *Saccharomyces cerevisiae* and *Candida albicans.* Future Microbiol **5,** 1125–1141.

Cousin, A., Mehrabi, R., Guilleroux, M., Dufresne, M., T, V.D.L., Waalwijk, C., Langin, T., and Kema, G.H. (2006). The MAP kinase-encoding gene MgFus3 of the non-appressorium phytopathogen *Mycosphaerella graminicola* is required for penetration and in vitro pycnidia formation. Mol Plant Pathol **7,** 269-278.

Csank, C., Schroppel, K., Leberer, E., Harcus, D., Mohamed, O., Meloche, S., Thomas, D.Y., and Whiteway, M. (1998). Roles of the *Candida albicans* mitogen-activated protein kinase homolog, Cek1p, in hyphal development and systemic candidiasis. Infection and immunity **66,** 2713–2721.

Dephoure, N., Gould, K.L., Gygi, S.P., and Kellogg, D.R. (2013). Mapping and analysis of phosphorylation sites: a quick guide for cell biologists. Mol Biol Cell **24,** 535–542.

Derewenda, U., Tarricone, C., Choi, W.C., Cooper, D.R., Lukasik, S., Perrina, F., Tripathy, A., Kim, M.H., Cafiso, D.S., Musacchio, A., and Derewenda, Z.S. (2007). The Structure of the Coiled-Coil Domain of Ndel1 and the Basis of Its Interaction with Lis1, the Causal Protein of Miller-Dieker Lissencephaly. Structure **15,** 1467-1481.

Di Pietro, A., Garcia-MacEira, F.I., Meglecz, E., and Roncero, M.I. (2001). A MAP kinase of the vascular wilt fungus *Fusarium oxysporum* is essential for root penetration and pathogenesis. Molecular Microbiology **39,** 1140–1152.

Di Stasio, M., Brefort, T., Mendoza-Mendoza, A., Munch, K., and Kahmann, R. (2009). The dual specificity phosphatase Rok1 negatively regulates mating and pathogenicity in *Ustilago maydis*. Molecular Microbiology **73,** 73–88.

Doehlemann, G., Berndt, P., and Hahn, M. (2006). Different signalling pathways involving a G alpha protein, cAMP and a MAP kinase control germination of *Botrytis cinerea* conidia. Molecular Microbiology **59,** 821–835.

Dohlman, H.G., Song, J., Ma, D., Courchesne, W.E., and Thorner, J. (1996). Sst2, a negative regulator of pheromone signaling in the yeast *Saccharomyces cerevisiae* : expression, localization, and genetic interaction and physical association with Gpa1 (the G-protein alpha subunit). Molecular and Cellular Biology **16,** 5194–5209.

Dunn, J.D., Reid, G.E., and Bruening, M.L. (2010). Techniques for phosphopeptide enrichment prior to analysis by mass spectrometry. Mass Spectrometry Reviews **29,** 29–54.

Eblen, S.T., Kumar, N.V., Shah, K., Henderson, M.J., Watts, C.K.W., Shokat, K.M., and Weber, M.J. (2003). Identification of Novel ERK2 Substrates through Use of an Engineered Kinase and ATP Analogs. Journal of Biological Chemistry **278,** 14926–14935.

Efimov, V.P., and Morris, N.R. (2000). The LIS1-related NUDF protein of *Aspergillus nidulans* interacts with the coiled-coil domain of the NUDE/RO11 protein. J Cell Biol **150,** 681-688.

Efimov, V.P. (2003). Roles of NUDE and NUDF proteins of *Aspergillus nidulans*: insights from intracellular localization and overexpression effects. Mol Biol Cell **14,** 871–888.

Elías-Villalobos, A., Fernández-Álvarez, A., and Ibeas, J.I. (2011). The General Transcriptional Repressor Tup1 Is Required for Dimorphism and Virulence in a Fungal Plant Pathogen. PLoS Pathog **7,** e1002235.

Elion, E.A., Satterberg, B., and Kranz, J.E. (1993). FUS3 phosphorylates multiple components of the mating signal transduction cascade: evidence for STE12 and FAR1. Molecular Biology of the Cell **4,** 495–510.

Feng, Y., Olson, E.C., Stukenberg, P.T., Flanagan, L.A., Kirschner, M.W., and Walsh, C.A. (2000). LIS1 regulates CNS lamination by interacting with mNudE, a central component of the centrosome. Neuron **28,** 665–679.

Feng, S., Ye, M., Zhou, H., Jiang, X., Jiang, X., Zou, H., and Gong, B. (2007). Immobilized Zirconium Ion Affinity Chromatography for Specific Enrichment of Phosphopeptides in Phosphoproteome Analysis. Molecular & Cellular Proteomics **6,** 1656–1665.

Folk, P., Puta, F., and Skruzny, M. (2004). Transcriptional coregulator SNW/SKIP: the concealed tie of dissimilar pathways. Cellular and molecular life sciences: CMLS **61,** 629–640.

Fuchs, U., Manns, I., and Steinberg, G. (2005). Microtubules are dispensable for the initial pathogenic development but required for long-distance hyphal growth in the corn smut fungus *Ustilago maydis*. Mol Biol Cell **16,** 2746–2758.

Fukunaga, R., and Hunter, T. (1997). MNK1, a new MAP kinase-activated protein kinase, isolated by a novel expression screening method for identifying protein kinase substrates.

Gao, Z.H., Metherall, J., and Virshup, D.M. (2000). Identification of casein kinase I substrates by in vitro expression cloning screening. Biochem Biophys Res Commun **268,** 562–566.

Garcia-Muse, T., Steinberg, G., and Perez-Martin, J. (2003). Pheromone-induced G2 arrest in the phytopathogenic fungus *Ustilago maydis.* Eukaryot Cell **2,** 494–500.

Garrido, E., Voss, U., Muller, P., Castillo-Lluva, S., Kahmann, R., and Perez-Martin, J. (2004). The induction of sexual development and virulence in the smut fungus *Ustilago maydis* depends on Crk1, a novel MAPK protein. Genes & Development **18,** 3117–3130.

Goodman, T., Schulenberg, B., Steinberg, T.H., and Patton, W.F. (2004). Detection of phosphoproteins on electroblot membranes using a small-molecule organic fluorophore. Electrophoresis **25,** 2533–2538.

Grimsrud, P.A., Swaney, D.L., Wenger, C.D., Beauchene, N.A., and Coon, J.J. (2010). Phosphoproteomics for the Masses. Acs Chemical Biology **5,** 105–119.

Grønborg, M., Kristiansen, T.Z., Stensballe, A., Andersen, J.S., Ohara, O., Mann, M., Jensen, O.N., and Pandey, A. (2002). A Mass Spectrometry-based Proteomic Approach for Identification of Serine/Threonine-phosphorylated Proteins by

Enrichment with Phospho-specific Antibodies: Identification of a Novel Protein, Frigg, as a Protein Kinase A Substrate. Molecular & Cellular Proteomics **1,** 517–527.

Gruhler, A., Olsen, J.V., Mohammed, S., Mortensen, P., Færgeman, N.J., Mann, M., and Jensen, O.N. (2005). Quantitative Phosphoproteomics Applied to the Yeast Pheromone Signaling Pathway. Molecular & Cellular Proteomics **4,** 310–327.

Guo, J., Dai, X., Xu, J.-R., Wang, Y., Bai, P., Liu, F., Duan, Y., Zhang, H., Huang, L., and Kang, Z. (2011). Molecular characterization of a Fus3/Kss1 type MAPK from *Puccinia striiformis f. sp. tritici*, PsMAPK1. Plos One **6,** e21895.

Hamel, L.P., Nicole, M.C., Duplessis, S., and Ellis, B.E. (2012). Mitogen-activated protein kinase signaling in plant-interacting fungi: distinct messages from conserved messengers. Plant Cell **24,** 1327–1351.

Hanahan, D. (1985). DNA Cloning: A Practical Approach (Glover, D.M., ed.). IRL Press, McLean, Virginia.

Hartmann, H.A., Kahmann, R., and Bolker, M. (1996). The pheromone response factor coordinates filamentous growth and pathogenicity in *Ustilago maydis*. EMBO Journal **15,** 1632–1641.

Heimel, K., Scherer, M., Schuler, D., and Kämper, J. (2010). The *Ustilago maydis* Clp1 Protein Orchestrates Pheromone and b-Dependent Signaling Pathways to Coordinate the Cell Cycle and Pathogenic Development. The Plant Cell Online **22,** 2908–2922.

Hoehenwarter, W., Thomas, M., Nukarinen, E., Egelhofer, V., Rohrig, H., Weckwerth, W., Conrath, U., and Beckers, G.J.M. (2013). Identification of Novel in vivo MAP Kinase Substrates in *Arabidopsis thaliana* Through Use of Tandem Metal Oxide Affinity Chromatography. Molecular & Cellular Proteomics **12,** 369–380.

Hoffman, C.S., and Winston, F. (1987). A ten-minute DNA preparation from yeast efficiently releases autonomous plasmids for transformation of *Escherichia coli*. Gene **57,** 267–272.

Hoffmann, B., Zuo, W., Liu, A., and Morris, N.R. (2001). The LIS1-related protein NUDF of *Aspergillus nidulans* and its interaction partner NUDE bind directly to specific subunits of dynein and dynactin and to alpha- and gamma-tubulin. J Biol Chem **276,** 38877–38884.

Holliday, R. (1974). *Ustilago maydis*. Handbook of genetics edited by R. C. King **1,** 575–595.

Holt, L.J., Tuch, B.B., Villen, J., Johnson, A.D., Gygi, S.P., and Morgan, D.O. (2009). Global Analysis of Cdk1 Substrate Phosphorylation Sites Provides Insights into Evolution. Science **325,** 1682–1686.

Hu, G.G., Kamp, A., Linning, R., Naik, S., and Bakkeren, G. (2007). Complementation of *Ustilago maydis* MAPK mutants by a wheat leaf rust, *Puccinia triticina* homolog: Potential for functional analyses of rust genes. Molecular Plant-Microbe Interactions **20,** 637–647.

Iida, N., Fujita, M., Miyazawa, K., Kobayashi, M., and Hattori, S. (2014). Proteomic identification of p38 MAP kinase substrates using in vitro phosphorylation. Electrophoresis **35,** 554–562.

Jenczmionka, N.J., Maier, F.J., Losch, A.P., and Schafer, W. (2003). Mating, conidiation and pathogenicity of *Fusarium graminearum*, the main causal agent of the head-blight disease of wheat, are regulated by the MAP kinase gpmk1. Curr Genet **43,** 87–95.

Jensen, O.N. (2004). Modification-specific proteomics: characterization of post-translational modifications by mass spectrometry. Current Opinion in Chemical Biology **8,** 33–41.

Jensen, S.S., and Larsen, M.R. (2007). Evaluation of the impact of some experimental procedures on different phosphopeptide enrichment techniques. Rapid communications in mass spectrometry: RCM **21,** 3635–3645.

Kaffarnik, F., Muller, P., Leibundgut, M., Kahmann, R., and Feldbrugge, M. (2003). PKA and MAPK phosphorylation of Prf1 allows promoter discrimination in *Ustilago maydis*. EMBO Journal **22,** 5817–5826.

Kämper, J. (2004). A PCR-based system for highly efficient generation of gene replacement mutants in Ustilago maydis. Mol Genet Genomics **271**, 103-110.

Kamper, J., Reichmann, M., Romeis, T., Bolker, M., and Kahmann, R. (1995). Multiallelic recognition: nonself-dependent dimerization of the bE and bW homeodomain proteins in *Ustilago maydis*. Cell **81,** 73–83.

Kamper, J., Kahmann, R., Bolker, M., Ma, L.-J., Brefort, T., Saville, B.J., Banuett, F., Kronstad, J.W., Gold, S.E., Muller, O., Perlin, M.H., Wosten, H.A.B., Vries, R.d., Ruiz-Herrera, J., Reynaga-Pena, C.G., Snetselaar, K., McCann, M., Perez-Martin, J., Feldbrugge, M., Basse, C.W., Steinberg, G., Ibeas, J.I., Holloman, W., Guzman, P., Farman, M., Stajich, J.E., Sentandreu, R., Gonzalez-Prieto, J.M.,

Kennell, J.C., Molina, L., Schirawski, J., Mendoza-Mendoza, A., Greilinger, D., Munch, K., Rossel, N., Scherer, M., Vranes, M., Ladendorf, O., Vincon, V., Fuchs, U., Sandrock, B., Meng, S., Ho, E.C.H., Cahill, M.J., Boyce, K.J., Klose, J., Klosterman, S.J., Deelstra, H.J., Ortiz-Castellanos, L., Li, W., Sanchez-Alonso, P., Schreier, P.H., Hauser-Hahn, I., Vaupel, M., Koopmann, E., Friedrich, G., Voss, H., Schluter, T., Margolis, J., Platt, D., Swimmer, C., Gnirke, A., Chen, F., Vysotskaia, V., Mannhaupt, G., Guldener, U., Munsterkotter, M., Haase, D., Oesterheld, M., Mewes, H.-W., Mauceli, E.W., DeCaprio, D., Wade, C.M., Butler, J., Young, S., Jaffe, D.B., Calvo, S., Nusbaum, C., Galagan, J., and Birren, B.W. (2006). Insights from the genome of the biotrophic fungal plant pathogen *Ustilago maydis*. Nature **444,** 97–101.

Kinane, J., and Oliver, R.P. (2003). Evidence that the appressorial development in barley powdery mildew is controlled by MAP kinase activity in conjunction with the cAMP pathway. Fungal Genetics and Biology **39,** 94–102.

Kinoshita, E., Kinoshita-Kikuta, E., and Koike, T. (2009). Separation and detection of large phosphoproteins using Phos-tag SDS-PAGE. Nat. Protocols **4,** 1513–1521.

Kinoshita, E., Kinoshita-Kikuta, E., and Koike, T. (2012). Phos-tag SDS-PAGE systems for phosphorylation profiling of proteins with a wide range of molecular masses under neutral pH conditions. Proteomics **12,** 192–202.

Kinoshita, E., Kinoshita-Kikuta, E., and Koike, T. (2014). Advances in Phos-tag-based methodologies for separation and detection of the phosphoproteome. Biochimica et biophysica acta.

Kinoshita, E., Kinoshita-Kikuta, E., Takiyama, K., and Koike, T. (2006). Phosphate-binding Tag, a New Tool to Visualize Phosphorylated Proteins. Molecular & Cellular Proteomics **5,** 749–757.

Klosterman, S.J., Martinez-Espinoza, A.D., Andrews, D.L., Seay, J.R., and Gold, S.E. (2007). Ubc2, an Ortholog of the Yeast Ste50p Adaptor, Possesses a Basidiomycete-Specific Carboxy Terminal Extension Essential for Pathogenicity Independent of Pheromone Response. Molecular Plant-Microbe Interactions **21,** 110–121.

Kramer, B., Thines, E., and Foster, A.J. (2009). MAP kinase signalling pathway components and targets conserved between the distantly related plant pathogenic fungi

Mycosphaerella graminicola and *Magnaporthe grisea*. Fungal Genetics and Biology **46,** 667–681.

Krantz, M., Becit, E., and Hohmann, S. (2006). Comparative genomics of the HOG-signalling system in fungi. Curr Genet **49,** 137–151.

Kruger, J., Loubradou, G., Regenfelder, E., Hartmann, A., and Kahmann, R. (1998). Crosstalk between cAMP and pheromone signalling pathways in *Ustilago maydis*. Mol Gen Genet **260,** 193–198.

Lanctot, A.A., Peng, C.Y., Pawlisz, A.S., Joksimovic, M., and Feng, Y. (2013). Spatially dependent dynamic MAPK modulation by the Nde1-Lis1-Brap complex patterns mammalian CNS. Dev Cell **25,** 241–255.

Lanver, D. (2011). Appressorienbildung von *Ustilago maydis* auf hydrophoben Oberflächen : Regulation durch Membranproteine.

Lanver, D., Mendoza-Mendoza, A., Brachmann, A., and Kahmann, R. (2010). Sho1 and Msb2-related proteins regulate appressorium development in the smut fungus *Ustilago maydis*. The Plant Cell **22,** 2085–2101.

Lanver, D., Berndt, P., Tollot, M., Naik, V., Vranes, M., Warmann, T., Munch, K., Rossel, N., and Kahmann, R. (2014). Plant surface cues prime *Ustilago maydis* for biotrophic development. Plos Pathogens **10,** e1004272.

Lassowskat, I., Böttcher, C., Eschen-Lippold, L., Scheel, D., and Lee, J. (2014). Sustained mitogen-activated protein kinase activation reprograms defense metabolism and phosphoprotein profile in *Arabidopsis thaliana*. Frontiers in Plant Science **5,** 554.

Leberer, E., Harcus, D., Dignard, D., Johnson, L., Ushinsky, S., Thomas, D.Y., and Schroppel, K. (2001). Ras links cellular morphogenesis to virulence by regulation of the MAP kinase and cAMP signalling pathways in the pathogenic fungus *Candida albicans*. Mol Microbiol **42,** 673–687.

Lee, N., and Kronstad, J.W. (2002). ras2 Controls morphogenesis, pheromone response, and pathogenicity in the fungal pathogen *Ustilago maydis*. Eukaryot Cell **1,** 954–966.

Lee, L.A., Lee, E., Anderson, M.A., Vardy, L., Tahinci, E., Ali, S.M., Kashevsky, H., Benasutti, M., Kirschner, M.W., and Orr-Weaver, T.L. (2005). Drosophila genome-scale screen for PAN GU kinase substrates identifies Mat89Bb as a cell cycle regulator. Developmental cell **8,** 435–442.

Lemmon, M.A. (2007). Pleckstrin homology (PH) domains and phosphoinositides. Biochemical Society symposium**,** 81–93.

Lengeler, K.B., Davidson, R.C., D'souza, C., Harashima, T., Shen, W.-C., Wang, P., Pan, X., Waugh, M., and Heitman, J. (2000). Signal Transduction Cascades Regulating Fungal Development and Virulence. Microbiology and Molecular Biology Reviews **64,** 746–785.

Lev, S., Sharon, A., Hadar, R., Ma, H., and Horwitz, B.A. (1999). A mitogen-activated protein kinase of the corn leaf pathogen Cochliobolus heterostrophus is involved in conidiation, appressorium formation, and pathogenicity: diverse roles for mitogen-activated protein kinase homologs in foliar pathogens. Proc Natl Acad Sci U S A **96,** 13542-13547.

Levine, M., and Hoey, T. (1998). Homeobox proteins as sequence-specific transcription factors. Cell **55,** 537–540.

Lewis, T.S., Hunt, J.B., Aveline, L.D., Jonscher, K.R., Louie, D.F., Yeh, J.M., Nahreini, T.S., Resing, K.A., and Ahn, N.G. (2000). Identification of Novel MAP Kinase Pathway Signaling Targets by Functional Proteomics and Mass Spectrometry. Molecular cell **6,** 1343–1354.

Li, J., Lee, W.L., and Cooper, J.A. (2005). NudEL targets dynein to microtubule ends through LIS1. Nat Cell Biol **7,** 686-690.

Liu, W., Zhou, X., Li, G., Li, L., Kong, L., Wang, C., Zhang, H., and Xu, J.-R. (2011). Multiple plant surface signals are sensed by different mechanisms in the rice blast fungus for appressorium formation. Plos Pathogens **7,** e1001261.

MA, A., R, B., RE, K., DD, M., JG, S., and JA, S. (1987). Current protocols in molecular biology. (John & Sons, Inc).

Ma, Y., Qiao, J., Liu, W., Wan, Z., Wang, X., Calderone, R., and Li, R. (2008). The sho1 sensor regulates growth, morphology, and oxidant adaptation in *Aspergillus fumigatus* but is not essential for development of invasive pulmonary aspergillosis. Infection and immunity **76,** 1695–1701.

Madhani, H.D., and Fink, G.R. (1997). Combinatorial control required for the specificity of yeast MAPK signaling. Science **275,** 1314–1317.

Mayorga, M.E., and Gold, S.E. (1999). A MAP kinase encoded by the ubc3 gene of *Ustilago maydis* is required for filamentous growth and full virulence. Molecular Microbiology **34,** 485–497.

Mendoza-Mendoza, A., Eskova, A., Weise, C., Czajkowski, R., and Kahmann, R. (2009a). Hap2 regulates the pheromone response transcription factor prf1 in *Ustilago maydis.* Molecular Microbiology **72,** 683–698.

Mendoza-Mendoza, A., Berndt, P., Djamei, A., Weise, C., Linne, U., Marahiel, M., Vranes, M., Kamper, J., and Kahmann, R. (2009). Physical-chemical plant-derived signals induce differentiation in *Ustilago maydis*. Molecular Microbiology **71,** 895–911.

Mey, G., Oeser, B., Lebrun, M.H., and Tudzynski, P. (2002). The Biotrophic, Non-Appressorium-Forming Grass Pathogen *Claviceps purpurea* Needs a Fus3/Pmk1 Homologous Mitogen-Activated Protein Kinase for Colonization of Rye Ovarian Tissue. Molecular Plant-Microbe Interactions **15,** 303–312.

Minke, P.F., Lee, I.H., Tinsley, J.H., Bruno, K.S., and Plamann, M. (1999). *Neurospora crassa* ro-10 and ro-11 genes encode novel proteins required for nuclear distribution. Mol Microbiol **32,** 1065–1076.

Morandell, S., Stasyk, T., Grosstessner-Hain, K., Roitinger, E., Mechtler, K., Bonn, G.K., and Huber, L.A. (2006). Phosphoproteomics strategies for the functional analysis of signal transduction. Proteomics **6,** 4047-4056.

Mori, D., Yano, Y., Toyo-oka, K., Yoshida, N., Yamada, M., Muramatsu, M., Zhang, D., Saya, H., Toyoshima, Y.Y., Kinoshita, K., Wynshaw-Boris, A., and Hirotsune, S. (2007). NDEL1 phosphorylation by Aurora-A kinase is essential for centrosomal maturation, separation, and TACC3 recruitment. Mol Cell Biol **27,** 352–367.

Morris, S.M., Albrecht, U., Reiner, O., Eichele, G., and Yu-Lee, L.y. (1998). The lissencephaly gene product Lis1, a protein involved in neuronal migration, interacts with a nuclear movement protein, NudC. Current Biology **8,** 603–606.

Mosch, H.U., Roberts, R.L., and Fink, G.R. (1996). Ras2 signals via the Cdc42/Ste20/mitogen-activated protein kinase module to induce filamentous growth in *Saccharomyces cerevisiae.* Proceedings of the National Academy of Sciences of the United States of America **93,** 5352–5356.

Muller, P., Aichinger, C., Feldbrugge, M., and Kahmann, R. (1999). The MAP kinase Kpp2 regulates mating and pathogenic development in *Ustilago maydis*. Molecular Microbiology **34,** 1007–1017.

Muller, P., Katzenberger, J.D., Loubradou, G., and Kahmann, R. (2003). Guanyl nucleotide exchange factor Sql2 and Ras2 regulate filamentous growth in *Ustilago maydis.* Eukaryotic Cell **2,** 609–617.

Müller, P., Weinzierl, G., Brachmann, A., Feldbrügge, M., and Kahmann, R. (2003b). Mating and Pathogenic Development of the Smut Fungus *Ustilago maydis* Are Regulated by One Mitogen-Activated Protein Kinase Cascade. Eukaryotic Cell **2,** 1187–1199.

New, L., Jiang, Y., Zhao, M., Liu, K., Zhu, W., Flood, L.J., Kato, Y., Parry, G.C., and Han, J. (1998). PRAK, a novel protein kinase regulated by the p38 MAP kinase. The EMBO journal **17,** 3372–3384.

Niethammer, M., Smith, D.S., Ayala, R., Peng, J., Ko, J., Lee, M.S., Morabito, M., and Tsai, L.H. (2000). NUDEL is a novel Cdk5 substrate that associates with LIS1 and cytoplasmic dynein. Neuron **28,** 697–711.

Ong, S.-E., Blagoev, B., Kratchmarova, I., Kristensen, D.B., Steen, H., Pandey, A., and Mann, M. (2002). Stable Isotope Labeling by Amino Acids in Cell Culture, SILAC, as a Simple and Accurate Approach to Expression Proteomics. Molecular & Cellular Proteomics **1,** 376–386.

Orsatti, L., Forte, E., Tomei, L., Caterino, M., Pessi, A., Talamo, F., and al, e. (2009). 2-D Difference in gel electrophoresis combined with Pro-Q Diamond staining: A successful approach for the identification of kinase/phosphatase targets. Electrophoresis **30. 14**.

Park, G., Bruno, K.S., Staiger, C.J., Talbot, N.J., and Xu, J.-R. (2004). Independent genetic mechanisms mediate turgor generation and penetration peg formation during plant infection in the rice blast fungus. Molecular Microbiology **53,** 1695–1707.

Park, G., Xue, C., Zhao, X., Kim, Y., Orbach, M., and Xu, J.-R. (2006). Multiple upstream signals converge on the adaptor protein Mst50 in *Magnaporthe grisea*. The Plant Cell **18,** 2822–2835.

Park, H.C., Song, E.H., Nguyen, X.C., Lee, K., Kim, K.E., Kim, H.S., Lee, S.M., Kim, S.H., Bae, D.W., Yun, D.-J., and Chung, W.S. (2011). Arabidopsis MAP kinase

phosphatase 1 is phosphorylated and activated by its substrate AtMPK6. Plant cell reports **30,** 1523–1531.

Peck, S.C. (2006). Analysis of protein phosphorylation: methods and strategies for studying kinases and substrates. Plant J **45,** 512–522.

Perez-Martin, J., Castillo-Lluva, S., Sgarlata, C., Flor-Parra, I., Mielnichuk, N., Torreblanca, J., and Carbo, N. (2006). Pathocycles: *Ustilago maydis* as a model to study the relationships between cell cycle and virulence in pathogenic fungi. Molecular genetics and genomics: MGG **276,** 211–229.

Perez-Nadales, E., Almeida Nogueira, M.F., Baldin, C., Castanheira, S., El Ghalid, M., Grund, E., Lengeler, K., Marchegiani, E., Mehrotra, P.V., Moretti, M., Naik, V., Oses-Ruiz, M., Oskarsson, T., Schäfer, K., Wasserstrom, L., Brakhage, A.A., Gow, N.A.R., Kahmann, R., Lebrun, M.-H., Perez-Martin, J., Di Pietro, A., Talbot, N.J., Toquin, V., Walther, A., and Wendland, J. (2014). Fungal model systems and the elucidation of pathogenicity determinants. Fungal Genetics and Biology **70,** 42–67.

Peter, M., Gartner, A., Horecka, J., Ammerer, G., and Herskowitz, I. (1993). FAR1 links the signal transduction pathway to the cell cycle machinery in yeast. Cell **73,** 747–760.

Pitzschke, A. (2015). Modes of MAPK substrate recognition and control. Trends in Plant Science **20,** 49–55.

Posewitz, M.C., and Tempst, P. (1999). Immobilized gallium (III) affinity chromatography of phosphopeptides. Analytical Chemistry **71,** 2883–2892.

Pryciak, P.M., and Huntress, F.A. (1998). Membrane recruitment of the kinase cascade scaffold protein Ste5 by the G beta gamma complex underlies activation of the yeast pheromone response pathway. Genes & Development **12,** 2684–2697.

Raitt, D.C., Posas, F., and Saito, H. (2000). Yeast Cdc42 GTPase and Ste20 PAK-like kinase regulate Sho1-dependent activation of the Hog1 MAPK pathway. The EMBO journal **19,** 4623–4631.

Ramezani-Rad, M. (2003). The role of adaptor protein Ste50-dependent regulation of the MAPKKK Ste11 in multiple signalling pathways of yeast. Current genetics **43,** 161–170.

Rauyaree, P., Ospina-Giraldo, M.D., Kang, S., Bhat, R.G., Subbarao, K.V., Grant, S.J., and Dobinson, K.F. (2005). Mutations in VMK1, a mitogen-activated protein kinase gene, affect microsclerotia formation and pathogenicity in *Verticillium dahliae*. Curr Genet **48,** 109–116.

Regenfelder, E., Spellig, T., Hartmann, A., Lauenstein, S., Bolker, M., and Kahmann, R. (1997). G proteins in *Ustilago maydis*: transmission of multiple signals? The EMBO journal **16,** 1934–1942.

Rispail, N., Soanes, D.M., Ant, C., Czajkowski, R., Grünler, A., Huguet, R., Perez-Nadales, E., Poli, A., Sartorel, E., Valiante, V., Yang, M., Beffa, R., Brakhage, A.A., Gow, N.A.R., Kahmann, R., Lebrun, M.-H., Lenasi, H., Perez-Martin, J., Talbot, N.J., Wendland, J., and Di Pietro, A. (2009). Comparative genomics of MAP kinase and calcium–calcineurin signalling components in plant and human pathogenic fungi. Fungal Genetics and Biology **46,** 287–298.

Roman, E., Nombela, C., and Pla, J. (2005). The Sho1 adaptor protein links oxidative stress to morphogenesis and cell wall biosynthesis in the fungal pathogen *Candida albicans*. Molecular and Cellular Biology **25,** 10611–10627.

Roman, E., Cottier, F., Ernst, J.F., and Pla, J. (2009). Msb2 signaling mucin controls activation of Cek1 mitogen-activated protein kinase in *Candida albicans*. Eukaryotic Cell **8,** 1235–1249.

Ruiz-Roldan, M.C., Maier, F.J., and Schafer, W. (2001). PTK1, a mitogen-activated-protein kinase gene, is required for conidiation, appressorium formation, and pathogenicity of *Pyrenophora teres* on barley. Mol Plant Microbe Interact **14,** 116-125.

Sambrook, J., Fritsch, E.F., and Maniatis, T. (1989). Molecular cloning: a laboratory manual. (Cold Spring Harbor, N.Y.: Cold Spring Harbor Laboratory).

Scherer, M., Heimel, K., Starke, V., and Kamper, J. (2006). The Clp1 protein is required for clamp formation and pathogenic development of *Ustilago maydis*. Plant Cell **18,** 2388–2401.

Schultz, J., Milpetz, F., Bork, P., and Ponting, C.P. (1998). SMART, a simple modular architecture research tool: identification of signaling domains. Proceedings of the National Academy of Sciences of the United States of America **95,** 5857–5864.

Schulz, B., Banuett, F., Dahl, M., Schlesinger, R., Schäfer, W., Martin, T., Herskowitz, I., and Kahmann, R. (1990). The b alleles of *U. maydis*, whose combinations program pathogenic development, code for polypeptides containing a homeodomain-related motif. Cell **60,** 295–306.

Smith, T.F., Gaitatzes, C., Saxena, K., and Neer, E.J. (1999). The WD repeat: a common architecture for diverse functions. Trends in Biochemical Sciences **24,** 181–185.

Spellig, T., Bolker, M., Lottspeich, F., Frank, R.W., and Kahmann, R. (1994). Pheromones trigger filamentous growth in *Ustilago maydis*. The EMBO journal **13,** 1620–1627.

Steinberg, G., and Perez-Martin, J. (2008). *Ustilago maydis,* a new fungal model system for cell biology. Trends in Cell Biology **18,** 61–67.

Steinberg, T.H., Agnew, B.J., Gee, K.R., Leung, W.-Y., Goodman, T., Schulenberg, B., Hendrickson, J., Beechem, J.M., Haugland, R.P., and Patton, W.F. (2003). Global quantitative phosphoprotein analysis using Multiplexed Proteomics technology. Proteomics **3,** 1128–1144.

Straube, A., Weber, I., and Steinberg, G. (2005). A novel mechanism of nuclear envelope break-down in a fungus: nuclear migration strips off the envelope. EMBO J **24,** 1674–1685.

Straube, A., Brill, M., Oakley, B.R., Horio, T., and Steinberg, G. (2003). Polar and Perinuclear Microtubule Organizing Centers in the Plant Pathogen *Ustilago maydis*. Mol Biol Cell **14,** 642–657.

Sturm, M., Leitner, A., Smått, J.-H., Lindén, M., and Lindner, W. (2008). Tin Dioxide Microspheres as a Promising Material for Phosphopeptide Enrichment Prior to Liquid Chromatography-(Tandem) Mass Spectrometry Analysis. Advanced Functional Materials **18,** 2381–2389.

Sugiyama, N., Masuda, T., Shinoda, K., Nakamura, A., Tomita, M., and Ishihama, Y. (2007). Phosphopeptide Enrichment by Aliphatic Hydroxy Acid-modified Metal Oxide Chromatography for Nano-LC-MS/MS in Proteomics Applications. Molecular & Cellular Proteomics **6,** 1103–1109.

Szabó, Z., Tönnis, M., Kessler, H., and Feldbrügge, M. (2002). Structure-function analysis of lipopeptide pheromones from the plant pathogen *Ustilago maydis*. Molecular Genetics and Genomics **268,** 362–370.

Tai, C.-Y., Dujardin, D.L., Faulkner, N.E., and Vallee, R.B. (2002). Role of dynein, dynactin, and CLIP-170 interactions in LIS1 kinetochore function. J Cell Biol **156,** 959–968.

Takáč, T., and Šamaj, J. (2015). Advantages and limitations of shot-gun proteomic analyses on Arabidopsis plants with altered MAPK signaling. Frontiers in Plant Science **6,** 107.

Takano, Y., Kikuchi, T., Kubo, Y., Hamer, J.E., Mise, K., and Furusawa, I. (2000). The *Colletotrichum lagenarium* MAP kinase gene CMK1 regulates diverse aspects of fungal pathogenesis. Mol Plant Microbe Interact **13,** 374-383.

Talbot, N.J. (2003). Exploring the biology of *Magnaporthe grisea*. Annu Rev Microbiol **57,** 177–202.

Taylor, B.L., and Zhulin, I.B. (1999). PAS Domains: Internal Sensors of Oxygen, Redox Potential, and Light. Microbiology and Molecular Biology Reviews **63,** 479–506.

Theisen, U., Straube, A., and Steinberg, G. (2008). Dynamic rearrangement of nucleoporins during fungal "open" mitosis. Molecular Biology of the Cell **19,** 1230–1240.

Thingholm, T.E., Jensen, O.N., and Larsen, M.R. (2009). Analytical strategies for phosphoproteomics. Proteomics **9,** 1451–1468.

Toyo-oka, K., Shionoya, A., Gambello, M.J., Cardoso, C., Leventer, R., Ward, H.L., Ayala, R., Tsai, L.H., Dobyns, W., Ledbetter, D., Hirotsune, S., and Wynshaw-Boris, A. (2003). 14-3-3epsilon is important for neuronal migration by binding to NUDEL: a molecular explanation for Miller-Dieker syndrome. Nat Genet **34,** 274–285.

Toyo-oka, K., Sasaki, S., Yano, Y., Mori, D., Kobayashi, T., Toyoshima, Y.Y., Tokuoka, S.M., Ishii, S., Shimizu, T., Muramatsu, M., Hiraiwa, N., Yoshiki, A., Wynshaw-Boris, A., and Hirotsune, S. (2005). Recruitment of katanin p60 by phosphorylated NDEL1, an LIS1 interacting protein, is essential for mitotic cell division and neuronal migration. Hum Mol Genet **14,** 3113–3128.

Tsukuda, T., Carleton, S., Fotheringham, S., and Holloman, W.K. (1988). Isolation and characterization of an autonomously replicating sequence from *Ustilago maydis*. Molecular and Cellular Biology **8,** 3703–3709.

Turra, D., Segorbe, D., and Di Pietro, A. (2014). Protein kinases in plant-pathogenic fungi: conserved regulators of infection. Annual Review of Phytopathology **52,** 267–288.

Ueda, K., Kosako, H., Fukui, Y., and Hattori, S. (2004). Proteomic identification of Bcl2-associated athanogene 2 as a novel MAPK-activated protein kinase 2 substrate. The Journal of biological chemistry **279,** 41815–41821.

Urban, M., Mott, E., Farley, T., and Hammond-Kosack, K. (2003). The *Fusarium graminearum* MAP1 gene is essential for pathogenicity and development of perithecia. Mol Plant Pathol **4,** 347–359.

Valinluck, M., Ahlgren, S., Sawada, M., Locken, K., and Banuett, F. (2010). Role of the nuclear migration protein Lis1 in cell morphogenesis in *Ustilago maydis.* Mycologia **102,** 493–512.

Vergnolle, M.A.S., and Taylor, S.S. (2007). Cenp-F Links Kinetochores to Ndel1/Nde1/Lis1/Dynein Microtubule Motor Complexes. Current Biology **17,** 1173–1179.

Wahl, R., Zahiri, A., and Kamper, J. (2010). The *Ustilago maydis* b mating type locus controls hyphal proliferation and expression of secreted virulence factors in planta. Molecular Microbiology **75,** 208–220.

Wang, L. (2011). Functional characterization of a seven-WD40 repeat protein Rak1 in *Ustilago maydis*. (Philipps-Universität Marburg).

Wang, Z., Dong, G., Singh, S., Steen, H., and Li, J. (2009). A simple and effective method for detecting phosphopeptides for phosphoproteomic analysis. Journal of Proteomics **72,** 831–835.

Wu, C., Jansen, G., Zhang, J., Thomas, D.Y., and Whiteway, M. (2006). Adaptor protein Ste50p links the Ste11p MEKK to the HOG pathway through plasma membrane association. Genes & Development **20,** 734–746.

Xiang, X., and Fischer, R. (2004). Nuclear migration and positioning in filamentous fungi. Fungal Genetics and Biology **41,** 411–419.

Xu, J.-R. (2000). MAP Kinases in Fungal Pathogens. Fungal Genetics and Biology **31,** 137–152.

Yamagata, A., Kristensen, D.B., Takeda, Y., Miyamoto, Y., Okada, K., Inamatsu, M., and Yoshizato, K. (2002). Mapping of phosphorylated proteins on two-dimensional polyacrylamide gels using protein phosphatase. Proteomics **2,** 1267–1276.

Yan, X., Li, F., Liang, Y., Shen, Y., Zhao, X., Huang, Q., and Zhu, X. (2003). Human Nudel and NudE as regulators of cytoplasmic dynein in poleward protein transport along the mitotic spindle. Mol Cell Biol **23,** 1239–1250.

Zarnack, K., Eichhorn, H., Kahmann, R., and Feldbrugge, M. (2008). Pheromone-regulated target genes respond differentially to MAPK phosphorylation of transcription factor Prf1. Molecular Microbiology **69,** 1041–1053.

Zhao, X., Kim, Y., Park, G., and Xu, J.R. (2005). A mitogen-activated protein kinase cascade regulating infection-related morphogenesis in *Magnaporthe grisea*. Plant Cell **17,** 1317–1329.

Zheng, L., Campbell, M., Murphy, J., Lam, S., and Xu, J.-R. (2000). The BMP1 Gene Is Essential for Pathogenicity in the Gray Mold Fungus *Botrytis cinerea*. Molecular Plant-Microbe Interactions **13,** 724–732.

Zhou, H., Tian, R., Ye, M., Xu, S., Feng, S., Pan, C., Jiang, X., Li, X., and Zou, H. (2007). Highly specific enrichment of phosphopeptides by zirconium dioxide nanoparticles for phosphoproteome analysis. Electrophoresis **28,** 2201–2215.

6 Supplementary data

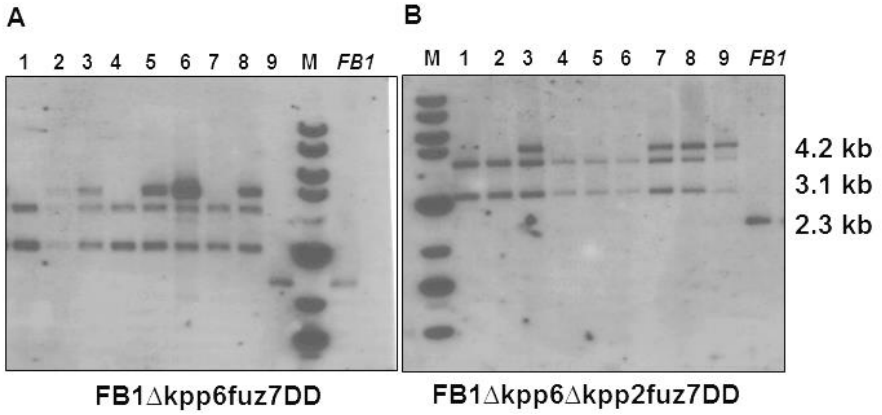

Supple figure 1: Construction of Fuz7DD strains. (A) Southern blot showing the DNA isolated from the colonies transformed with p123crg1fuz7DD into FB1Δkpp6 and FB1Δkpp6Δkpp2 and control strain FB1 (WT). Showing the integration of *fuz7DD* into FB1Δkpp6 lane 1, 4, 7 were positive for integration. (B) Showing the integration of fuz7DD into FB1Δkpp6Δkpp2 lanes 1, 2, 4-6 are positive. Expected bands for control strain was 2333 bp and for integration strains was 4269 bp and 3094 bp.Enzymes used for DNA digetion were EcoRV and Acc65I.

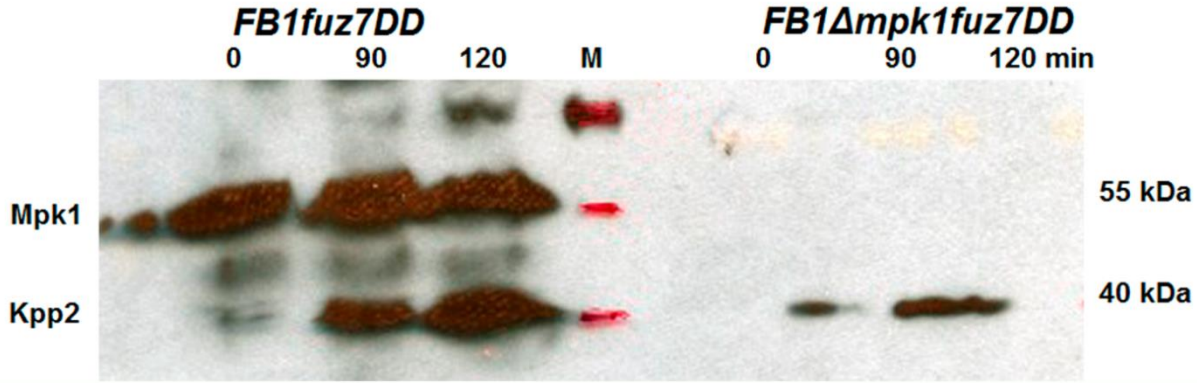

Supple figure 2: Phosphorylation of the MAP kinase Kpp2 after fuz7DD induction shows cell wall integrity protein kinase Mpk1. (A) Analysis of the phosphorylation status of MAP kinase Kpp2 in the strains FB1fuz7DD and FB1Δmpk1fuz7DD. The expression of Kpp2 was induced for 0, 90 and 120 min as indicated. Phosphorylation was detected by western-blot analysis using a phospho-specific antibody recognizing the phosphorylated TEY motif in MAPKs (α-p44/p42).

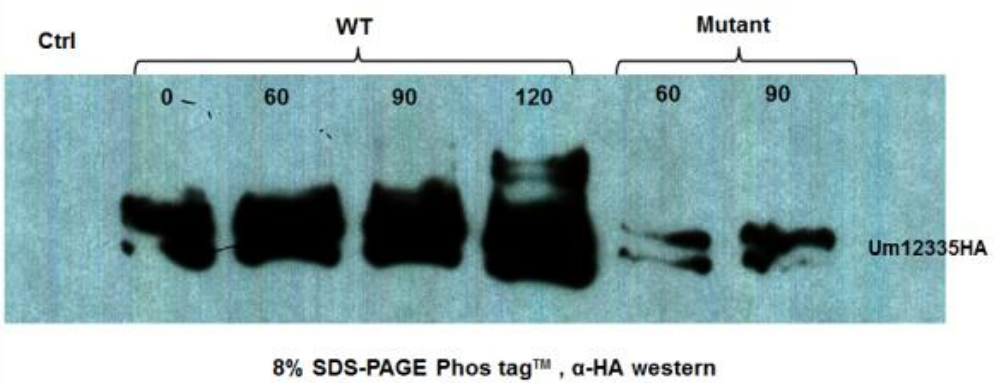

Supple figure 3: Phosphorylation of Um12335-HA after induction of fuz7DD. (A) Strain FB1fuz7DD (Ctrl), FB1fuz7DDPotef-um12335HA (WT) and FB1Δkpp6Δkpp2fuz7DD-Potef-um12335HA (Mutant) were induced for *fuz7dd* at the different time points indicated. 50mM Phos-tag SDS-PAGE was used for detecting the mobility shift in the HA tagged Um12335 after induction. Bands were detected using anti-HA antibodies.

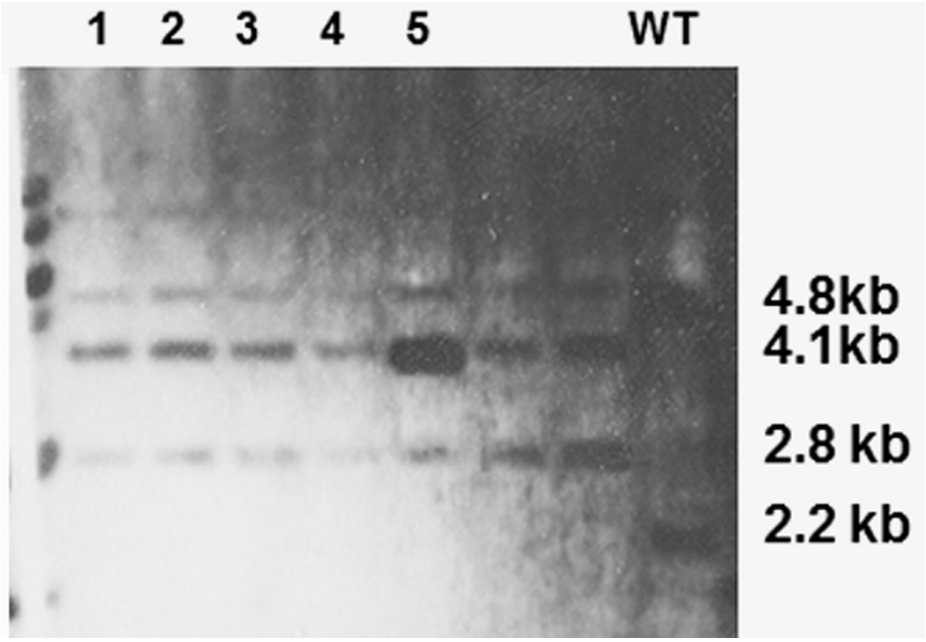

Supple figure 4: Southern blot for the deletion of *um05364.* Southern blot showing the DNA isolated from the colonies transformed with pum05364hyg in SG200 and control strains *SG200* (WT) digested with restriction enzymes BsrGI and EcoRI. Blotted with DIG probe generated using plasmid pum05364hyg. Lane 1-4 was the deletion strains SG200Δum05364. Expected bands for control strain was 4838 bp and 2252 bp and for deletion strains was 4128 bp and2874.

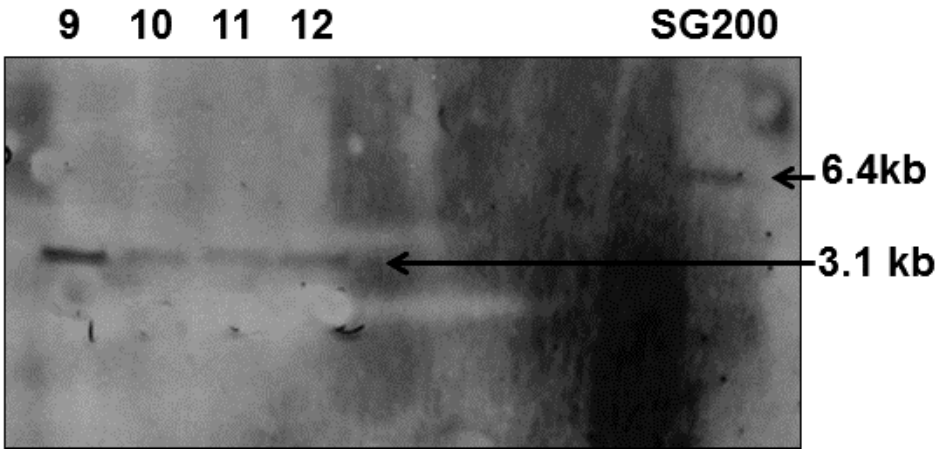

Supple figure 5: Southern blot for the deletion of *um11960*. The DNA isolated from the transformed strains and control strains SG200 was digested with restriction enzyme PsiI/NdeI were probed with DIG probe generated using plasmid pum11960hyg. Lane 9 to 12 was the deletion strains SG200Δum11960. Expected bands for control strain was 6436 bp and for deletion strains was 3150 bp.

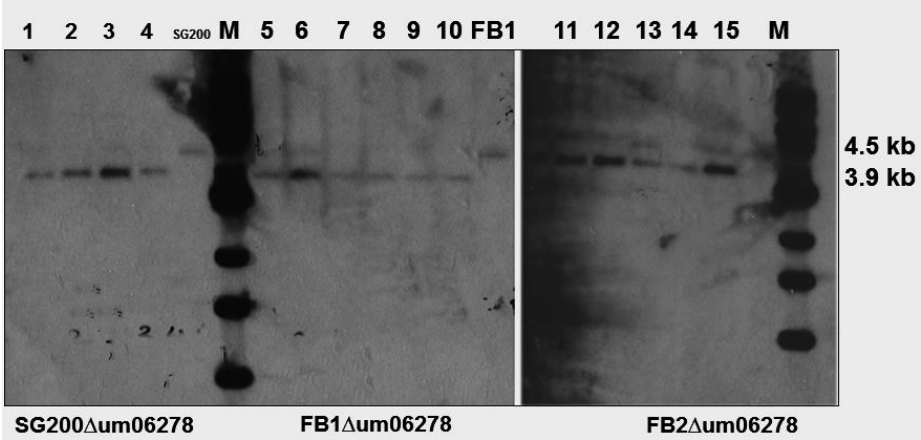

Supple figure 6: Southern blot for the deletion of *um06278*. Southern blot showing the DNA isolated from the transformed strains and control strains SG200 and FB1, digested with restriction enzyme Hind III Probed with DIG probe generated using pum06278hyg. Lane 1,2,3,4 was the deletion strains SG200Δum06278 and lane 6 to 10 were the deletion strains FB1Δum06278 and lane 12 to 15 were the deletion strains FB2Δum06278. Expected band for control strain was 4548 bp and a deletion strain was 3893. M is 1 kb marker.

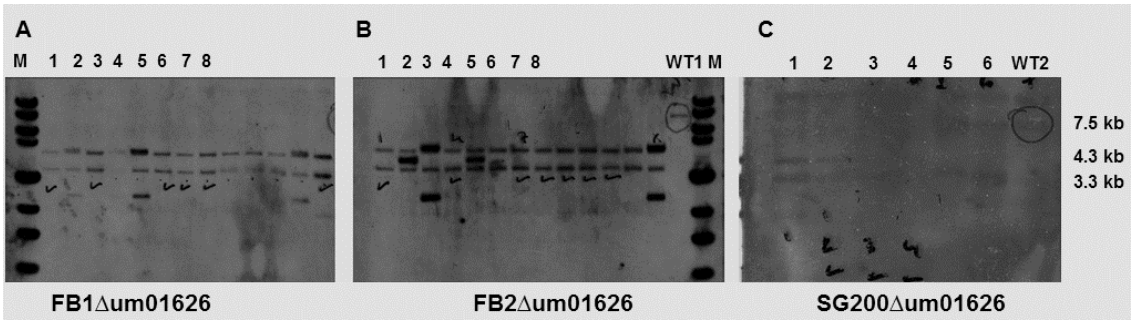

Supple figure 7: Southern blot for the deletion of *um*01626. Southern blot showing the DNA isolated from the transformed strains and control strains FB1 (WT1) and SG200 (WT2) digested with restriction enzyme Nde1/BamH1. Developed with DIG probe generated using pum01626hyg. (A) Lane 1-4, 6-8 were the deletion strains FB1Δum01626. (B) Lane 1, 4, 7 and 8 were the deletion strains FB2Δum01626. (C) Lane 1, 2, 3 were the deletion strains SG200Δum01626. Expected bands for control strain was 7519 bp and deletion strains were 4309 bp and 3358 bp shown on the right side. M is 1 kb marker.

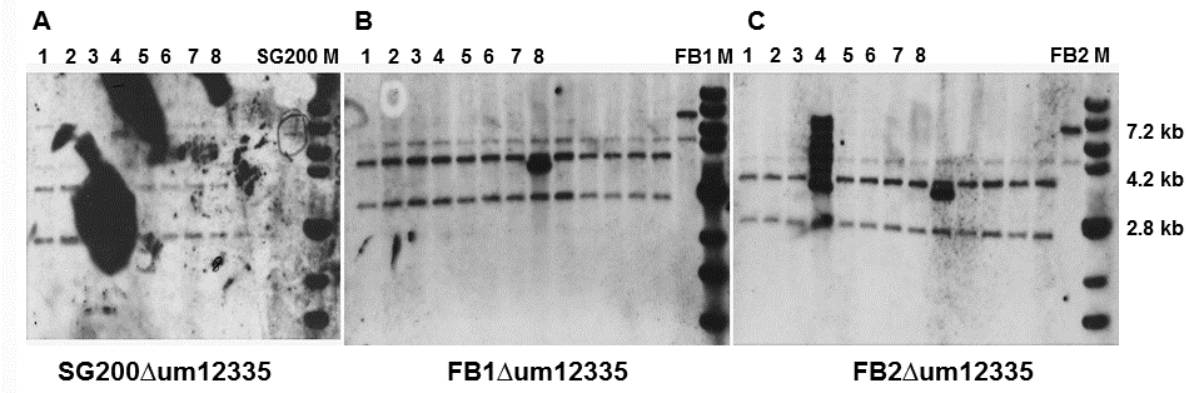

Supple figure 8: Southern blot for the deletion of *um12335*. Southern blot showing the DNA isolated from the transformed strains and control strains SG200, FB1 and FB2 digested with restriction enzyme Not1/BamH1. Developed with DIG probe generated using pum12335hyg. (A) Lane 1, 2, 5-7 were the deletion strains SG200Δum12335. (B) Lane 1 to 8 was the deletion strains FB1Δum12335. (C) Lane 1 to 8 were the deletion strains FB2Δum12335. Expected bands for control strain was 7243 bp and deletion strains were 4251 bp and 2795 bp. M is 1 kb marker.

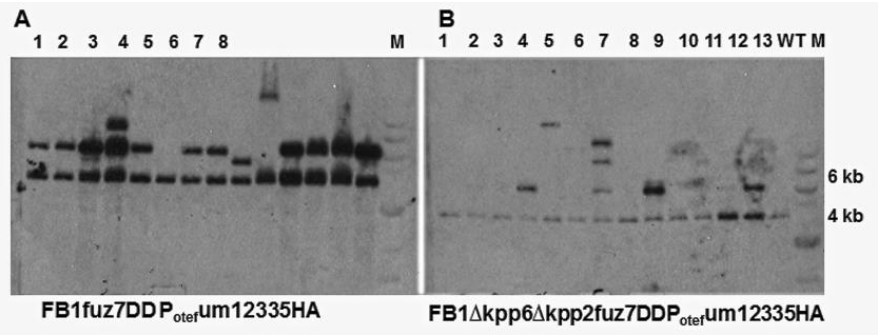

Supple figure 9: Integration of *um12335HA*. Southern blot showing the DNA isolated from the transformed strains and control strain FB1fuz7DD digested with restriction enzyme PciI. Developed with DIG probe generated using ORF of um12335. (A) Lane 1, 2, 3 and 5, 7, 8 were the strains showing the integration of um12335HA into FB1fuz7DD. (B) Lane 4, 9 and 13 were the strains showing the integration of *um12335HA* into FB1Δkpp6Δkpp2fuz7DD. Expected bands for control strain 4096 bp and for integration strains were 4096bp and 6059 bp. M is 1 kb marker.

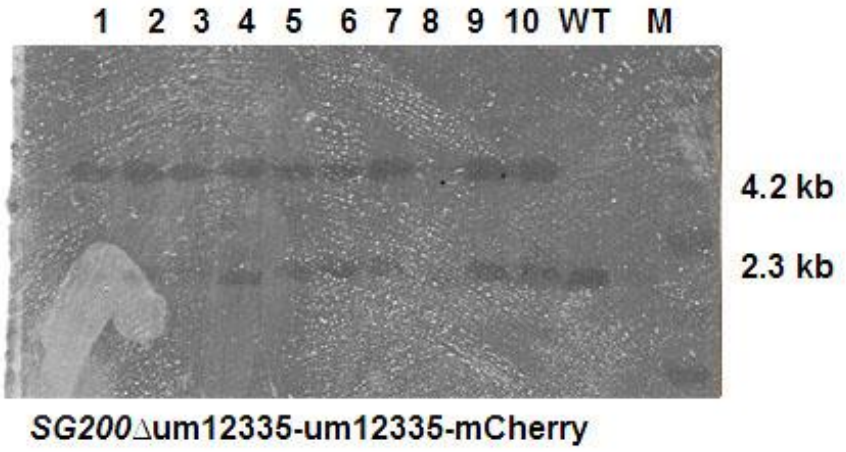

Supple figure 10: Integration of *um12335-m Cheryy* into SG200Δum12335. Southern blot showing the DNA isolated from the transformed strains and control strains SG200 digested with restriction enzymes Acc65I and EcoRV, were developed with *cbx* probe generated using p123crg1fuz7DD . Lane 4, 5, 6, 9 and 10 are the strains showing the integration of *um12335-mCherry* into SG200Δum12335. Expected bands for control strain was 2333 bp and deletion strains was 2426 bp and 4269 bp. M is 1 kb marker

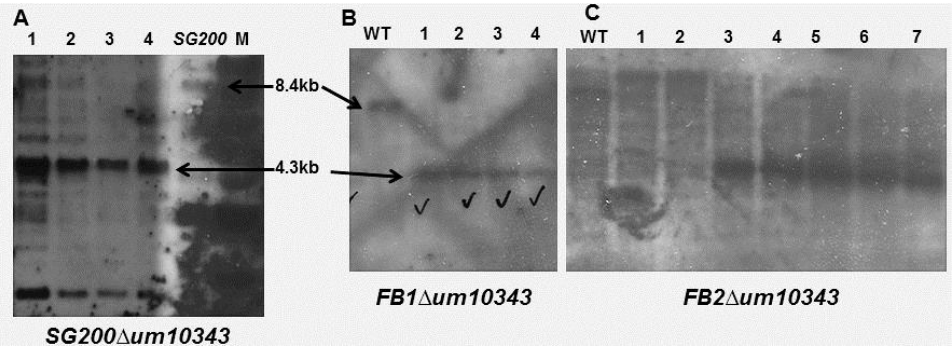

Supple figure 11: Southern blot for the deletion of *um10343.* Southern blot showing the DNA isolated from the colonies transformed with pum10343hyg in SG200, FB1, FB2 and control strains SG200, FB1 (WT) digested with restriction enzymes PciI. Developed with DIG probe generated using plasmid pum10343hyg. (A) Lane 1 to 4 was deletion strains SG200Δum10343. (B) Lane 1 to 4 was the deletion strains FB1Δum10343. (C) Lane 3 to 7 are the deletion strains FB2Δum10343. Expected bands for control strain was 8473 bp and for deletion strains was 4304 bp. M is 1 kb marker.

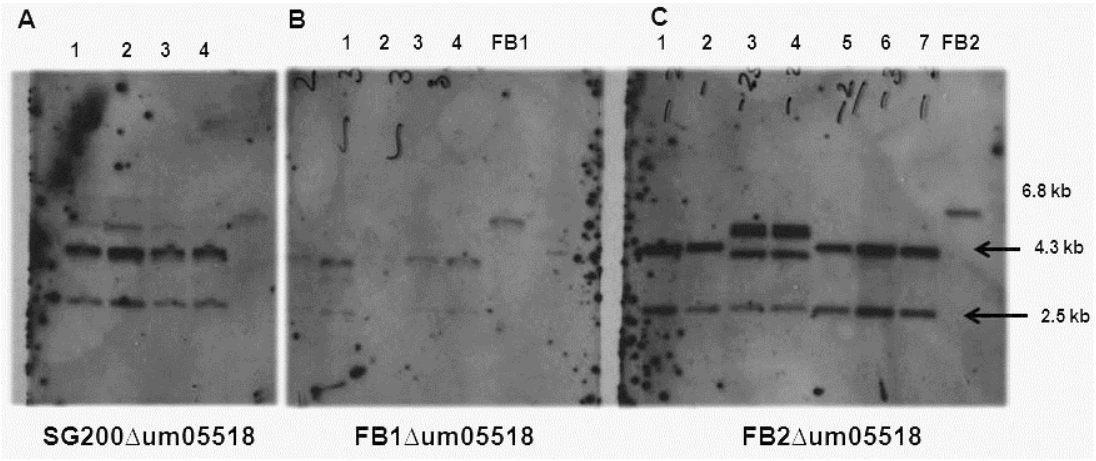

Supple figure 12: Southern blot for the deletion of *um05518*. Southern blot showing the DNA isolated from the transformed strains and control strains FB1 and FB2 digested with restriction enzyme Acc65I/Not1. Developed with DIG probe generated using pum05518hyg. (A) Lane 1-4 was the deletion strains SG200Δum05518. (B) Lane 1, 3, 4 were the deletion strains FB1Δum05518. (C) Lane 1, 2, 5, 6, 7 were the deletion strains FB2Δum05518. Expected bands for control strain was 6801 bp and deletion strains were 4362 bp and 2533 bp.

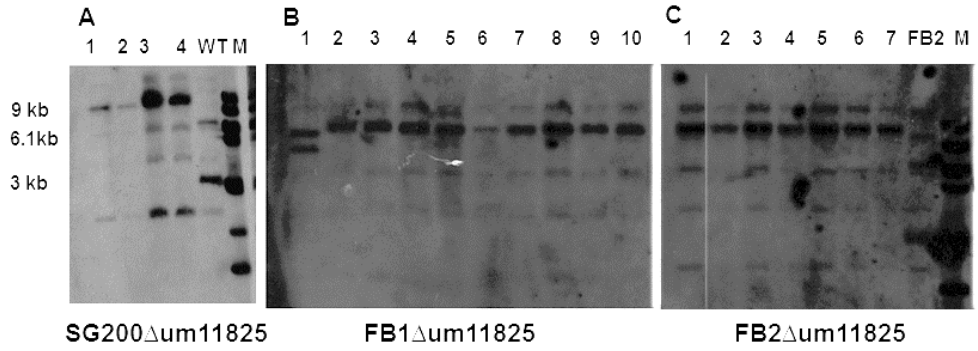

Supple figure 13: Southern blot for the deletion of *um11825*. Southern blot showing the DNA isolated from the transformed strains and control strains SG200 (WT) and FB2 digested with restriction enzyme Bgl II. Developed with DIG probe generated using pum11825hyg. (A) Lane 1 -4 was the deletion strains SG200Δum11825. (B) Lane 2 – 9 were the deletion strains FB1Δum11825. (C) Lane 2, 3, 4, were the deletion strains FB2Δum11825. Expected bands for control strain was 6180 bp, 3098 bp and deletion strains was 8997 bp

.

Acknowledgements

Foremost, I would like to express my sincere gratitude to my advisor Prof. Dr. Regine Kahmann for the continuous support during my Ph.D study and research, for her patience, motivation, enthusiasm, and immense knowledge. I would like to thank my PhD thesis committee Prof. Dr. Michael Bölker, Dr. Stefan Zauner, Prof. Dr. Hans-Ulrich Mösch for their insightful comments and hard questions.

I am great full to Dr. Gerold J. M. Beckers for supervising me in doing phospho proteomics experiments in his lab. I am especially thankful to Dr. Wolfgang Hoehenwarter for doing massspec analysis. I am also thankful to Dr. Stefanie Reißmann for support in discussion and encouragement for my experiments.

I thank my fellow past and current lab members from Kahmann lab and department of orgnismic interactions. Special thanks to Marino, Lei wang, Daniel, Liang, Nina, Nancy and all those who lend their support throughout my stay in lab. I want to express my gratitude to all my Ariadne friends, especially Sonia, Elisabetta for their inspiration during my PhD study.

I am sincerely grateful to Karin Münch, Nicole Rössel, Volker Vincon for encouragement and assistance in the lab, Rolf Rösser for computational support, Stefan Schmidt, Anita Boos, Ria Faber, Vera Matschiske-Peters, for their assistance and generous help during my stay in lab. I also would like to extend my thanks to Mr. Christian Bengelsdorff for all the support in dealing with administrative work.

I also would like to acknowledge Marburg Graduate School 1216 and financial support through Marie-curie ITN and MPI.

Finally, I would like to thank my family and best friend Filomena for support, love, encouragements and laughter. They have been the source of my energy and self-confidence during all this time.

Curriculum Vitae

Vikram Naik

Personal Information

Date of Birth	03.May.1982
Nationality	Indian
Residence	Sirsi, Karnataka

Education

08/2010 – 06/2015	**PhD** project funded by Marie Curie EU-ITN Max Plank Institute for Terrestrial Microbiology - Marburg, Germany **PhD** thesis - **The *Ustilago maydis* MAP kinase signaling pathway: Identification of MAP kinase targets by phospho-peptide enrichment.**
07/2006 - 10/2008	**Master of Science in Biotechnology** University of Calicut - Kerala, India **Molecular biology, Immunology, Cell biology and Microbiology, Fermentation and Bioreactors, Genetic Engineering, Plant biotechnology.** Project - Cell cycle effects of *Rivina humilis* on the synchronous plasmodial cultures of *Physarum polycephalum*.
06/2000 - 05/2003	**Bachelor of Science** Karnatak University - Sirsi, India English, Fundamental knowledge in Chemistry, Botany and Zoology